EMEP/MSC-E Technical Note 11/2005

May 2005

Hemispheric model (MSCE-Hem) of persistent toxic substances dispersion in the environment

A.Gusev, E. Mantseva, V. Shatalov, O. Travnikov

Meteorological Synthesizing Centre - East

Leningradsky prospekt, 16/2, 125040 Moscow
Russia
Tel./Fax: +7 095 214 39 93
E-mail: msce@msceast.org
Internet: www.msceast.org

CONTENTS

1. MODEL DESCRIPTION 3

1.1. Model domains 3

1.2. Atmospheric transport 3

2. HM MODEL 7

2.1. Atmospheric chemistry 7

2.2. Dry deposition 13

2.3. Wet deposition 24

2.4. Boundary and initial conditions 26

2.5. Input information 26

3. POP MODEL 28

3.1. The atmospheric compartment 29

3.2. Soil compartment 33

3.3. Vegetation compartment 37

3.4. Seawater compartment 39

3.5. Input information 45

REFERENCES 47

Annex A CALCULATION OF THE VERTICAL VELOCITY 53

Annex B PHYSICAL CHEMICAL PROPERTIES OF SELECTED POPs AND SUBSTANCE-SPECIFIC PARAMETERS 55

B.1. Subcooled liquid-vapour pressure 55

B.2. Henry's law constant and air/water partition coefficient 57

B.3. Dry deposition velocities over land, sea, and forest 58

B.4. Washout ratio 59

B.5. Degradation rate constants in environmental media 60

B.6. Octanol-water partition coefficient 63

B.7. Organic carbon-water partition coefficient 63

B.8. Octanol-air partition coefficient 64

B.9. Molecular diffusion coefficients in air and water 67

Annex C INPUT DATA 69

C.1. Meteorological data 69

C.2. Land cover data

1. MODEL DESCRIPTION

The hemispheric models MSCE-Hem-HM and MSCE-Hem-POP has been developed in MSC-East to meet the tasks of the Convention on Long-Range Transboundary Air Pollution on the assessment of the atmospheric transport and depositions of heavy metal and persistent organic pollutants in the Northern Hemisphere, evaluation of the intercontinental transport and support of the regional pollution modelling with the boundary conditions.

1.1. Model domain

Both MSCE-Hem-HM and MSCE-Hem-POP are three-dimensional models of Eulerian type. The model computation domain covers the whole Northern Hemisphere with spatial resolution 2.5° both in zonal and meridional directions. To avoid a singularity at the pole point, peculiar to the spherical coordinates, the grid has a special circular mesh of radius 1.25° including the North Pole. In the vertical direction the model domain consists of eight irregular levels of terrain-following sigma-pressure (σ-p) coordinate defined as a ratio of local atmospheric pressure to the ground surface pressure [*Jacobson*, 1999].

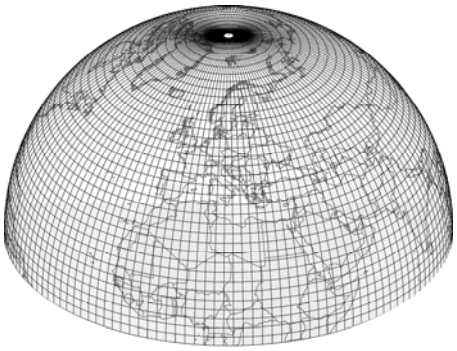

Fig.1.1. *Horizontal structure of the regional and hemispheric model domains. Red line depicts the EMEP region. Geographical coordinates with 2.5° x 2.5° resolution and the pole grid cell*

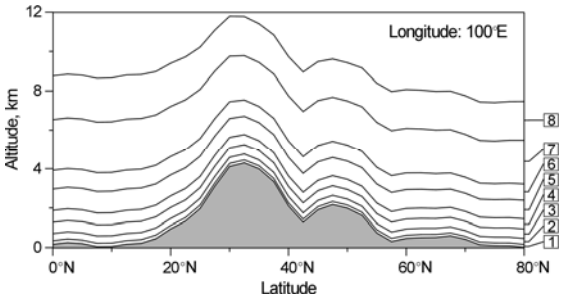

Fig.1.2. *Vertical grid structure of the hemispheric model domain. Eight terrain-following s-levels: 1 - σ = 0.99; 2 - 0.96; 3 - 0.91; 4 - 0.85; 5 - 0.77; 6 - 0.68; 7 - 0.55; 8 - 0.4*

1.2. Atmospheric transport

The models description of atmospheric transport is based on the three-dimensional advection-diffusion equation adapted to the (σ–p) coordinate [see e.g. *Jacobson*, 1999]:

$$\frac{\partial}{\partial t}(qp_s) = -\nabla_H \cdot (qp_s \mathbf{V}_H) - \frac{\partial}{\partial \sigma}(qp_s\dot{\sigma}) + \frac{\partial}{\partial \sigma}\left[K_z \frac{g^2\rho^2}{p_s^2}\frac{\partial}{\partial \sigma}(qp_s)\right] + C + S - R \qquad (1.1)$$

Here $q = c/\rho$ is air pollutant mixing ratio;

c_i and ρ are the volume concentration and the local air density;

$\dot{\sigma} = d\sigma/dt$ is the vertical scalar velocity in the σ–p coordinate;

∇_H and $\mathbf{V}_H$ denote vectors of horizontal divergence operator and horizontal wind velocity respectively;

K_z is the vertical eddy diffusion coefficient; and g is the gravitational acceleration.

In Eq. (1.1) we omitted horizontal components of eddy diffusion because of the coarse horizontal grid resolution. The local air density ρ is coupled with air temperature T_a and surface pressure p_s through the equation of state:

$$\rho = \frac{\sigma p_s}{R_a T_a}, \tag{1.2}$$

where R_a is the humid air gas constant.

The first two terms on the right hand side of Eq. (1.2) describe horizontal and vertical advection of a pollutant in the atmosphere. The third term represents vertical eddy diffusion, the fourth considers species mutual chemical transformations (C), and the last two terms describe bulk pollutant sources (S) and removal processes (R). Eq. (1.1) is solved by means of the time-splitting technique [*Yanenko*, 1971; *Marchuk*, 1975; *McRae et al.*, 1982]. Following this method, Eq. (1.2) is decomposed into several separate sub-equations describing different physical and chemical processes, which are solved successively during each time step.

Advection

In spherical coordinates the sub-equation of Eq. (1.1) describing horizontal advection has the following form:

$$\frac{\partial}{\partial t}(qp_s) = -\frac{1}{R_E \cos\varphi}\left[\frac{\partial}{\partial \lambda}(qp_s V_\lambda) + \frac{\partial}{\partial \varphi}(qp_s V_\varphi \cos\varphi)\right] \tag{1.3}$$

where λ and φ are the geographical longitude and latitude;

R_E is the Earth radius;

V_λ and V_φ are zonal and meridional components of the wind velocity respectively.

Moreover, the former term in the square brackets describes the zonal advective transport, while the latter term represents the meridional one.

Eq. (1.3) is numerically solved using Bott flux-form advection scheme [*Bott*, 1989a; 1989b]. This scheme is mass conservative, positive-definite, monotone, and is characterized by comparatively low artificial diffusion [see e.g. *Dabdub and Seinfeld*, 1994]. In order to reduce the time-splitting error in strong deformational flows the scheme has been modified according to [*Easter*, 1993]. The original Bott scheme has been derived in the Cartesian coordinates. To apply the scheme to the transport in spherical coordinates it has been modified taking into account peculiarities of the spherical geometry. Detailed description of the Bott advection scheme in the spherical coordinates is presented in [*Travnikov*, 2001].

The vertical advection part of Eq. (1.1) is written as follows:

$$\frac{\partial}{\partial t}(qp_s) = -\frac{\partial}{\partial \sigma}(qp_s \dot{\sigma}). \tag{1.4}$$

This one-dimensional advection equation is solved using the original Bott scheme generalized for a grid with variable step $\Delta\sigma$.

Eddy diffusion

Vertical eddy diffusion is described by the following equation:

$$\frac{\partial}{\partial t}(qp_s) = \frac{\partial}{\partial \sigma}\left[K_z \frac{g^2\rho^2}{p_s^2} \frac{\partial}{\partial \sigma}(qp_s) \right]. \qquad (1.8)$$

Vertical eddy diffusion coefficient $K_z = K_z(\lambda,\varphi,\sigma)$ is supplied by the atmospheric boundary layer module of the meteorological data preparation system. Non-linear diffusion Eq. (1.8) has been approximated by the second-order implicit numerical scheme in order to avoid restrictions of the time step caused by possible sharp gradients of species mixing ratio $q(\sigma)$. The obtained finite-difference equation is solved by means of the sweep method.

Mass consistency

A very important issue for any air quality model is the mass consistency. It means that off-line fields of wind and surface pressure supplied by the meteorological pre-processor should satisfy the continuity equation:

$$\frac{\partial p_s}{\partial t} + \nabla_H \cdot (p_s \mathrm{V}_H) + \frac{\partial}{\partial \sigma}(p_s \dot{\sigma}) = 0 . \qquad (1.5)$$

In the terms of an air quality model it implies that the model maintain a uniform mass mixing ratio field of an inert tracer [*Odman and Russel*, 2000]. It can be exactly realized only if the air quality model and a meteorological model supplying input data have the same discretization, i.e. grid structure, time step, and finite-difference formulation. However, many transport models (including considered one) have the discretization different from that used in the weather prediction model (WPM) supplying the data. Besides, time resolution of the off-line meteorological data (6 hours for the model involved) is often considerably lower than the model time resolution (10-30 minutes) defined by the numerical stability of the explicit scheme. It requires temporal interpolation of the meteorological data. All mentioned above can lead to a considerable mass inconsistency and the uniform tracer field cannot be maintained. A possible approach to adjust the input meteorological fields to the model discritization is derivation of vertical wind velocity $\dot{\sigma}$ from the continuity Eq. (1.5) at each time step [*Odman and Russel*, 2000].

For the exact mass conservation it is important to apply to solution of Eq. (1.5) the same numerical scheme used for species advection description. The solution is performed in two steps:

Step 1. Solution of the horizontal constituent of the air continuity equation for p_s using Bott advection scheme:

$$\frac{\partial p_s}{\partial t} = -\nabla_H \cdot \left(p_s \mathrm{V}_H\right). \qquad (1.6)$$

For the initial condition the surface pressure at the beginning of the time step $(p_s)_t$ is used. As a result a tree-dimensional distribution of the intermediate pressure $(p_s)_{t+\Delta t/2} = f(x,y,\Delta)$ is obtained.

Step 2. Solution of the vertical constituent of the air continuity equation for the vertical velocity:

$$\frac{\partial p_s}{\partial t} = -\frac{\partial}{\partial \sigma}(p_s \dot{\sigma}) . \qquad (1.7)$$

The intermediate pressure $(p_s)_{t+\Delta t/2}$ from the Step 1 is used as the initial condition; and the surface pressure at the end of the time step $(p_s)_{t+\Delta t}$ = f(x,y) interpolated from the input data is considered as a final condition. The vertical velocity is derived from Eq. (1.7) analytically by inversion of the Bott scheme applied for the vertical transport description.

Details of the vertical velocity calculation procedure are presented in Annex A.

2. HM MODEL

The heavy metal version of the hemispheric model (MSCE-HM-Hem) describes HM fate in the atmosphere from its emission till deposition to the Earth surface including (beside the atmospheric transport) such processes as the scavenging of a pollutant with precipitation, dry uptake by the Earth`s surface as well as physical and chemical transformations of mercury. A general scheme of the main processes governing HM cycling in the atmosphere is shown in Fig.2.1. More detailed description of the model parameterization of these processes is presented in the following sections.

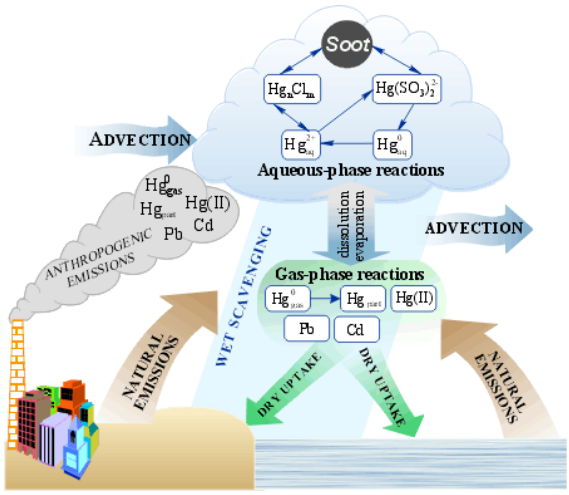

Fig. 2.1. *The model scheme of HM behaviour in the atmosphere*

2.1. Atmospheric chemistry

Such heavy metals as lead and cadmium and their compounds are characterized by very low volatility. It is assumed in the model that these metals (as well as some others – nickel, chromium, zinc etc.) are transported in the atmosphere only in the composition of aerosol particles. It is believed that their possible chemical transformations do not change properties of their particles-carriers with regard to removal processes.

On the contrary, mercury transformations in the atmosphere include transitions between the gaseous, aqueous and solid phases, chemical reactions in the gaseous and aqueous environment. Hereafter we shall use the term “aqueous phase” for all species dissolved in cloud water and those in composition of solid particles suspended in a droplet. Besides, we shall distinguish three main mercury forms in the atmospheric air: gaseous elemental mercury (GEM), total particulate mercury (TPM) and reactive gaseous mercury (RGM). The last form mostly consists of divalent mercury compounds in gaseous phase, the most typical of which is mercury chloride ($HgCl_2$). The general scheme of mercury transformations in the atmosphere is illustrated in Fig. 2.2.

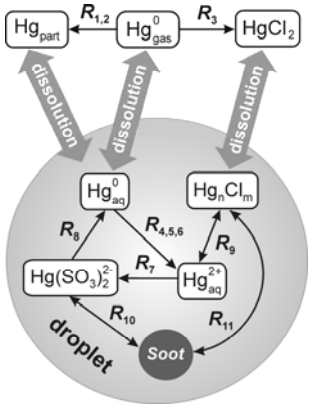

Fig. 2.2. *Scheme of chemical transformations of mercury in the atmosphere*

Inter-phase equilibrium

All gaseous mercury compounds are soluble to some extent in cloud- and rainwater. Size of cloud droplets is small enough to establish the equilibrium between the solution and the gas rather rapidly. The equilibrium described by Henry’s law has pronounced temperature dependence. The expression for the Henry’s law constants (in the form of the ratio of a species concentration in liquid to its air concentration, M·cm^3/molec) are given by:

$$H = A_H T \exp\left[B_H\left(\frac{T_0}{T} - 1\right)\right], \tag{2.1}$$

where T_0 = 298.15 K; coefficients A_H and B_H for gaseous mercury forms and other gases of interest are presented in Table 2.1.

Table 2.1. *Coefficients of Henry's low constants*

Compound	A_H	B_H	Reference
Hg^0	$1.76 \cdot 10^{-23}$	9.08	*Andersson et al.*, 2004
$HgCl_2$	$1.75 \cdot 10^{-16}$	18.75	*Ryaboshapko et al.*, 2001
O_3	$1.58 \cdot 10^{-24}$	7.8	*Sander*, 1997
$^{\cdot}OH$	$3.41 \cdot 10^{-21}$	17.72	*Jacobson*, 1999
Cl_2	$4.48 \cdot 10^{-16}$ *		*Lin and Pehkonen*, 1999

* - no temperature dependence is available

Besides, we expect that half of particulate mercury mass in cloud- and rainwater is represented by soluble compounds [*Brosset and Lord*, 1991; *Fitzgerald et al.*, 1991; *Lamborg et al.*, 1995]. On the other hand, it is assumed that all mercury mass in the aqueous phase is transformed to the particulate form if the cloud droplet is evaporated.

Gas-phase reactions

One of the most important gas phase reactions is oxidation of elemental mercury by ozone:

$$Hg^0_{(gas)} + O_{3(gas)} \rightarrow Hg(II)_{(part)} + products \tag{2.2}$$

Since, ozone is always in plenty under ordinary atmospheric conditions this second-order reaction is described by a first-order rate expression with the reaction rate constant depending on the reactant concentration:

$$R_1 = -\frac{d[Hg^0_{(gas)}]}{dt} = k_1'[Hg^0_{(gas)}], \tag{2.3}$$
$$k_1' = k_1[O_{3(gas)}], \quad k_1 = A\exp(-E_a/(R_{univ}T))$$

where A = $2.1 \cdot 10^{-18}$ $cm^3/(molec \cdot s)$ [*Hall*, 1995];
E_a = 10.36 kJ/mole;
R_{univ} = 8.31 J/(mole·K);
$[O_{3(gas)}]$ is ozone concentration, $molec/cm^3$.

It is believed that the product of the reaction – mercury oxide is in particulate form due to its poor volatility [*Sommar et al*., 2001; *Schroeder and Munthe*, 1998].

Recently investigated reaction of mercury oxidation by hydroxyl radical in gaseous phase is expected to be very significant or even prevailing sink of elemental mercury in the troposphere [*Sommar et al.*, 1999; 2001; *Pal and Ariya*, 2004]:

$$Hg^0_{(gas)} + {}^{\bullet}OH_{(gas)} \rightarrow Hg(II)_{(part)} + products, \tag{2.4}$$

$$R_2 = -\frac{d[Hg^0_{(gas)}]}{dt} = k'_2[Hg^0_{(gas)}], \qquad k'_2 = k_2[^{\bullet}OH_{(gas)}], \tag{2.5}$$

where k_2 = 8.7·10^{-14} cm^3/(molec·s) [*Sommar et al.*, 2001];
[$^{\cdot}OH_{(gas)}$] is hydroxyl radical concentration, molec/cm^3.

Gas phase oxidation of elemental mercury by chlorine can be noticeable in the ocean boundary layer during nighttime [*Seigneur et al.*, 1994; *Tokos et al.*, 1998; *Ariya et al.*, 2002]:

$$Hg^0_{(gas)} + Cl_{2(gas)} \rightarrow Hg(II)_{(gas)}, \tag{2.6}$$

$$R_3 = -\frac{d[Hg^0_{(gas)}]}{dt} = k'_3[Hg^0_{(gas)}], \qquad k'_3 = k_3[Cl_{2(gas)}], \tag{2.7}$$

where k_3 = 2.6·10^{-18} cm^3/(molec·s) [*Ariya et al.*, 2002];
[$Cl_{2(gas)}$] is chlorine concentration, molec/cm^3.

Aqueous-phase reactions

Dissolved elemental mercury is oxidized by ozone producing mercury oxide *HgO*, which is very short-lived in the liquid phase and is rapidly transformed to the mercury ion Hg^{2+}_{aq}. Thus, the resulting reaction can be written as follows:

$$Hg^0_{(aq)} + O_{3(aq)} \rightarrow Hg^{2+}_{(aq)} + products, \tag{2.8}$$

with the reaction rate expression:

$$R_4 = -\frac{d[Hg^0_{(aq)}]}{dt} = k'_4[Hg^0_{(aq)}], \qquad k'_4 = k_4 H_{O3}[O_{3(gas)}]. \tag{2.9}$$

Here k_4 = 4.7·10^7 M^{-1}s^{-1} [*Munthe*, 1992];
[$O_{3(gas)}$] is ozone concentration, molec/cm^3;
H_{O3} is Henry's constant for ozone.

Another important reaction of mercury oxidation in aqueous phase is reaction with hydroxyl radical:

$$Hg^0_{(aq)} + {}^{\bullet}OH_{(aq)} \rightarrow Hg^{2+}_{(aq)} + products. \tag{2.10}$$

Reaction rate expression for this reaction has the following form:

$$R_5 = -\frac{d[Hg^0_{(aq)}]}{dt} = k'_5[Hg^0_{(aq)}]; \qquad k'_5 = k_5 H_{OH}[^{\bullet}OH_{(gas)}] \tag{2.11}$$

where k_5 = 2.4·10^9 M^{-1}s^{-1} [*Gårdfeldt et al.*, 2001];
[$^{\cdot}OH_{(gas)}$] is hydroxyl radical concentration, molec/cm^3;
H_{OH} is Henry's constant for hydroxyl radical.

Elemental mercury in aqueous phase is also oxidized by dissolved chlorine $Cl(I)_{aq}$ with formation of mercury ion Hg^{2+}_{aq}:

$$Hg^0_{(aq)} + Cl(I)_{(aq)} \rightarrow Hg^{2+}_{(aq)} + products\ , \tag{2.12}$$

$$R_6 = -\frac{d[Hg^0_{(aq)}]}{dt} = k'_6[Hg^0_{(aq)}]\ ; \qquad k'_6 = k_6 H_{Cl2}[Cl_{2(gas)}]\ , \tag{2.13}$$

where $k_6 = 2\cdot10^6\ M^{-1}s^{-1}$ [*Lin and Pehkonen*, 1999];
$[Cl_{2(gas)}]$ is chlorine concentration, molec/cm^3;
H_{Cl2} is Henry's constant for chlorine.

Mercury ion Hg^{2+}_{aq} reacts in the solution with sulphite ions SO^{2-}_3 resulting in the formation of mercury sulphite complex $Hg(SO_3)^{2-}_2$ [*Pleijel and Munte*, 1995]:

$$Hg^{2+}_{(aq)} + 2SO^{2-}_{3(aq)} \rightarrow Hg(SO_3)^{2-}_{2(dis)}\ . \tag{2.14}$$

The reaction rate is determined by the air concentration of SO_2 and the cloud water *pH*:

$$R_7 = -\frac{d[Hg^{2+}_{(aq)}]}{dt} = k'_7[Hg^{2+}_{(aq)}]\ , \qquad k'_7 = k_7[SO_{2(gas)}]^2\cdot10^{4\,pH}\ , \tag{2.15}$$

where $k_7 = 1.1\cdot10^{-21}\ s^{-1}$, and $[SO_{2(gas)}]$ is in ppbv. In all calculations we use fixed value for cloud water *pH* = 4.5.

The sulphite complex $Hg(SO_3)^{2-}_{2(dis)}$ is dissociated to mercury sulphite $HgSO_3$, which is unstable, and is readily reduced to $Hg^0_{(aq)}$. Thus, the reduction process can be described as:

$$Hg(SO_3)^{2-}_{2(dis)} \rightarrow Hg^0_{(aq)} + products \tag{2.16}$$

with the reaction rate expression:

$$R_8 = -\frac{d[Hg(SO_3)^{2-}_{2(dis)}]}{dt} = k_8[Hg(SO_3)^{2-}_{2(dis)}]\ , \tag{2.17}$$

where $k_8 = 4.4\cdot10^{-4}\ s^{-1}$.

This process increases the amount of dissolved elemental mercury in a droplet hampering further dissolution of gaseous mercury. Hence, the scheme implies negative feedback controlling elemental mercury uptake from the air.

Mercury ion $Hg^{2+}_{(aq)}$ also takes part in a number of reactions leading to the formation of various chloride complexes Hg_nCl_m (R_9). These reversible reactions in the first approximation can be replaced by equilibrium concentrations of free mercury ions and mercury in the aggregate of chloride complexes ($[HgCl^+]$, $[HgCl_2]$, $[HgCl_3^-]$, $[HgCl_4^{2-}]$). The equilibrium ratio of the appropriate mercury concentrations depends upon water content of chloride ion $[Cl^-]$ and is defined as follows [*Lurie*, 1971]:

$$r_1 = \frac{[Hg_nCl_{m(dis)}]}{[Hg^{2+}_{(aq)}]} = \frac{[Cl^-_{(aq)}]}{1.82\cdot10^{-7}} + \frac{[Cl^-_{(aq)}]^2}{6.03\cdot10^{-14}} + \frac{[Cl^-_{(aq)}]^3}{8.51\cdot10^{-15}} + \frac{[Cl^-_{(aq)}]^4}{8.51\cdot10^{-16}}\ . \tag{2.18}$$

The chloride ion concentration in cloud water is taken as $7 \cdot 10^{-5}$ M [*Acker et al.*, 1998]. Sulphite and chloride complexes in the aqueous phase can be adsorbed and desorbed by soot particles (R_{10}, R_{11}). Comparatively fast equilibrium of these two reverse processes can also be described by means of "dissolved-to-adsorbed ratio". Based on the appropriate reaction rates it could be taken equal to 0.2 in both cases [*Petersen et al.,* 1998]:

$$r_2 = \frac{[Hg(SO_3)^{2-}_{2(dis)}]}{[Hg(SO_3)^{2-}_{2(soot)}]} = \frac{[Hg_nCl_{m(dis)}]}{[Hg_nCl_{m(soot)}]} \approx 0.2 \,. \qquad (2.19)$$

Summary of all chemical transformations of mercury included into the model is presented in Table 2.2.

Table 2.2. *Summary of mercury transformations included into the model*

Reactions and equilibriums	*k* or *H*	Units	Reference
$Hg^0_{(gas)} + O_{3(gas)} \rightarrow Hg(II)_{(part)} + products$	$2.1 \cdot 10^{-18} \exp(-1247/T)$	$cm^3/(molec \cdot s)$	*Hall*, 1995
$Hg^0_{(gas)} + {}^{\bullet}OH_{(gas)} \rightarrow Hg(II)_{(part)} + products$	$8.7 \cdot 10^{-14}$	$cm^3/(molec \cdot s)$	*Sommar et al.*, 2001
$Hg^0_{(gas)} + Cl_{2(gas)} \rightarrow Hg(II)_{(gas)}$	$2.6 \cdot 10^{-18}$	$cm^3/(molec \cdot s)$	*Ariya et al.,* 2002
$Hg^0_{(aq)} + O_{3(aq)} \rightarrow Hg^{2+}_{(aq)} + products$	$4.7 \cdot 10^{7}$	$M^{-1}s^{-1}$	*Munthe*, 1992
$Hg^0_{(aq)} + {}^{\bullet}OH_{(aq)} \rightarrow Hg^{2+}_{(aq)} + products$	$2.4 \cdot 10^{9}$	$M^{-1}s^{-1}$	*Gårdfeldt et al.*, 2001
$Hg^0_{(aq)} + Cl(I)_{(aq)} \rightarrow Hg^{2+}_{(aq)} + products$	$2 \cdot 10^{6}$	$M^{-1}s^{-1}$	*Lin and Pehkonen*, 1999
$Hg^{2+}_{(aq)} + 2SO^{2-}_{3(aq)} \rightarrow Hg(SO_3)^{2-}_{2(aq)}$	$1.1 \cdot 10^{-21} [SO_{2(gas)}]^{2} \cdot 10^{4pH}$ *	s^{-1}	*Petersen et al.,* 1998
$Hg(SO_3)^{2-}_{2(aq)} \rightarrow Hg^0_{(aq)} + products$	$4.4 \cdot 10^{-4}$	s^{-1}	*Petersen et al.,* 1998
$Hg_nCl_{m(dis)} \leftrightarrow Hg^{2+}_{(aq)}$	$f([Cl])$ **	1	*Lurie*, 1971
$Hg_nCl_{m(dis)} \leftrightarrow Hg_nCl_{m(soot)}$	0.2	1	*Petersen et al.,* 1998
$Hg(SO_3)^{2-}_{2\,(dis)} \leftrightarrow Hg(SO_3)^{2-}_{2\,(soot)}$	0.2	1	*Petersen et al.,* 1998
$Hg^0_{(gas)} \leftrightarrow Hg^0_{(aq)}$	$1.76 \cdot 10^{-23} T \exp(9.08(T_0/T\text{-}1))$	$M \cdot cm^3/molec$	*Andersson et al.*, 2004
$HgCl_{2(gas)} \leftrightarrow HgCl_{2(aq)}$	$1.75 \cdot 10^{-16} T \exp(18.75(T_0/T\text{-}1))$	$M \cdot cm^3/molec$	*Ryaboshapko et al.*, 2001
$O_{3(gas)} \leftrightarrow O_{3(aq)}$	$1.58 \cdot 10^{-24} T \exp(7.8(T_0/T\text{-}1))$	$M \cdot cm^3/molec$	*Sander*, 1997
${}^{\bullet}OH_{(gas)} \leftrightarrow {}^{\bullet}OH_{(aq)}$	$3.41 \cdot 10^{-21} T \exp(17.72(T_0/T\text{-}1))$	$M \cdot cm^3/molec$	*Jacobson*, 1999
$Cl_{2(gas)} \leftrightarrow Cl(I)_{(aq)}$	$4.48 \cdot 10^{-16}$	$M \cdot cm^3/molec$	*Lin and Pehkonen*, 1999

* - $[SO_{2(gas)}]$ is in ppbv

** - see Eq. (2.18)

As it was mentioned above one can distinguish three groups of mercury compounds being in equilibrium. The first group (*A*) contains elemental mercury in the gaseous and dissolved phase; the second one (*B*) consists of the mercury sulphite complex both dissolved and on soot particles; and the third group (*C*) includes free mercury ions, mercury chloride complexes dissolved and adsorbed by soot particles and gaseous mercury chloride:

$$A = Hg^0_{(gas)} + Hg^0_{(aq)},$$

$$B = Hg(SO_3)^{2-}_{2(dis)} + Hg(SO_3)^{2-}_{2(soot)}, \qquad (2.20)$$

$$C = Hg^{2+}_{(aq)} + Hg_nCl_{m(dis)} + Hg_nCl_{m(soot)} + HgCl_{2(gas)}.$$

According to this simplified scheme and introduced notations mercury transformations in the liquid phase are described by the following system of the first-order differential equations:

$$\begin{cases} \dfrac{d[A]}{dt} = -\alpha(k_4' + k_5' + k_6')[A] + \beta k_8[B], \\ \dfrac{d[B]}{dt} = -\beta k_8[B] + \gamma k_7'[C], \\ \dfrac{d[C]}{dt} = -\gamma k_7'[C] + \alpha(k_4' + k_5' + k_6')[A]. \end{cases} \qquad (2.21)$$

Here $\alpha = H_{Hg}C_w / (\rho_w + H_{Hg}C_w)$ is the fraction of mercury in the *A* group corresponding to the dissolved form; ρ_w is water density; C_w is cloud liquid water content defined as mass of cloud water per unit volume. Parameter $\beta = r_2 / (1 + r_2)$ denotes mercury fraction of the *B* group in the dissolved phase. Value $\gamma = r_2 r_3 / (r_1 r_3 + r_2 r_3 + r_1 r_2)$ is the fraction of mercury in the *C* group corresponding to the mercury ion Hg_{aq}^{2+}. Parameter $r_3 = H_{HgCl2}C_w / (\rho_w + H_{HgCl2}C_w)$ is the fraction of mercury chloride $HgCl_2$ in cloud water. The analytical solution of the equations system with appropriate initial conditions defines mercury evolution in the aqueous phase during one time step.

Mercury depletion events (MDE)

Rapid transformation of elemental mercury to divalent forms with subsequent intensive deposition has been observed in the Arctic during springtime [*Schroeder et al*., 1998; *Berg et al*., 2001; *Lu et al*., 2001; *Lindberg et al*., 2002; *Ebinghaus et al*., 2002]. This phenomenon, which named as *Mercury Depletion Events* (MDE), could be crucial for the Arctic contamination with mercury and adverse impacts on its vulnerable ecosystems. The kinetic mechanism of the phenomenon associated with halogen-related chemistry is not clear understood yet as well as very few measurement data on the reactions kinetics are available. A simplified parameterization of the MDE phenomenon have been developed to assess the overall effect of the phenomenon on mercury depositions in the Arctic. The main assumptions of the parameterization are presented below:

1. We assume that MDE can occur only over open seawater areas, which were previously covered with ice during winter period. We exclude a possibility of penetration of halogen precursors through ice cover. Hence, we think that MDE can take place over coastal zones of the Arctic Ocean. Only those grid cells are taken into account, which cover both land and see.

2. We suppose that the water surface was previously covered with ice if air temperature in a given point was permanently lower than -3°C during wintertime (assumed seawater freezing point). Then in springtime the temperature became higher than 0°C, and ice melting started. Besides, during springtime ice-drift becomes more intensive and areas of open water appear. Conditionally we “switch on” the MDE module if air temperature during previous 24 hours was higher that 0°C. We understand the conventional character of such a “trigger” because open water can appear in reality at low negative temperatures.

3. We assume that total duration of MDE during springtime in any point does not exceed 4 weeks and MDE takes place every day (instantly at noon) during this period. The MDE module can be “switched on” only within the period from April to June.

4. We believe that during the MDE concentration of elemental mercury near the surface layer drops down from its usual level to 0.1 ng/m^3. Oxidation of Hg^0 leads to the formation of RGM (50%) and

Hg_{part} (50%). The oxidized products are partly scavenged from the atmosphere within a given modelling grid cell, partly transported outside it and scavenged later.

5. We accept that the MDE covers the lowest 1-kilometer height layer of the atmosphere. Within this layer the intensity of the phenomenon linearly decreases with height to zero at the top of the layer. Hence, during the MDE elemental mercury has rising profile from 0.1 ng/m^3 at the surface to its usual values at 1 km height. Contrary, oxidized forms have dropping profile from their maximum at the surface to their usual values at 1 km height.

We applied the Arctic definition adopted in the AMAP programme (Fig. 2.3). It covers the terrestrial and marine areas north of the Arctic Circle, north of 62°N in Asia and 60°N in North America, modified to include the marine areas north of the Aleutian chain, Hudson Bay, and parts of the North Atlantic Ocean including the Labrador Sea.

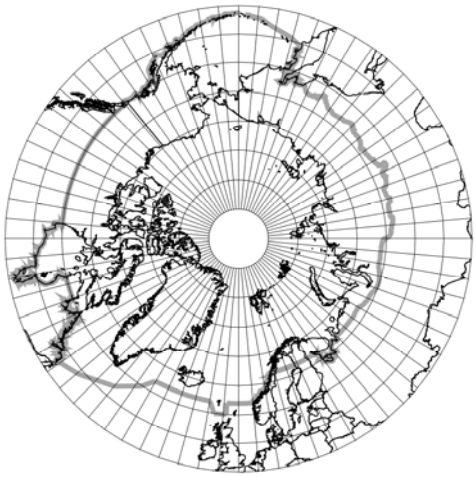

Fig. 2.3. *AMAP Arctic area [AMAP, 1998]*

2.2. Dry deposition

One of the processes accounting for removal of heavy metals from the atmosphere is dry deposition. Heavy metals in aerosol composition or in gaseous form interact with ground surface (buildings, trees, grass, soil, water surface etc.). As a result they stick or react with the surface and are removed from the air. Dry deposition of a substance to a particular surface type i is described by the equation:

$$\frac{\partial q}{\partial t} = -\Lambda^i_{dry} q \ , \tag{2.22}$$

where Λ^i_{dry} is the surface dependent dry deposition coefficient, proportional to dry deposition velocity V^i_d:

$$\Lambda^i_{dry} = \frac{V^i_d}{\Delta\sigma_1}\left|\frac{\partial\sigma}{\partial z}\right|, \ \frac{\partial\sigma}{\partial z} = -\frac{g}{R_a T_a}\left(\sigma_1 + \frac{p_t}{p^*}\right). \tag{2.23}$$

Here $\Delta\sigma_1$ and σ_1 are depth and mid-level of the lowest σ-layer respectively.

The pollutant mixing ratio averaged over a gridcell after the dry deposition is given by:

$$q^{t+\Delta t} = q^t \sum_i f_i \exp(-\Lambda^i_{dry}\Delta t) \tag{2.24}$$

where f_i is area fraction of a surface type i in a gridcell and summing is performed over all surface types in the cell.

Commonly the dry deposition velocity is calculated using the resistance analogy [e.g. *Wesely and Hicks*, 2000]. For gases it has the following form:

$$V_d^i = \frac{1}{R_a + R_b + R_c}\,, \tag{2.25}$$

where R_a is the aerodynamic resistance between a reference height (mid-level of the lowest σ–layer) and the quasi-laminar sub-layer above the surface;

R_b is the quasi-laminar sub-layer resistance;

R_c is the surface resistance to chemical, physical and biological interactions.

Dry deposition velocities of aerosol differ from those of gases (Eq. (2.25)) by absence of the surface resistance and influence of the gravitational sedimentation [*Seinfeld and Pandis*, 1997]:

$$V_d^i = \frac{1}{R_a + R_b + R_a R_b V_g} + V_g\,, \tag{2.26}$$

where V_g is the gravitational sedimentation velocity.

Aerodynamic resistance

The aerodynamic resistance can be approximated from the similarity theory as [*Jacobson*, 1999]:

$$R_a = \frac{1}{k u_*} \int_{z_{0h}}^{z_{ref}-d} \Phi_h \frac{dz}{z}\,, \tag{2.27}$$

where k is the von Kármán constant taken as 0.4;

u_* is the friction velocity;

z_{ref} is the reference height (mid-level of the lowest σ-layer);

d is the displacement height;

z_{oh} is the energy roughness length; and Φ_h is the dimensionless potential temperature gradient.

The friction velocity is given by:

$$u_* = k U_{ref} \left(\int_{z_{0m}}^{z_{ref}-d} \Phi_m \frac{dz}{z} \right)^{-1}\,, \tag{2.28}$$

where U_{ref} is wind velocity at the reference height;

z_{0m} is the roughness length for momentum;

Φ_m is the dimensionless wind shear.

The momentum roughness length z_{0m} for different land cover types along with the displacement heights (Table 2.3). The roughness length for water surfaces is a function of the friction velocity [*Garratt*, 1999].

Table 2.3. *Characteristics of different landcover categories used in the model*

		Land cover category					
		Coniferous forest	Deciduous forest	Low vegetation	Urban	Barren land	Water surface*
z_{0m} (m)	1	0.9	1.05	0.05	1	0.04	f(u*)
	2	0.9	1.05	0.05	1	0.04	f(u*)
	3	0.9	0.95	0.03	1	0.04	f(u*)
	4	0.9	0.55	0.01	1	0.04	f(u*)
	5	0.9	0.75	0.03	1	0.04	f(u*)
d (m)	1	15	15	0.4	-	-	-
	2	15	15	0.4	-	-	-
	3	15	7	0.2	-	-	-
	4	15	7	0	-	-	-
	5	15	10	0.2	-	-	-
H (m)		20	20	0.5	-	-	-

* - function of the friction velocity (see Eq. (2.29))

$$z_{0m} = \alpha_c u_*^2 / g + 0.11\nu / u_* , \tag{2.29}$$

where $\alpha_c \approx 0.016$ is the Charnock constant; and ν is the kinematic viscosity of air.

The energy roughness length is expressed through that of momentum for a wide variety of surfaces [*Garratt*, 1999]:

$$\ln\left(\frac{z_{0m}}{z_{0h}}\right) \approx \begin{cases} 2 & \text{rough surface} \\ k(13.6\,\mathrm{Pr}^{2/3} - 12) & \text{water surface} \end{cases}, \tag{2.30}$$

where $\mathrm{Pr} = \nu\rho\, c_{pm}/\kappa$ is the Prandtl number;

ρ is air density;

c_{pm} is the specific heat of moist air;

κ is the thermal air conductivity.

The integrals of Φ_h and Φ_m in Eqs. (2.27) and (2.28) are calculated as follows [*Jacobson*, 1999]:

$$\int_{z_{0h}}^{z} \Phi_h \frac{dz}{z} = \begin{cases} \mathrm{Pr}_t \ln\dfrac{z}{z_{0h}} + \dfrac{\beta_h}{L}\left(z - z_{0h}\right) & z/L > 0 \quad (\textit{stable}) \\ \mathrm{Pr}_t\left[\ln\dfrac{(1-\gamma_h\, z/L)^{1/2} - 1}{(1-\gamma_h\, z/L)^{1/2} + 1} - \ln\dfrac{(1-\gamma_h\, z_{0h}/L)^{1/2} - 1}{(1-\gamma_h\, z_{0h}/L)^{1/2} + 1}\right] & z/L < 0 \quad (\textit{unstable}) \\ \mathrm{Pr}_t \ln\dfrac{z}{z_{0h}} & z/L = 0 \quad (\textit{neutral}) \end{cases} \tag{2.31}$$

$$\int_{z_{0h}}^{z} \Phi_m \frac{dz}{z} = \begin{cases} \ln\dfrac{z}{z_{0m}} + \dfrac{\beta_m}{L}\left(z - z_{0m}\right) & z/L > 0 \quad (\textit{stable}) \\ \ln\dfrac{(1-\gamma_m\, z/L)^{1/4} - 1}{(1-\gamma_m\, z/L)^{1/4} + 1} - \ln\dfrac{(1-\gamma_m\, z_{0m}/L)^{1/4} - 1}{(1-\gamma_m\, z_{0m}/L)^{1/4} + 1} & \\ \quad + 2\tan^{-1}\left(1-\gamma_m\dfrac{z}{L}\right)^{1/4} - 2\tan^{-1}\left(1-\gamma_m\dfrac{z_{0m}}{L}\right)^{1/4} & z/L > 0 \quad (\textit{unstable}) \\ \ln\dfrac{z}{z_{0m}} & z/L = 0 \quad (\textit{neutral}) \end{cases} \tag{2.32}$$

Here $\mathrm{Pr}_t \approx 0.95$ is the turbulent Prandtl number;

$\beta_h = 7.8$; $\gamma_h = 11.6$; $\beta_m = 6.0$; $\gamma_m = 19.3$;

L is the Monin-Obukhov length.

Gridcell averaged values of the Monin-Obukhov length are supported by the meteorological pre-processor. To obtain values specific for each land cover type we use the following expression for L [*Jacobson*, 1999]:

$$L = -\frac{c_{pd}\rho\theta_v}{kgH_f}u_*^3\,, \tag{2.33}$$

where c_{pd} is the specific heat of dry air;

θ_v is the potential virtual temperature;

H_f is the vertical turbulent sensible-heat flux.

The Eqs. (2.28) and (2.33) are iterated for u_* and L using the cell averaged values for the initial estimate.

Aerosol deposition

Dry deposition velocities of aerosol is described by Eq. (2.26), where the gravitational sedimentation velocity V_g is given as follows:

$$V_g = \frac{d_p^2\rho_p g}{18\eta}G_{cunn}\,. \tag{2.34}$$

Here d_p and ρ_p are the aerosol diameter and density respectively;

G_{cunn} = 1 + Kn (1.249 + 0.42 exp(-0.87 / Kn)) is the Cunningham correction factor [*Jacobson*, 1999];

Kn = 2λ / d_p is the Knudsen number; and λ is the mean free path of air molecules.

In the moist atmospheric air condensation of water vapor on aerosol particles leads to increase of their size. The diameter of an aerosol that is in equilibrium with the air moisture depends upon ambient humidity [*Fitzgerald*, 1975]:

$$d_p = Ad_d^B\ ; \qquad A = 1.2\exp\left(\frac{0.066S}{1.058-S}\right);\quad B = \exp\left(\frac{0.00077S}{1.009-S}\right), \tag{2.35}$$

where d_d is the dry diameter of an aerosol;

S is the air saturation ratio.

In this parameterization we expect that the water absorbing mass fraction of the aerosol is equal to unity.

Vegetated surfaces

The size-segregated approach developed for dry deposition to vegetated surfaces is based on theoretical work [*Slinn*, 1982] and fitted to experimental data. Empirical parameterizations based on extensive field measurements [*Ruijgrok et al.*, 1997; *Wesely et. al.*, 1985] are used for selection of the model parameters. A similar approach is suggested by *L.Zhang et al*. [2001]. Following [*Slinn*, 1982] the deposition velocity is expressed in simplified form:

$$V_d^{veg} = \frac{1}{R_a + R_s} + V_g\,. \tag{2.36}$$

Here R_s is the resistance of the interfacial sub-layer (the layer within and just above the roughness elements) also called as the 'canopy resistance'.

This resistance is calculated as follows:

$$R_s = \frac{U_h}{E u_*^2}, \tag{2.37}$$

where E is the total efficiency of particles collection by the surface;

U_h is the wind velocity at the canopy height H given as:

$$U_h = \frac{u_*}{k} \int_{z_{0m}}^{H-d} \Phi_m \frac{dz}{z}. \tag{2.38}$$

Following *W.G.N.Slinn* [1982] and *L.Zhang et al*. [2001] the collection efficiency has the following form:

$$E = \varepsilon_0 (E_b + E_{in} + E_{im}) r_{off}, \tag{2.39}$$

where E_b, E_{in}, E_{im} are constituents of the collection efficiency from Brownian diffusion, interception and impaction respectively;

r_{off} represents reduction of the efficiency caused by particles bounce-off;

ε_0 is the empirical constant taken from fitting to the experimental data.

The diffusion term is given as [*Slinn*, 1982]:

$$E_b = \mathrm{Sc}^{-2/3}, \tag{2.40}$$

where $\mathrm{Sc} = \nu / D_p$ is the Schmidt number;

D_p is the particle Brownian diffusion coefficient.

We use a generalized form of the impaction term suggested in [*Peters and Eiden*, 1992]:

$$E_{im} = \left(\frac{\mathrm{St}}{\alpha + \mathrm{St}} \right)^{\beta}, \tag{2.41}$$

where $\mathrm{St} = u_* V_g / (g \hat{A})$ is the Stokes number for vegetated surfaces;

$\hat{A}$ is the characteristic collector width given below;

α and β are constants chosen to fit the experimental data.

The interception term is the most uncertain part of the collection efficiency. *W.G.N.Slinn* [1982] parameterized it composing contributions of small (vegetative hairs) and large (grass blades, needles etc.) collectors:

$$E_{in} = F \frac{d_p}{d_p + \check{A}} + (1 - F) \frac{d_p}{d_p + \hat{A}}, \tag{2.42}$$

where $\check{A}$ and $\hat{A}$ are characteristics width of small and large collectors taken as 10 μm and 1 mm respectively;

F and (1-F) are the contributions of these two collector types, where F = 0.01.

The choice of these parameters is arbitrary to some extent since there is no experimental or theoretical data on their values. However, the sensitivity analysis has shown that the interception term is insignificant in comparison with two other terms.

The bounce-off correction factor is taken in the form [*Slinn*, 1982]:

$$r_{off} = \exp(-\gamma\,\mathrm{St}^{\delta}), \tag{2.43}$$

where γ an δ are the fitting constants.

It is assumed that the particles bounce-off takes place from dry surfaces only. The surface is supposed to be dry if no precipitation occurred during current 6-hours meteorological period for grass and during current and previous periods for forest.

Forests

To evaluate the constants of the deposition scheme described above for tall vegetation (forests) the scheme was fitted to empirical parameterization developed by *W.Ruijgrok et al*. [1997]. This parameterization is based on extensive measurements of dry deposition velocities of aerosol particles over needleleaf and some mixed forests. It takes into account dependence of the dry deposition velocity on the friction velocity and relative humidity of the ambient air. Particles of two size ranges are described: fine fraction with mass median diameter (MMD) = 0.6 μm (NH_4, SO_4, NO_3) and coarse fraction with MMD = 5.12 μm (*Na*). Parameters of dry deposition of different particles in the fine fraction vary insignificantly therefore mean values of the coefficients were used. The fitting constants of the dry deposition scheme obtained for forests are presented in Table 2.4.

Table 2.4. *Empirical constants of the dry deposition scheme for vegetated surfaces*

Constant	Forests	Low vegetation
α	1	1
β	0.5	0.5
γ	2	2
δ	0.25	0.25
ε_0	1.4	0.22
Λ	–	100

A comparison of the collection efficiency of the Ruijgrok's parameterization with the model scheme is shown in Figs. 2.4 and 2.5 for particles with d_p = 0.6 μm over a wet surface. As seen both schemes give similar functional dependencies on the ambient air relative humidity and the friction velocity. The model scheme predicts more intensive increase of the collection efficiency for relative humidity close to 100%. Similar results are also obtained for a dry surface and for particles with d_p = 5.12 μm.

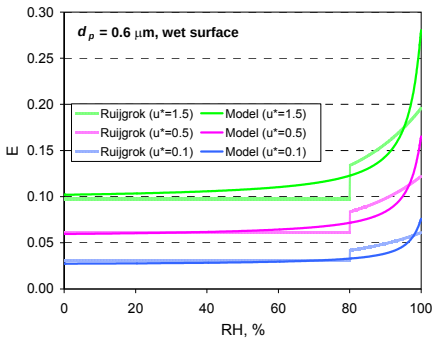

Fig. 2.4. *Collection efficiency over forest (wet surface) as a function of the ambient air relative humidity*

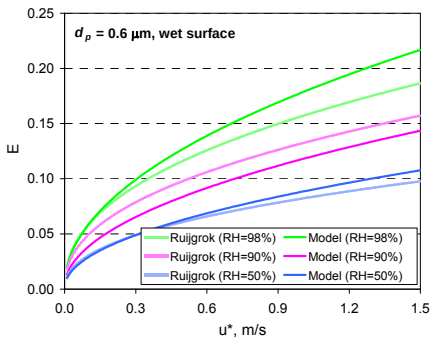

Fig. 2.5. *Collection efficiency over forest (wet surface) as a function of the friction velocity*

Figs. 2.6. and 2.7 shows the dry deposition velocity of aerosol particles over wet and dry forest surface respectively as a function of a particle size. The solid line presents the model scheme, filled squares show the Ruijgrok's parameterization for particles with MMD 0.6 μm and 5.12 μm. As seen from the figures both schemes are in good agreement. The dry deposition velocity of coarse particles over a dry surface is somewhat lower than that over a wet surface because of the bounce-off effect. Besides, the model scheme was tested using the full set of meteorological data. Fig. 2.8 shows the cumulative distribution function of dry deposition velocity over coniferous forests in Europe obtained for the year 2000 by the model scheme and the Ruijgrok's parameterization. As seen from the figure the results practically coincide.

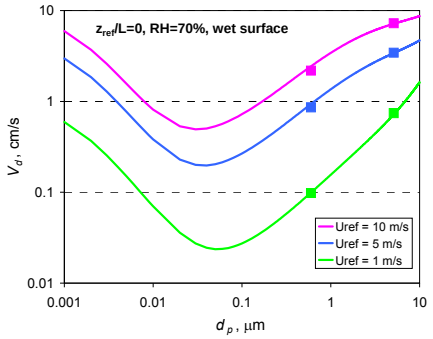

Fig. 2.6. *Dry deposition velocity to forest (wet surface) as a function of a particle size. Solid lines show the model results, the filled squares depict the Ruijgrok's parameterization*

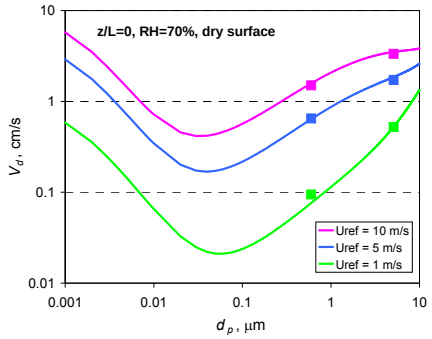

Fig. 2.7. *Dry deposition velocity to forest (dry surface) as a function of particle size. Solid lines show the model results, the filled squares depict the Ruijgrok's parameterization*

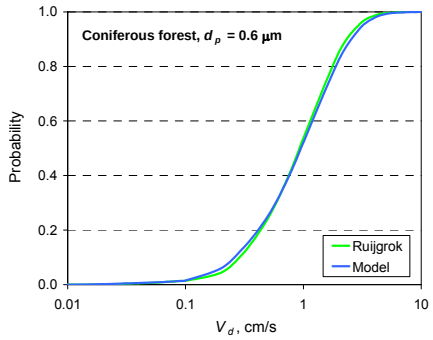

Fig. 2.8. *Cumulative distribution function of dry deposition velocity over coniferous forests in Europe*

Low vegetation

For low vegetation (grassland, crops, wetland etc.) a procedure similar to that described above was used to evaluate the constants of the dry deposition scheme. The scheme was fitted to the empirical parameterization developed from field measurements of particles dry deposition to grass [*Wesely et. al.*, 1985]. The expression for the interfacial sub-layer resistance (2.37) was modified to take into account the atmospheric stability conditions as suggested by *M.L.Wesely et al.* [1985]:

$$R_s = \begin{cases} \dfrac{U_h}{Eu_*^2} & L \geq 0 \\ \dfrac{U_h}{Eu_*^2}\left[1+\left(-\dfrac{\mathrm{A}}{L}\right)^{2/3}\right]^{-1} & L < 0 \end{cases}, \qquad (2.44)$$

where A is a fitting constant.

Values of the fitting constants of the model dry deposition scheme for low vegetation are presented in Table 2.4. Fig. 2.9 shows the comparison of the model scheme for grass with the Wesely's parameterization. As seen the interfacial sub-layer conductivity (reciprocal resistance) given by the Wesely's parameterization lies between those predicted by the model for dry and wet surfaces. The dry deposition velocity over grass (dry surface) as a function of a particle size is illustrated in Fig. 2.10. The cumulative distribution function of dry deposition velocity over grassland in Europe for conditions of 2000 is shown in Fig. 2.11. As seen from the figure the model somewhat underestimates the Wesely's parameterization for small deposition velocities.

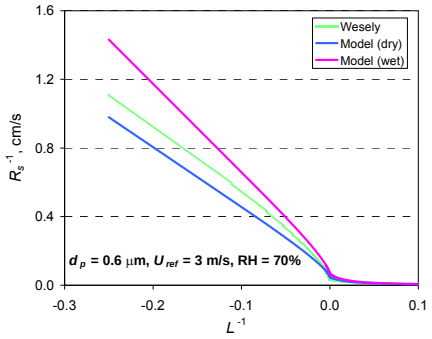

Fig. 2.9. *Reciprocal resistance of the interfacial sub-layer over grass as a function of the stability conditions*

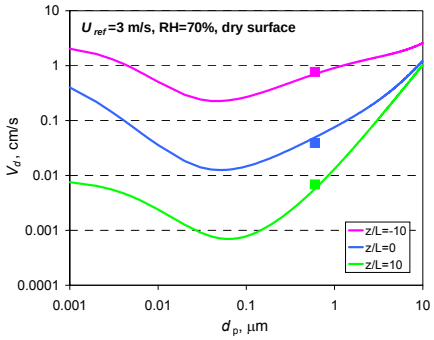

Fig. 2.10.* *Dry deposition velocity to grass (dry surface) as a function of particle size. Solid lines show the model results, the filled squares depict the Ruijgrok's parameterization*

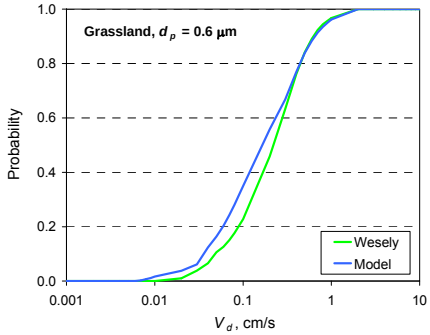

Fig. 2.11. *Cumulative distribution function of dry deposition velocity over grassland in Europe*

Water surface

The parameterization of dry deposition to water surfaces is based on the approach suggested by *R.M. Williams* [1982] taking into account the effects of wave breaking and aerosol washout by seawater spray. A similar approach was developed in [*Pryor et al.*, 1999]. The modified resistance scheme of aerosol particles dry deposition over water surface is illustrated in Fig. 2.12. Following the procedure from [*Williams*, 1982] one can obtain an expression for the dry deposition velocity:

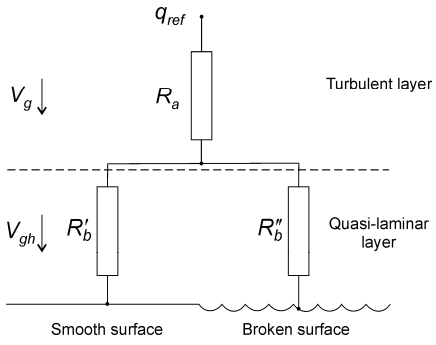

Fig. 2.12. *Resistance scheme of aerosol particles dry deposition over water surface*

$$V_d^{water} = \frac{(1+R_a V_g)(1+R_b V_{gh})}{R_a + R_b + R_a R_b V_{gh}}, \tag{2.45}$$

where V_{gh} is the gravitational sedimentation velocity in the humid quasi-laminar layer near the air-water interface.

The relative air humidity of this layer can be significantly higher that of the turbulent layer. It results in more intensive particle growth. Since due to Raoult's law the relative humidity over salt water cannot exceed 98.3%, the constant value of 98% is accepted in the model for the humid layer. The quasi-laminar layer resistance R_b consists of the resistance over the smooth surface R'_b and the resistance over the broken one R''_b:

$$R_b = \left(\frac{1-\alpha_b}{R'_b} + \frac{\alpha_b}{R''_b} \right). \tag{2.46}$$

Here α_b is the fraction surface area broken due to the wind force [*Wu*, 1979]:

$$\alpha_b = 1.7 \cdot 10^{-6} U_{10}^{3.75}, \tag{2.47}$$

where U_{10} is the wind speed at 10 m height.

The quasi-laminar layer resistance over the smooth surface is determined mostly by the Brownian diffusion and impaction [*Slinn and Slinn*, 1980]:

$$R'_b = \frac{k U_{ref}}{u_*^2} \left(E_b + E_{im} \right)^{-1}, \qquad E_b = \mathrm{Sc}^{-1/2}, \qquad E_{im} = 10^{-3/\mathrm{St}}, \tag{2.48}$$

where the Stokes number for water surfaces is $\mathrm{St} = u_*^2 V_{gh} / (g\nu)$;

the Schmidt number is $\mathrm{Sc} = \nu / D_{ph}$, D_{ph} is the diffusion coefficient in the humid layer.

The broken surface resistance R''_b governed by scavenging of particles due to impaction and coagulation with spray droplets is expected to be quite low. Because of lack of reliable estimates for this resistance a tentative value of 10 s/m [*Williams*, 1982] is used. Fig. 2.13 illustrates the velocity of dry deposition to water surface as a function of particle size for different values of wind speed. The influence of the broken surface resistance on the dry deposition velocity over water surfaces is illustrated in Fig. 2.14. The lowest case corresponds to water surface with no broken area.

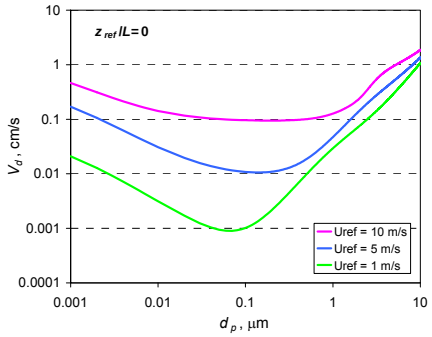

Fig. 2.13. *Dry deposition velocity to water surface as a function of particle size for different values of wind speeds*

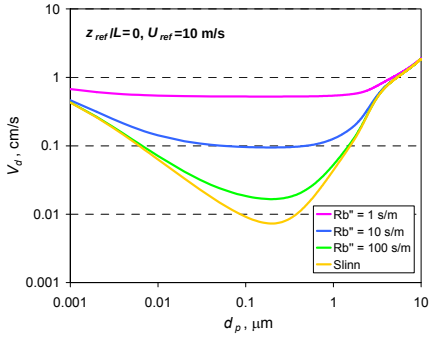

Fig. 2.14. *Dry deposition velocity to water surface as a function of particle size for different values of the broken surface resistance*

Non-vegetated surfaces

The dry deposition to non-vegetated surfaces (deserts, glaciers etc.) is described by Eq. (2.26), where the resistance of the quasi-laminar layer has the following form:

$$R_b = \frac{kU_{ref}}{u_*^2}\left(E_b + E_{im}\right)^{-1} \quad , \qquad E_b = \mathrm{Sc}^{-2/3}, \qquad E_{im} = 10^{-3/\mathrm{St}}. \tag{2.49}$$

The Schmidt and the Stokes numbers are Sc = ν / D_p and St = $u_*^2 V_g$ /($g\nu$) respectively. The particular case of non-vegetated surfaces is urban area characterized by bluff roughness elements. For urban areas we used a different form of the impaction term E_{im} = St^2 / (400 + St^2) [*Giorgi*, 1986].

Fig. 2.15 shows dry deposition velocities of particles with d_p = 0.6 μm to different land cover categories in the EMEP region calculated for meteorological conditions of 2000. As seen the highest deposition velocities correspond to forests (around 1 cm/s), whereas the lowest – to barren land and permanent ice areas (glaciers) (below 0.01 cm/s on average).

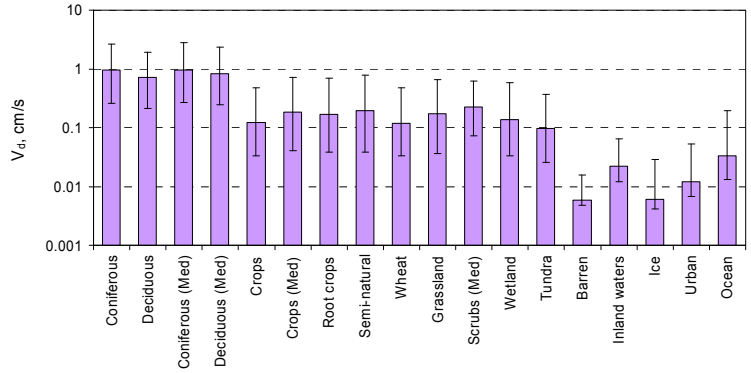

Fig. 2.15. *Dry deposition velocities of particles (d_p = 0.6 μm) to different land cover categories in the EMEP region. Bars show median values of 6-hour averages during 2000. Error bars depict 90%-confidence intervals*

The current version of the model describes particles carrying heavy metal as mono-disperse fraction with appropriate MMD: Pb – 0.55 μm, Cd – 0.84 μm, Hg – 0.61 μm [*Milford and Davidson*, 1985].

Reactive gaseous mercury deposition

The dry deposition of reactive gaseous mercury (RGM) is described by Eq. (2.25). The quasi-laminar resistance is given as follows [*Erisman et al.*, 1994]:

$$R_b = \frac{2}{ku_*}\left(\frac{\mathrm{Sc}}{\mathrm{Pr}}\right)^{2/3}, \tag{2.50}$$

where Schmidt number Sc = ν/ D_g;

D_g is the molecular diffusion coefficient of RGM.

Since solubility of RGM is similar to those of nitric acid vapor [*Petersen et al.*, 1995] the surface resistance R_c is taken to be zero [*Wesely and Hicks*, 2000].

Dry deposition velocities of RGM to different land cover categories in the EMEP region calculated for meteorological conditions of 2000 are shown in Fig. 2.16. The highest deposition velocities are to forests and urban areas (3 cm/s on average), the lowest velocities are to inland waters (0.5 cm/s).

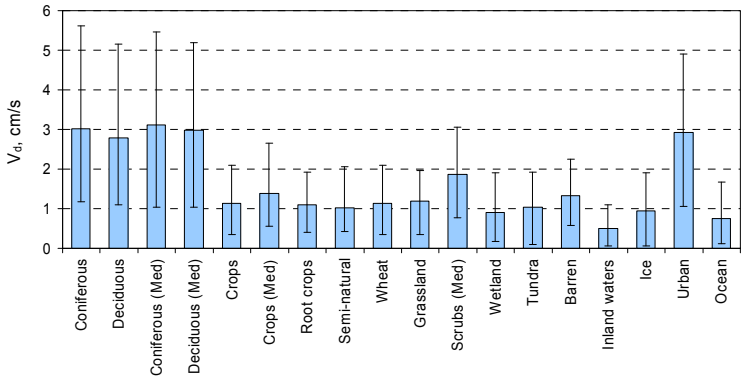

Fig. 2.16. *Dry deposition velocities RGM to different land cover categories in the EMEP region. Bars show median values of 6-hour averages during 2000. Error bars depict 90%-confidence intervals*

Gaseous elemental mercury deposition

Dry deposition of elemental gaseous mercury by various types of underlying surface is not adequately defined yet. Some experts [*US EPA*, 1997] suppose that this type of mercury removal is not an essential sink on a regional and global scale. According to another viewpoint [*Lin and Pehkonen*, 1999] dry uptake of elemental mercury is considered to be the dominating mechanism of mercury removal from the atmosphere. Summarizing available literature data [*Travnikov and Ryaboshapko*, 2002] we adopt the following simplified parameterization of the process. There is no dry uptake of elemental gaseous mercury by water surface and land surface not covered by vegetation. It is also absent during nighttime. Over the vegetated surface during daytime dry deposition velocity is given by:

$$V_d^{veg} = \begin{cases} 0\ , & T_s \le T_0 \\ \mathrm{B}\dfrac{T_s - T_0}{T_1 - T_0}\cos\theta_s\ , & T_0 < T_s \le T_1 \\ \mathrm{B}\cos\theta_s\ , & T_s > T_1 \end{cases}\ , \qquad (2.51)$$

where T_s is the surface temperature, T_0 = 273K and T_1 = 293K;

B is equal to 0.03 cm/s for forests and 0.01 cm/s for low vegetation;

θ_s is the solar zenith angle calculated according to [*Jacobson*, 1999].

Fog deposition

Mercury aqueous forms in fog droplets can be removed from the atmosphere through the fog interaction with the ground surface. The fog dry deposition is described in the model similar to that of aerosol particles with mass median diameter 20 μm.

2.3. Wet deposition

Another important process accounting for heavy metal removal from the atmosphere is wet deposition. Particle-bound heavy metals as well as soluble gaseous species are scavenged form the atmospheric air both in cloud environment and below the cloud base. Wet deposition of a substance is described by the equation:

$$\frac{\partial q}{\partial t} = -\Lambda_{wet} q \,, \tag{2.52}$$

where Λ_{wet} is the wet deposition coefficient depending on the local precipitation rate R_p.

We used the following expression for the wet deposition coefficient based on measurement data:

$$\Lambda_{wet} = A\left(\frac{R_p}{F}\right)^B . \tag{2.53}$$

Here A and B are empirical constants;
F is a fraction of the grid cell where precipitation occurs.

We adopt $F = 0.3$ for convective precipitation and $F = 1$ for stratiform one following the discussion in [*Walton et al.*, 1988]. The pollutant mixing ratio averaged over a grid cell after the wet deposition is given by:

$$q^{t+\Delta t} = q^t\left[1 - F\left(1 - \exp(-\Lambda_{wet}\Delta t)\right)\right] \tag{2.54}$$

The model distinguishes in-cloud scavenging (ICS) and below-cloud scavenging (BCS).

In-cloud scavenging

In the cloud environment soluble gases dissolve very quickly in the cloud water coming into the equilibrium with the solution, while aerosol particles are taken up by cloud droplets due to nucleation or impaction scavenging. Further collection of cloud drops by falling raindrops leads to removal of the pollutants from the atmosphere. The efficiency of aerosol scavenging by cloud droplets depends upon the cloud liquid water content (LWC). Fig. 2.17 shows the scavenging efficiencies (i.e. the ratio of aerosol concentration in cloud water to its concentration in interstitial air) for *Pb* and SO_4 measured by *A.Kasper et al.* [1998] as a function of the LWC. For values of the LWC higher than 0.5 g/m^3 the efficiency commonly exceeds 0.8 and it drops down when the LWC become lower 0.1 g/m^3. For the approximation of the dependence we used the following expression:

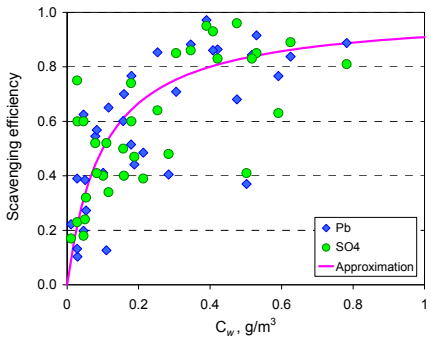

Fig. 2.17. *Efficiency of aerosol scavenging by cloud droplets for lead and sulphate as a function of cloud LWC. Symbols show measurement data from [Kasper et al., 1998], solid line – approximation*

$$\varepsilon_w = \frac{C_w}{C_w + \varepsilon_{w0}} , \tag{2.55}$$

where the liquid water content C_w is in g/m^3;
constant ε_{w0} is equal to 0.1.

Thus for the in-cloud scavenging Eq. (2.54) is transformed to:

$$q^{t+\Delta t} = q^t\left[1-\varepsilon_w F\left(1-\exp(-\Lambda_{wet}\Delta t)\right)\right], \tag{2.56}$$

where the scavenging efficiency ε_w for aerosol particles is defined by Eq. (2.55) and $\varepsilon_w = 1$ for aqueous forms.

Parameters of the wet deposition coefficient expression (2.53) for in-cloud scavenging estimated or measured by different authors are presented in Table 2.5. Taking into account values in the table and sensitivity calculations we adopted the parameters: $A_{in} = 3\cdot10^{-4}$, $B_{in} = 0.8$ for all heavy metal species incorporated into cloud water.

Table 2.5. *Parameters of the wet deposition coefficient for in-cloud scavenging (A_{in} is in units of s^{-1}; R_p is in units of mm/h)*

Reference	A_{in} ($\times10^{-4}$)	B_{in}	Method
Scott, 1982	3.5	0.78	Calculation
Penner et al., 1991	1.31	1	Estimation *
Brandt et al., 2002	3.36	0.79	Estimation
Andrinache, 2004	3.97	0.81	Measurement **

* - ICS plus BCS of HNO_3; ** - Calculations based on measured ICS plus BCS

Below-cloud scavenging

Below the cloud base aerosol particles and soluble gases are collected by falling raindrops and removed from the air. The model parameterization of below-cloud scavenging is mostly based on empirical estimates. Table 2.6 presents parameters of the wet deposition coefficient for BCS of particles and highly soluble gases based on measurement data. As seen different estimates of A_{below} varies roughly from $0.5\cdot10^{-4}$ to $2.5\cdot10^{-4}$ s^{-1}; and B_{below} is within the range 0.62-0.79. There is no principal difference between values of the parameters for sub-micron aerosol particles and highly soluble gases. Basing on the data from the table and the sensitivity runs we adopted the values $A_{below} = 1\cdot10^{-4}$ and $B_{below} = 0.7$ both particle-bound heavy metals and highly soluble gaseous species (RGM).

Table 2.6. *Parameters of the wet deposition coefficient for below-cloud scavenging (A_{below} is in units of s^{-1}; R_p is in units of mm/h)*

Reference	A_{below} ($\times10^{-4}$)	B_{below}	Method
Ragland and Wilkening, 1983	1.22	0.63	Estimation
Barries, 1985	1	0.67	Measurement
Jylhä, 1991	1	0.64	Measurement
Asman, 1995	0.52-0.99	0.62	Calculation *
Okita et al., 1996	1.38	0.74	Measurement
Brandt et al., 2002	0.84	0.79	Estimation
Andrinache, 2003	0.67 – 2.44	0.7	Calculation **

* - for highly soluble gases; ** - theoretical calculations based on measured aerosol size spectra

2.4. Boundary and initial conditions

The model computation domain has two boundaries: upper and equatorial. Long residence time of mercury in the atmosphere requires setting appropriate initial and boundary conditions to take into account mercury contained in the computation domain before the computations and the input fluxes of mercury through the boundaries.

According to the numerous measurements carried out for last decades [e.g. see *R.Ebinghaus et al.*, 1999] elemental mercury Hg^0 is more or less uniformly distributed over the Northern Hemisphere (background concentrations are around 1.7 ng/m^3). Vertical distribution of Hg^0 is also rather uniform [*Banic et al.*, 1999]. Therefore we prescribed uniform distribution of elemental mercury concentration at the upper boundary – 0.185 pptv (corresponding to about 1.5 ng/m^3 at 1 atm and 20°C). On the other hand, some gradient of total gaseous mercury (TGM) was observed over the ocean between the Northern and Southern Hemispheres [e.g. see *Banic et al.*, 1999]. According to *R.Ebinghaus et al.* [2001] mean concentrations of TGM over the Northern and Southern Hemispheres are 1.7 and 1.3 ng/m^3 respectively. Elemental mercury makes up the main part of TGM. Summarizing the measurement data from [*Slemr*, 1996] we set the gradient of Hg^0 to 0.05 ng/m^3/degree at the equatorial boundary. Since the residence time of other mercury species in the atmosphere is considerably shorter we neglected their input through the boundaries. Currently, only atmospheric module is adequately developed for the mercury transport description. Therefore, the lower boundary at the Earth surface is closed. The mercury fluxes through the lower boundary are indirectly considered by deposition and "natural emission and re-emission" processes.

To fill up the model domain with mercury from anthropogenic sources of different regions and continents (it is necessary for the inter-continental transport assessment) we performed a computation run for the period of one year without any boundary and initial conditions. Then we used the obtained concentrations of mercury species as initial conditions for the regular computation run. Besides, the contribution of different sources to mercury incoming through the upper boundary is assumed to be the same as at the highest atmospheric layer.

2.5. Input information

The MSCE-HM-Hem model input information includes emission data, meteorological and geophysical information, and chemical reactants data. Meteorological data and land cover information are described in Annex C.

Emissions

Anthropogenic emission of mercury in the Northern Hemisphere was evaluated basing on the global emission inventory for 1995 published by *J.Pacyna et al.* [2003]. According to these data, anthropogenic emission of mercury in the Northern Hemisphere is about 1900 t/y. Available data on the natural emission of mercury are rather uncertain. To take into account natural emission of mercury we used global estimates by *C.H.Lamborg et al.* [2002]. Spatial distribution of natural emission fluxes (including re-emission) was obtained by scattering the total value throughout the globe depending on mercury content in soils and the surface temperature. The total natural emission and re-emission of mercury in the Northern Hemisphere is estimated as much as 1600 t/y. More details in the emission data used in the hemispheric model can be found in [*Travnikov and Ryaboshapko*, 2002; *Dutchak et al*., 2003].

Chemical reactants data

Mercury species take part in chemical reactions of oxidation and reduction both in the gaseous and aqueous phase. To describe chemical transformations one should know spatial and temporal distribution of the reactant concentrations (such as ozone, sulfur dioxide and hydroperoxy radical) in the atmosphere.

Global monthly mean data on ozone, SO_2 concentration in the atmosphere were kindly provided by Dr. Malcolm Ko [*Wang et al.*, 1998; *Chin M. et al.*, 1996]. For hydroperoxy radical (HO_2) we used monthly mean data from Dr. Clarissa Spivakovsky [*Spivakovsky et al.*, 2000]. The original data were interpolated to the model grid for the Northern Hemisphere. In order to take into account diurnal cycle of OH radical we assume zero concentration at night and concentrations proportional to the cosine of the solar zenith angle during daytime. Besides, air concentrations of OH were decreased by a factor of 10 in the cloud environment and below clouds to account for reduction of its photochemical activity [*Seigneur et al*., 2001].

The model chemistry also considers oxidation of elemental mercury by chlorine both in gaseous and aqueous phase. To date, the direct production of Cl_2 is very poorly characterized. As it is mentioned in [*Keene et al*., 1999] sea-salt aerosol is the major source of reactive Cl gases (particularly Cl_2) in the global troposphere. Following *C.Seigneur et al.* [2001] we adopt air concentration of molecular chlorine in the lowest model layer over the ocean to be 100 ppt at night and 10 ppt during daytime and zero concentration over land.

3. POP MODEL

The model considers main environmental compartments (atmosphere, soil, seawater, vegetation) and includes basic processes describing POP emission, long-range transport, deposition, degradation, and gaseous exchange between the atmosphere and the underlying surface and POP behaviour in the environmental compartments (Fig. 3.1).

The hemispheric model is used for calculations of POP transport and accumulation on hemispheric scale, for evaluation of pollution of European region by remote sources, for evaluation of intercontinental transport, for assessing of pollution of remote regions like, for example, the Arctic region.

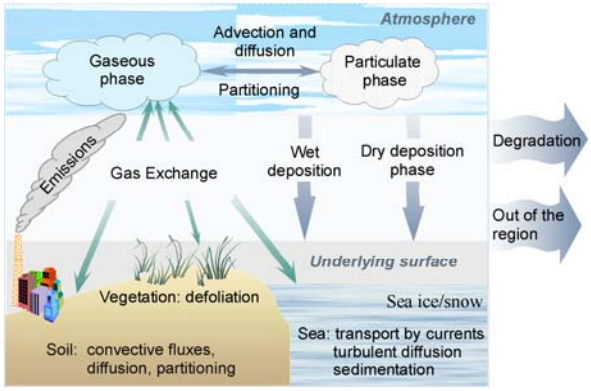

Fig. 3.1. *The scheme of processes included into the MSCE-POP-Hem model*

Compartments and basic processes

Current version of the model considers partitioning of POPs between the following environmental compartments: the atmosphere, soil, seawater, vegetation, and forest litter (Fig. 3.1). Selection of compartments and processes is based on current understanding of their importance with regard to the description of POP dispersion and accumulation in the environment.

The following processes affecting the long-range transport of POPs are included in the model:

Atmosphere:

- advective transport and turbulent diffusion;
- partitioning between the gaseous and particulate phase;
- wet and dry deposition of POP in particulate and gaseous phase to the underlying surface;
- degradation.

Vegetation:

- gaseous exchange with the atmosphere;
- degradation;
- defoliation and transfer to upper soil layer.

Soil:

- gaseous exchange with the atmosphere;
- partitioning in soil between the gaseous, solid and liquid phases;
- vertical transport due to convective water fluxes, diffusion, and bioturbation;
- degradation.

Seawater:

- gaseous exchange with the atmosphere;
- advective transport by sea currents and turbulent diffusion;
- partitioning between the dissolved and particulate phase;
- sedimentation;
- degradation.

3.1. The atmospheric compartment

The atmospheric part of MSCE-POP-Hem model domain is defined similar to MSCE-HM-Hem model (Section 1.1). The processes included are the following: advection, turbulent diffusion, partitioning of a pollutant between the gaseous and particulate phase, wet and dry deposition of both phases to the underlying surface, and degradation. MSCE-POP-Hem model shares the same description of advective transport and turbulent diffusion of pollutants within the atmosphere as the MSC-E-HM-Hem model. The description of dry and wet deposition of POPs in particulate phase within the MSCE-POP-Hem model is in general similar to the approach used in MSCE-HM-Hem model (Section 2.2 and 2.3).

Gas/particle partitioning

Characterization of POP partitioning between the gaseous and particulate phase is performed using the Junge-Pankow model [*Junge*, 1977; *Pankow*, 1987] based on subcooled liquid vapour pressure p_{OL} (Pa). According to this model the POP fraction φ adsorbed on atmospheric aerosol particles equals to:

$$\varphi = \frac{c \cdot \theta}{p_{OL} + c \cdot \theta}, \tag{3.1}$$

where c is the constant dependant on the thermodynamic parameters of the adsorption process and on the properties of aerosol particle surface; it is assumed c = 0.17 Pa·m [*Junge*, 1977] for background aerosol;

θ is the specific surface of aerosol particles, m^2/m^3.

The spatial distribution and temporal variations of aerosol specific surface were kindly provided by Dr. Sunling Gong (Canada). Parameter p_{OL} is pollutant-dependent and depends greatly on temperature. Coefficients of p_{OL} temperature dependencies used in model parameterisation for the selected POPs are presented in Annex B (B.1. “Subcooled liquid vapour pressure”).

Dry deposition of the particulate phase

Dry deposition flux of the particulate phase F^P_{dry} ($ng/m^2/s$) is a product of dry deposition velocity V_d (m/s) and air concentration C_P (ng/m^3) of a pollutant in the particulate phase taken at an air reference level coinciding with the middle of the lowest atmospheric layer:

$$F^P_{dry} = V_d C_P, \tag{3.2}$$

The dry deposition velocity V_d from the reference level z_a is calculated according to the resistance analogy using the equation:

$$V_d = \left(R_a + 1/V_d^{surf}\right)^{-1}, \tag{3.3}$$

where R_a is the aerodynamic resistance for turbulent transport of a pollutant from z_a to z_b, s/m;

z_b is the height of the surface layer, m;

V_d^{surf} is the surface dry deposition velocity from the surface layer height z_b.

Aerodynamic resistance R_a is calculated using the following equation (See [*Tsyro and Erdman*, 2000]):

$$R_a = \frac{0.74}{\kappa u_*}\left[\ln\left(\frac{z_a}{z_b}\right) - \psi_h\left(\frac{z_a}{L}\right) + \psi_h\left(\frac{z_b}{L}\right)\right], \tag{3.4}$$

where κ = 0.4 is the van Karman constant;

u_* is the friction velocity, m/s;

ψ_h is the similarity function for heat.

The values of deposition velocity to the underlying surface V_d^{surf} are calculated in different way for different types of underlying surface, namely, for sea, soil and forest separately.

<u>*Sea*</u>. Velocity of dry deposition to sea (V_d^{sea}, z_b = 10 m) is calculated using the equation:

$$V_d^{sea} = A_{sea}u_*^2 + B_{sea}, \tag{3.5}$$

where A_{sea} and B_{sea} are the constants dependant on the effective diameter of particle-carriers of a considered pollutant;

u_* is the friction velocity, m/s;

(regression equation obtained by *M.Pekar* [1996] from [*Lindfors et al*., 1991] data).

<u>*Soil*</u>. Velocity of dry deposition over land (V_d^{land}, z_b = 1 m) is given as follows:

$$V_d^{land} = \left(A_{soil}u_*^2 + B_{soil}\right)z_0^{C_{soil}}, \tag{3.6}$$

where as above u_* is the friction velocity;

z_0 is the surface roughness, mm;

A_{soil}, B_{soil}, C_{soil} are the constants dependant on effective diameters of particle-carriers of considered POP;

(regression equation obtained by *M.Pekar* [1996] from [*Sehmel*, 1980] data).

<u>*Forest*</u>. Velocity of dry deposition to a forest (V_d^{forest}, z_b = 20 m), (adapted by *L.Erdman* [*Tsyro and Erdman*, 2000] from [*Ruijgrok et al.,* 1997]):

$$V_d^{forest} = E\frac{u_*^2}{u_h}, \tag{3.7}$$

where u_h is the wind speed at forest height $h = z_b$;

$$E = \alpha\, u_*^{\beta}\left(1+\gamma \exp\left(\left(RH-80\right)/20\right)\right) \quad (3.8)$$

is the total collection efficiency for particles within the forest canopy and α, β and γ are the experimental coefficients, depending on effective diameters of particles-carriers.

In the current model version it is assumed that the relative humidity of air (*RH*) is 80% of the average. Wind speed at forest height u_h (m/s) is calculated using the following equation:

$$u_h = \frac{u_*}{\kappa}\left[\ln\left(\frac{z_b - d_0}{z_0}\right) - \psi_m\left(\frac{z_b - d_0}{L}\right) + \psi_m\left(\frac{z_0}{L}\right)\right], \quad (3.9)$$

where κ = 0.4 is the van Karman constant;
d_0 = 15 m is zero-plane displacement;
z_0 = 2 m is the roughness length;
L is the Monin-Obukhov parameter;
ψ_m is the universal correction function for the atmospheric stability for momentum.

Two types of forest are distinguished in the model: deciduous forest and coniferous forest. It is assumed that dry deposition velocities to forest are calculated by Eq. (3.7) for deciduous forests during the vegetative period (from May to September). For the remaining time, dry deposition velocities for areas covered by deciduous forests are calculated as for soil Eq. (3.6). For areas covered by coniferous forests dry deposition velocities are calculated by Eq. (3.7) throughout the year.

The amount of pollutant deposited to forest is distributed between soil and leaves/needles in accordance with the distribution coefficient K_{vs}, which is pollutant-dependent.

The coefficients A_{sea}, B_{sea}, A_{soil}, B_{soil}, C_{soil}, α, β and γ, as well as the distribution coefficient K_{vs} between soil and leaves/needles for forests, are a part of model parameterization for a particular chemical. Their values for the selected POPs are given in the Annex B. (B.3. “Dry deposition velocities over land, sea, and forest”).

Wet deposition

Wet deposition of POPs in gaseous and particulate phase is distinguished in the MSCE-POP-Hem model. Making an assumption that the pollutant does not redistribute between dissolved and particulate phase within a raindrop, total dimensionless ratio W_T for a substance washout with precipitation is determined by the following equation:

$$W_T = W_g\,(1 - \varphi) + W_P\,\varphi, \quad (3.10)$$

where W_g is the washout ratio of the POP gaseous phase;
W_P is the washout ratio of a substance associated with aerosol particles;
φ is the substance fraction associated with aerosol particles in the atmosphere.

For the description of gaseous phase scavenging with precipitation, the instantaneous equilibrium between the gaseous phase in the air and the dissolved phase in precipitation is assumed:

$$C_w^d = W_g\, C_a^g, \quad (3.11)$$

where C_w^d is the dissolved phase concentration in precipitation water, ng/m^3;
C_a^g is the gaseous phase concentration in air, ng/m^3;
$W_g = 1/K'_H$ is the dimensionless washout ratio for the gaseous phase;
K'_H is the dimensionless Henry’s law constant.

The Henry's law constant (K'_H) is temperature dependant. Temperature dependence and its parameters for selected POPs can be found in Annex B (B.2. "Henry`s law constant and air/water partition coefficient").

For the description of particle bound phase scavenging with precipitation, the washout ratio determined experimentally is used:

$$C_w^s = W_p C_a^p , \tag{3.12}$$

where C_a^p is the particle bound phase concentration in the air surface layer, ng/m^3;
C_w^s is the suspended phase concentration in precipitation water, ng/m^3;
W_p is the dimensionless washout ratio for the particulate phase.

The W_p is a parameter specific for each POP which values can be found in Annex B (B.4. "Washout ratio").

Degradation in air

Degradation process of POPs in the atmosphere is considered as the gas-phase reaction of pollutants with hydroxyl radicals and all other reactions are neglected. The degradation process in the atmosphere is described by the equation of the second order:

$$\frac{dC}{dt} = -k_{air} \cdot C \cdot [\mathrm{OH}], \tag{3.13}$$

where C is the pollutant concentration in air (gaseous phase), ng/m^3;
[OH] is the concentration of OH radical, molec/cm^3;
k_{air} is the degradation rate constant for air, cm^3/(molec·s).

In the MSCE-POP-Hem model for some of considered POPs the degradation rate constant due to reaction with OH-radical in the atmosphere is taken to be temperature dependent. Temperature dependence of degradation rate constant of the gas-phase reaction with OH-radical is described using Arrenius equation (see Annex B, B.5 "Degradation rate constants in environment media"). OH radical concentrations in the atmosphere vary substantially depending on many factors (latitude, cloudiness, day time, season, some atmospheric properties, etc.). Data on temporal and spatial variations of OH radical concentrations are described in Section 2.5. "Chemical reactants data".

The process of degradation of POPs associated with particles is not included in the model due to lack of information on this topic.

Gaseous exchange with underlying surface

The gaseous exchange of POPs between the atmosphere and underlying surface (soil, vegetation, and seawater) is described on the basis of the resistance analogy. Description of this process is given below in sections devoted to corresponding media, namely, soil, vegetation, and seawater.

3.2. Soil compartment

The soil module is based on the model developed by *C.M.J. Jacobs and W.A.J. van Pul* [1996]. The soil compartment is represented by upper 20 cm soil layer which is separated into seven horizontal sub-layers of different thickness, namely, Δz_i = 0.1, 0.3, 0.6, 1, 2, 5 and 11 cm.

In the current version of the model the following processes are included: partitioning of the pollutant between various phases in soil, vertical transport due to diffusion and convective water fluxes, bioturbation, gaseous exchange with the atmosphere, and the degradation.

Partitioning in soil

Several phases of POPs within the soil are considered in the model: gaseous phase, dissolved phase, phase sorbed on the dissolved organic carbon, and phase sorbed on organic carbon within the solid soil fraction (Fig. 3.3). To take into account the dynamic character of the redistribution between POP sorbed on solid organic carbon and other POP phases in soil, total content of solid organic carbon (OC) was split into two separate fractions: easily accessible and potentially accessible [*Vassilyeva and Shatalov,* 2002]. It is assumed that the equilibrium between all POP phases except sorbed on potentially accessible soil OC fraction is established instantaneously.

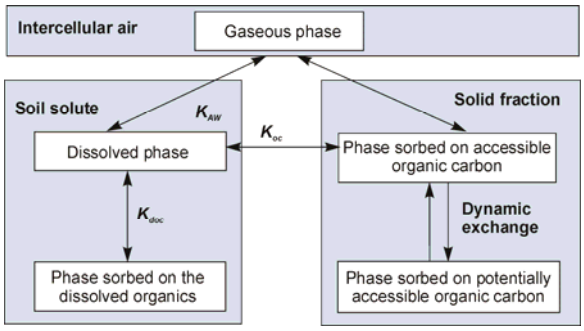

Fig. 3.3. *POP fractions in soil, exchange processes and partitioning coefficients*

The process of partitioning between these phases is governed by the following three partitioning coefficients:

- Air/water partitioning coefficient ($K_{AW,}$ dimensionless):

$$K_{AW} = \frac{K_H}{RT} \tag{3.14}$$

where K_H is the air-water Henry's law constant, Pa·m^3/mol;
T is soil temperature, K;
R = 8.314 J/(mol·K) is the universal gas constant.

- Organic carbon/water partitioning coefficient K_{oc}, m^3/kg.
- Dissolved organic carbon/water partitioning coefficient K_{doc}, dm^3/kg.

For the Henry's law constant in the dimensionless form (K'_H), temperature dependence determined by the Eq. (B.3) (Annex B) is assumed, where coefficients K_{H0} and a_H are pollutant-dependant.

The other two partitioning coefficients are calculated via the octanol/water partitioning coefficient K_{OW} of a pollutant in question by the following regression equations:

$$K_{OC} = 0.41\ K_{OW} \quad [\textit{Karikhoff,}\ 1981] \tag{3.15}$$

and $\log K_{doc} = 0.98 \log K_{OW} - 0.39$ for PAHs (3.16)

$\log K_{doc} = 0.93 \log K_{OW} - 0.54$ for PCBs (3.17)

[*Poershman and Kopinke*, 2001].

The latter relation obtained for a number of POPs with wide range of K_{OW} can also be used for other POPs (PCDD/Fs, HCB, γ-HCH) [*Vassilyeva and Shatalov*, 2002]. Values of K_{OW} and K_{OC} used in model parameterization are given in Annex B (B.6 "Octanol-water partition coefficient", B.7 "Organic carbon-water partition coefficient").

Following [*Jacobs and van Pul,* 1996], we express total POP concentration in soil C_T (ng/m^3) via concentrations C_s (ng/kg), C_g (ng/m^3), C_d (ng/m^3) and C_{doc} (ng/m^3) of solid, gaseous, dissolved and sorbed on dissolved organics fraction by the equation:

$$C_T = \rho_s C_s + \alpha_w (C_d + C_{doc}) + \alpha_a C_g \,, \tag{3.18}$$

where ρ_s is the bulk density of solid soil material, kg/m^3;

α_w is the volumetric water content of the soil;

α_a is the volumetric air content of the soil.

Relations between concentrations in different POP phases in soil are as follows:

$$C_g = K_{aw}\, C_d, \tag{3.19a}$$

$$C_{doc} = c_{doc}\, K_{doc}\, C_d, \tag{3.19b}$$

$$C_s = f_{oc}\, K_{oc}\, C_d, \tag{3.19c}$$

where f_{oc} is the fraction of organic carbon in soil,

c_{doc} is the concentration of dissolved organic carbon in soil solute (mobile fraction, kg/L).

The fraction f_{oc} of organic carbon varies widely depending on soil type (from 0.1 to 30% in Europe). The value of c_{doc} was chosen for calculations using the assumption that the fraction f_{doc} of soil organic carbon contained in mobile soil solute is about 0.5% of total organic carbon content in soil. This leads to the dissolved organic matter concentration in soil solute of about 170 mg/L at fraction f_{oc} of soil organic carbon equal to 5%. This value agree with that obtained by measurements (see [*Vassilyeva and Shatalov*, 2002]).

From formulas (3.18), (3.19 a-c) we obtain:

$$C_T = R_l\, C_l = R_s\, C_s = R_g\, C_g, \tag{3.20}$$

where $C_l = C_d + C_{doc} = C_d\,(1 + c_{doc}\, K_{doc})$ is the POP concentration in soil solute, and soil partitioning coefficients R_l, R_s and R_g are calculated by:

$$R_l = \alpha_w + (\rho_s f_{oc} K_{oc} + \alpha_a K_{aw})/(1 + c_{doc} K_{doc}) \,, \tag{3.21a}$$

$$R_s = R_l (1 + c_{doc} K_{doc})/(f_{oc} K_{oc}), \tag{3.21b}$$

$$R_g = R_l (1 + c_{doc} K_{doc})/K_{aw} \,. \tag{3.21c}$$

The exchange between a pollutant sorbed on easily accessible (C_0) and on potentially accessible (C_1) solid OC fractions is assumed to be a process of first order:

$$\frac{dC_0}{dt} = k(C_1 + C_0)$$
$$\frac{dC_1}{dt} = k(C_0 + C_1) \qquad (3.22)$$

where mass transfer coefficient k is chosen in such a way that the characteristic time for the exchange process equals to 1 year. The fraction f_{acc} of easily accessible fraction was assumed to be 30%.

Vertical transport in soil and exchange with the atmosphere

The migration of a pollutant over the vertical profile in soil is assumed to be due to diffusion and transport with the convective water flux J_w (equal to mean annual precipitation intensity h_p, m/c). The corresponding equation is:

$$\frac{\partial C_T}{\partial t} = \frac{\partial}{\partial z}\left(D_E \frac{\partial C_T}{\partial z} - V_E C_T \right). \qquad (3.23)$$

In the latter formula the effective diffusion coefficient D_E is given by:

$$D_E = \frac{\xi_g D_a}{R_g} + \frac{\xi_l D_w}{R_l} + D_b. \qquad (3.24)$$

where ξ_g and ξ_l are gas and liquid tortuosity factors;

$\xi_g = a_a^{10/3} / \phi^2$; $\xi_l = a_w^{10/3} / \phi^2$;

ϕ is the porosiry of the soil;

D_a and D_w are molecular diffusion coefficients in air and water;

D_b is bioturbation coefficient, $D_b = 6 \cdot 10^{-12}$ m^2/s [*McLachlan et al.,* 2002].

Bioturbation in the description of POP behavior in soil is treated as additional diffusion process and is based on the paper [*McLachlan et al.,* 2002].

The effective solute velocity V_E is defined as:

$$V_E = J_W / R_l \qquad (3.25)$$

At this stage the convective water flux J_w is assumed to be the same as the precipitation rate. Dynamic character of convective water flux will be taken into account later. In current version of MSCE-POP-Hem model the description of vertical transport of POPs in soil is rather simplified. This approach is used since the model is aimed at calculation of monthly and annual averages of POP concentrations and fluxes. For the description of POP vertical transport with upward water fluxes it is supposed that during some period T_{inv} (inverse flux period) after each precipitation event an upward water flux takes place. This flux is supposed to be constant in time. Its value is chosen in such a way that the amount of water transported by this flux to soil surface during the inverse flux period constitutes certain fraction f_{inv} of the amount fallen down during the precipitation event. The parameter f_{inv} is chosen to be 0.6 (60%) since the fraction of evaporated water from land is estimated as 60% from total precipitation amount on the average over Europe [*Atmosphere Handbook*, 1991].

To complete the description of POP vertical transport in soil, it is necessary to write down the expression of fluxes through upper and lower boundaries of the soil calculation domain.

The flux F_{as} at the atmosphere/soil interface is given by the following equation:

$$F_{as} = \frac{C_a - C_T / K_{as}}{R_a + R_b + R_s}, \tag{3.26}$$

where C_a is air concentration;

K_{as} is effective air/soil distribution coefficient.

This parameterization is based on the resistance analogy. The gaseous flux of POP from the atmosphere to the soil is driven by the difference between atmospheric gas concentration C_a at the air reference level z_a (equal to half the height of the lowest model atmospheric layer) and gaseous phase concentration C_T in soil at the reference level z_s=Δz_1/2 (Δz_1 – is the upper soil layer thickness). In the course of pollutant transport from the air reference level to the soil reference level it overcomes three resistances (see Fig. 3.4).

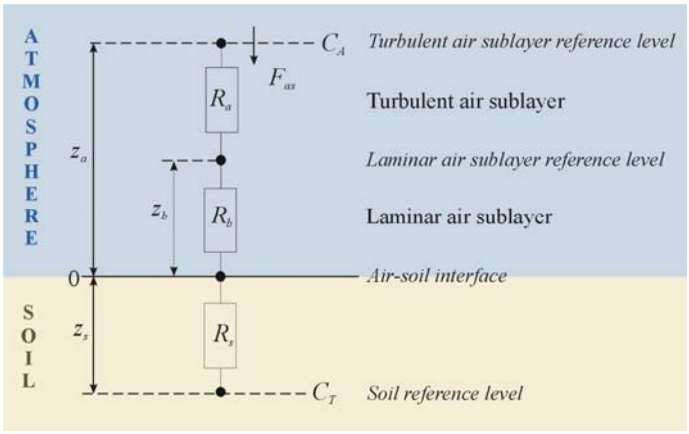

Fig. 3.4. *Resistance scheme used for the description of gaseous exchange between the atmosphere and the soil*

- Turbulent air sublayer resistance R_a, s/m is the resistance to transport through the turbulent air sublayer (from z_a to z_b).

- Laminar surface air sublayer resistance R_b, s/m is the resistance to transport through the laminar surface air sublayer (z_b) to the interface;

- Surface soil resistance R_s, s/m, is the resistance to transport from the surface soil interface to the soil reference level (z_s).

The resistance of upper soil layer r_s and effective air/soil distribution coefficient K_{as} are given by:

$$R_s = \frac{1}{R_g\left(\frac{2D_E}{\Delta z_1} + pV_E\right)}, \qquad K_{as} = \frac{1}{r_s\left(\frac{2D_E}{\Delta z_1} + qV_E\right)} \tag{3.27}$$

where Δz_1 is the thickness of the upper layer of the soil calculation grid;

p = 1, q = 0 for downward water flux (V_E > 0) and p = 0, q = 1 for upward water flux (V_E < 0).

The flux at the lower boundary of soil calculation domain is assumed to be zero.

Eq. (3.25) with the above boundary conditions is numerically solved by explicit scheme. The number of vertical calculation layers in the soil calculation domain and their thickness are chosen in an appropriate way. The criterion for the choice of these parameters is the stability of the value of net gaseous flux with respect to further subdivision of soil layers. As a result, 7 layers with thickness 0.1, 0.3, 0.6, 1, 2, 5 and 11 cm downwards are used.

Degradation in soil

The degradation process in soil is described as a first-order process by the equation:

$$\frac{dC}{dt} = -k_{soil} C, \tag{3.28}$$

where C is the pollutant concentration in soil, ng/m^3;

k_{soil} is the degradation rate constant for soil, s^{-1}.

The degradation rate constant k_{soil} is a part of model parameterization for a given pollutant (see Annex B (B.5. Degradation rate constants in environmental media).

3.3. Vegetation compartment

Three types of vegetation are distinguished in the model: coniferous forest, deciduous forest, and grass. The information on vegetation types is based on the land cover data described in MSCE-HM-Hen model description. Coefficients governing exchange processes between the atmosphere and vegetation are determined separately for each of the above vegetation types. Furthermore, we consider forest litter as an intermediate medium between vegetation and soil. In essence this medium can be viewed as an upper soil layer.

Gaseous exchange with the atmosphere

The equation describing atmosphere/vegetation exchange has the following form:

$$\frac{dC_V}{dt} = \frac{1}{R_{tot}} (C_a^g - C_V / K_{Va}), \tag{3.29}$$

where C_a^g is the air concentration of a pollutant;

C_V is the concentration in vegetation of a given type;

K_{va} is the bioconcentration factor *(BCF)*;

R_{tot} is the total resistance to the gaseous exchange given by the formula:

$$R_{tot} = R_a + a_V / k, \tag{3.30}$$

where R_a is the aerodynamic resistance of the turbulent atmospheric layer;

k is the mass transfer coefficient, m/s;

a_V is the specific surface area of vegetation, m^2/m^3 (assumed value is 8000, see [*Duyzer and van Oss*, 1997]).

The total amount of pollutant in vegetation of a given type in a certain grid cell is then expressed by the equation:

$$Q = C_V \frac{S \cdot \mathrm{LAI}}{a_V}, \tag{3.31}$$

where S is the area covered by vegetation of a given type within a grid cell;

LAI is the particular leaf area index for the considered type of vegetation.

Parameterization of BCF. The bioconcentration factor is determined by the following equation [*McLachlan and Horstmann*, 1998]:

$$K_{Va} = mK_{OA}^{n}, \tag{3.32}$$

where K_{OA} is the partitioning coefficient between octanol and air;

m, n are the regression coefficients presented in Table 3.1.

Table 3.1. *Regression parameters for Eq. (3.32)*

	Grass [*Thomas et al.*, 1998]	Forest [*McLachlan and Horstmann*, 1998]	
		Coniferous	Deciduous
m	22.91	38	14
n	0.445	0.69	0.76

While calculating BCF using Eq. (3.32) the temperature dependence of K_{OA} should be taken into account. Coefficients of K_{OA} temperature dependencies used in model parameterisation for the selected POPs are presented in Annex B (B.8. "Octanol-air partitioning coefficient").

Parameterization of the mass transfer coefficient k. According to [*Pekar et al.,* 1999], the mass transfer coefficient is directly proportional to the value of K_{OA}. Hence, for the evaluation of the temperature dependence of k the following formula can be used:

$$k = k_0 \exp\left[a_K\left(\frac{1}{T} - \frac{1}{T_0}\right)\right], \tag{3.33}$$

where k_0 is the k value at the reference temperature, based on the data given in [*McLachlan and Horstmann,* 1998] for forests and in [*Pekar et al.,* 1999] for grass;

a_K is the coefficient of K_{OA} temperature dependence, K.

The values of a_K for the selected POPs are given in the Annex B (B.8. "Octanol-air partitioning coefficient").

Defoliation and transport to soil from forest litter

The description of the defoliation process is also included in the model. It is assumed that part of the pollutant transported from vegetation to the forest litter is proportional to the decrease of leaf area index for deciduous forest and grass. For coniferous trees defoliation was described as a first-order process with a half-life $T_{1/2}$ = 2 years.

The transmission of a pollutant from fallen leaves to the underlying soil is described as a first order process with the half-life of about 10 years as a preliminary rough hypothesis.

Degradation in vegetation

There is very little data on degradation rates of considered chemicals in vegetation. For this reason, the degradation process in vegetation is not considered at present. A more detailed discussion of this question with rough estimation of degradation rates in vegetation for some POPs can be found in [*Pekar et al.*, 1999]. On the basis of preliminary investigations, the degradation process in forest litter was introduced to the model as a first-order process with a degradation constant rate two times higher than that in soil.

3.4. Seawater compartment

This section contains a general description of the processes included in the seawater module of the MSCE-POP-Hem model.

The calculation domain is divided into 15 vertical layers with depths of 12.5, 37.5, 65, 105, 165, 250, 375, 550, 775, 1050, 1400, 1900, 2600, 3500, 4600 metres. Horizontal resolution is 1.25°x1.25°, that is, two times less than the atmospheric one. More detailed spatial resolution for the ocean module allows for consideration of dynamical processes in the ocean on appreciably smaller scales than in the atmosphere. For example, this spatial resolution produces a reasonable description of sea currents nearby the coastal line.

Basic equation

The equation for the dynamics of total concentration, including a description of advection, turbulent diffusion, degradation and sedimentation can be written as follows:

$$\frac{Dc}{Dt} = K_H \Delta_H c + \frac{\partial}{\partial z}(K_V \frac{\partial c}{\partial z}) - v_{sed} \frac{\partial c_p}{\partial z} - k_d c \,, \tag{3.34}$$

where c, c_p are POP total and particulate phase concentrations;

$\frac{D}{Dt}$ is the total derivative in time;

Δ_H is the Laplace operator in horizontal variables;

$K_V(z)$ and K_H are the coefficients of vertical and horizontal diffusion;

v_{sed} is the sedimentation rate constant, which is estimated by the Stokes formula:

$$v_{sed} = \frac{g(\rho_p - \rho_w) d_p{}^2}{12\mu} \tag{3.35}$$

where g is gravitational acceleration, m/s^2;

ρ_p is mean density of particles, kg/m^3;

ρ_w is water density, kg/m^3;

d_p is the diameter of seawater particles, m;

μ is dynamic viscosity of seawater, kg/m/s.

Fields of sea current velocities, and the depth of the upper mixed layer, used to calculate vertical turbulent diffusion, are taken from the ocean dynamic model.

POP partitioning between different phases

POP redistribution between the dissolved phase, and the phase associated with particles, essentially affects the dynamics of POP concentration fields in the marine environment. Under the condition of instantaneous phase equilibrium establishment it is possible to consider that the relationship is always fulfilled:

$$c^p = k^p c^d \tag{3.36}$$

where c^p is the concentration of POP sorbed on particles;

c^d is the concentration of POP dissolved in water;

k^p is the partition coefficient between the particle and dissolved phase.

In its turn k^p may be estimated by the expression:

$$k^p = k_p^o K_p c_{prt} \tag{3.37}$$

where k_p^o is the fraction of organic matter in a particle;

K_p is the equilibrium constant for sorption/desorption processes (proportional to the octanol-water coefficient K_{OW});

C_{prt} is particle concentration.

Air/seawater mass exchange

For POP flux through the sea surface the following expression is used:

$$F_z\big|_{z=0} = \alpha_1(c_a^g / K'_H(T) - c^d)((1-\alpha_2)D_w/\delta + \alpha_2 K_{HR}\dot{h}_f) + F_{gw} + F_{pd} + F_{pw}, \tag{3.38}$$

where: $\delta = \delta_0 \exp(-0.15 \cdot U_a)$,

$\alpha_1 = 1.75 - 0.75\exp(-0.18 \cdot U_a)$,

$\alpha_2 = 1 - \exp(-0.01 \cdot U_a)$.

c_a^g is the POP gas-phase concentration in the lower layer of the atmosphere;

c^d is the dissolved POP concentration in upper layer of the sea;

$K'_H(T)$ is the dimensionless Henry's law constant depending on temperature;

D_w is the molecular diffusion coefficient in water;

δ_0 is the surface molecular layer depth at zero wind speed;

U_a is the wind speed absolute value near the surface;

$\dot{h}_f$ is the foam settling rate at the sea surface;

F_{gw} is the POP gas-phase flux with precipitation;

F_{pd} is the flux of POP associated with particles in the atmosphere as a result of particle dry deposition;

F_{pw} is the flux of POP associated with particles in the atmosphere as a result of particle washout with precipitation;

α_1 is the coefficient introduced for the description of surface sea area increase due to wave disturbance;

α_2 describes the relative sea surface area covered with foam at strong wind.

A more detailed description of these processes is given in [*Strukov et al.*, 2000].

Further development of the hemispheric model is associated with the refinement of the partitioning of a pollutant between the dissolved and particle phase, as well as sedimentation process. These processes strongly influence the fate of pollutants in the marine environment, and affect air concentrations over sea through gaseous exchange fluxes.

POP transport with ice cover

While POP transport modeling takes place within the scale of the globe it is necessary to consider the effect of ice coverage over the vast areas of the polar region. Sea ice plays the role of a screen between the seawater and the atmosphere. At the same time POP may be accumulated in ice itself and in the snow on it. The process of POP exchange with the atmosphere takes place on the upper snow-ice surface. When snow and ice are melting on the upper surface, or ice is melting on the lower or lateral surfaces, POP passes to the water environment. In the case of ice accretion on the lower or lateral ice surfaces, POP can penetrate into the ice medium. Furthermore, POP trapped by the sea ice and snow may be transported with ice drift. The scheme of basic processes in the atmosphere/snow/ice/seawater system is presented in Fig. 3.5.

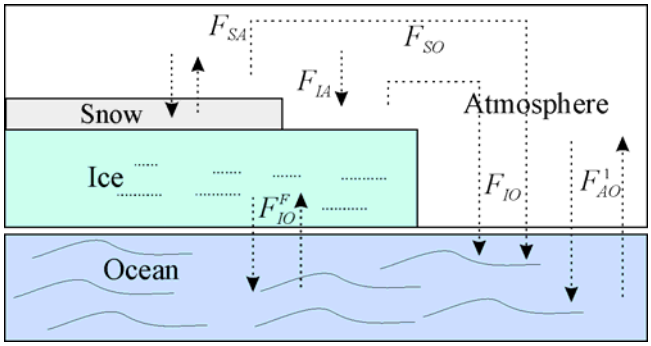

Fig. 3.5. *The scheme of POP fluxes in the system atmosphere-snow/ice-seawater*

F_{SA} – flux between the atmosphere and the snow pack (snow on the ice surface), F_{SO} - flux from the upper surface of the snow pack into seawater (snow on the ice surface), F_{IA} – flux from the atmosphere onto the upper ice surface (no snow), F_{IO} – flux into the seawater from the upper ice surface (no snow), F_{IO}^{p} – flux between the seawater and the ice medium (particle phase only). Fluxes downward are considered to be positive

POP flux between the atmosphere and seawater without sea ice may be represented as:

$$F_{AO}^{0} = F_z\big|_{z=0} = F_d^g + F_w^g + F_d^p + F_w^p \,, \tag{3.39}$$

where F_d^g is POP gas phase flux between the seawater and the atmosphere;

F_w^g is the gas phase flux from the atmosphere to the seawater with precipitation;

F_d^p is the atmospheric dry deposition flux of POP with particles to the seawater;

F_w^p is the flux of POP with particles depositing with precipitation.

To take into account the screening effect of sea ice, F_{AO}^{0} should be substituted for the expression:

$$F_{AO}^{1} = F_{AO}^{0}(1-A)\,, \tag{3.40}$$

where A is ice compactness in dimensionless units ($A = S_i / S$, S_i – ice square on sea square S).

POP molecules in the snow-ice environment may be found in different physical states: in the gaseous phase, in snow-ice pores, sorbed on surface ice crystals (the surface phase), incorporated into organic particles contained in the snow-ice medium (the particle phase), dissolved in water, if any, in the snow or ice medium. As a first approximation the following simplifications are made:

- equilibrium between POP different phases is instantly established;
- snow and ice are not saturated by water, i.e. the POP aqueous phase is absent in the ice coverage;
- POP entering the ice surfaces with the help of active vertical mixing mechanisms (hummocking and others) are distributed in the ice medium.

In accordance with these assumptions the total concentration of the gaseous and surface phase (kg/m^3) in snow pack is denoted as c_{sn}; the total concentration of the gaseous and surface phase in the ice medium (kg/m^3) – as c_{ic}; concentration of the particle phase in the snow (kg/m^3) – as c^p_{sc}; and the concentration of the particle phase in the ice thickness (kg/m^3) – as c^p_{ic}. The thickness of the snow cover on the ice and the ice thickness are denoted by h_{sn} and $h_{ic,}$ respectively. The values of $h_{sn,}$ h_{ic}, may depend on the horizontal co-ordinates λ, φ and time t concentration. Values c_{sn}, c_{in}, c^p_{sn}, c^p_{ic} may also depend on the vertical co-ordinate z. In view of the essentially smaller vertical scale, in comparison with the horizontal, vertically averaged values of concentrations c_{sn}, c_{in}, c^p_{sn}, c^p_{ic} will be considered. The area specific mass of different POP phases for the snow and ice, in accordance with ice compactness, may be represented by the expression:

$$m_{sn} = Ac_{sn}h_{sn}\,,\quad m^p_{sn} = Ac^p_{sn}h_{sn}\,,\quad m^p_{ic} = Ac^p_{ic}h_{ic}\,,\quad m_{is} = Ac_{is}h_{ic} \tag{3.41}$$

The balance equation of the considered POP fluxes for snow and ice medium and for the ice surface may be written as:

- for the sum of gaseous and surface phases of the snow pack:

$$\frac{dm_{sn}}{dt} = (F^{',g}_d + F^g_w + F_{SO})A - F_{Sd}\,, \tag{3.42}$$

where $F^{',g}_d$ is the atmospheric dry deposition flux of gaseous POP between the atmosphere and snow;

F^g_w is the atmospheric wet deposition flux of gaseous POP from the atmosphere (previously defined);

F_{SO} is the flux of the gaseous and surface phases of POP from the upper snow surface into seawater;

F_{Sd} is the degradation rate of gaseous and surface phases in snow.

- for the particle phase in the snow pack:

$$\frac{dm^p_{sn}}{dt} = (F^p_d + F^p_w + F^p_{SO})A - F^p_{Sd}\,, \tag{3.43}$$

where F^p_d, F^p_w are the atmospheric dry and wet deposition fluxes of POP with particles (previously defined);

F^p_{SO} is the flux of the particle phase of POP from the upper snow surface into seawater;

F^p_{Sd} is the degradation rate of the particle phase in snow.

- for the sum of the gaseous and surface phase in the ice:

$$\frac{dm_{is}}{dt} = (F^g_w + F_{IO})A - F_{Id}\,, \tag{3.44}$$

where F_{IO} is the flux of the surface phase of POP from the upper ice surface into seawater;

F_{Id} is the degradation rate of the surface phase in ice.

The gaseous phase in the ice medium is neglected due to the small volume of the pores in the ice.

- for the particle phase in the ice medium:

$$\frac{dm_{ic}^{p}}{dt} = (F_{d}^{p} + F_{w}^{p} + F_{IO}^{p})A - F_{Id}^{p} . \tag{3.45}$$

where F_{IO}^{p} is the flux of the particle phase of POP between bottom and lateral ice surfaces and seawater;

F_{Id}^{p} is the degradation rate of the particle phase in ice.

In these balance equations the total derivative for the two-dimensional problem is taken into consideration. Horizontal POP mass transport is realized with the ice drift along velocity fields (u_{ic}, v_{ic}), where u_{ic} – meridian, v_{ic} – zonal components of ice velocities.

The undefined mass fluxes in the right sides of Eq. (1.42 – 1.45) are represented by the following relationships.

The flux of the gaseous phase between the atmospheric and snow pack.

$$F_{d}^{'g} = \frac{(c_{a}^{g} - c_{surf})}{r + r_{surf}} . \tag{3.46}$$

Here c_{a}^{g} is the gas phase concentration in the atmosphere;

r is resistance to the atmospheric flux;

$r_{surf} = \frac{h_{sn}}{2\phi_{sn}^{4/3} D_{g}}$; $c_{surf} = c_{gsn} = c_{sn} / R_{sn}^{g}$;

D_{g} is the POP molecular diffusion coefficient in gas;

$\phi = \frac{\rho_{w} - \rho_{sn}}{\rho_{w}}$ is snow porosity;

ρ_{w}, ρ_{sn} are water and snow density respectively,

The expression for $F_{d}^{'g}$ may be derived from the model of POP exchange between soil and the atmosphere [*Pekar et al.,* 1998] under the condition that the water phase is absent. The coefficient R_{sn}^{g} in the relationship for c_{surf} is expressed through snow porosity, snow density, specific surface area of crystals s_{sn} and the coefficient of equilibrium between the gas and surface phase K_{ia} [*Koziol and Pudykiewicz,* 2001].

$$R_{sn}^{g} = \phi + \rho_{sn} s_{sn} K_{ia} \tag{3.47}$$

The values K_{ia} are connected with the POP solubility C_{W} and the Henry's law constant:

$$\log(K_{ia}) = 0.769 \cdot \log(C_{W}) - 5.966 - \log(K'_{H}(T_{sn})) , \tag{3.48}$$

where T_{sn} is snow temperature.

- For the sum of gaseous and surface phase fluxes from snow surface into the seawater (snow on the ice surface), presuming that in the majority of cases melting water leaks into the seawater through cracks and ice-holes on the ice cover (because of ice compactness *A* almost everywhere is less than 1):

$$F_{SO} = -dh_{sn} c_{sn} \quad \text{at} \quad h_{sn} > 0\,, \tag{3.49}$$

where dh_{sn} is snow cover melting rate.

- For the particle phase flux between the seawater and snow with the same assumptions

$$F^p_{SO} = -dh_{sn} c^p_{sn} \quad \text{at} \quad h_{sn} > 0 \tag{3.50}$$

- For the surface phase flux into seawater from the upper ice surface.

$$F_{IO} = -dh_{is} c_{ic} \quad \text{at} \quad h_{is} > 0, \tag{3.51}$$

where dh_{is} is the ice melting rate on the upper ice surface.

- For the particle flux into seawater from the upper ice surface.

$$F^p_{IO} = -dh_{is} c^p_{ic} \quad \text{at} \quad h_{is} > 0, \tag{3.52}$$

For the particle phase between the ice medium and seawater on the bottom / lateral surfaces of ice:

$$F^p_{IO} = -dh_{ib} c^p_{ic} \quad \text{at} \quad dh_{ib} > 0 \quad \text{(melting)} \tag{3.53}$$

$$F^p_{IO} = -dh_{ib} c^p_{w} \quad \text{at} \quad dh_{ib} \le 0\,, \quad \text{(accretion)}$$

where dh_{ib} is the ice melting rate on the lower ice surface;

c^p_w is concentration of the particle phase in the water surface layer.

It is considered that at ice bottom/lateral surfaces accretion POP gas and surface phase do not enter the new ice ("freezing" effect). POPs on particles in water enter the forming ice with the particles. The availability of organic particles trapped by sea ice with POP adsorbed molecules is confirmed by numerous observations [*Pfirman et al.,* 1995].

POP degradation rates are represented by appropriate linear dependence on POP concentration:

$$F_{Sd} = k_{snd} m_{sn}, \quad F^p_{Sd} = k^p_{snd} m^p_{sn}\,, \quad F_{id} = k_{icd} m_{ic}, \quad F^p_{Id} = k^p_{icd} m^p_{ic}\,, \tag{3.54}$$

where k_{snd}, k^p_{snd}, k_{icd}, k^p_{icd} are the degradation rate constants of a substance.

Computation of POP exchange between the atmosphere and ice compartment in MSCE-POP-Hem model requires the following input information, namely, ice compactness, ice cover thickness, snow cover thickness, ice and snow melting rates, surface temperature. These data were obtained from the CSIM2 model developed at NCAR in the framework of CCSM model project [*Bruce et al*., 2001] and adapted for supplying the MSCE-POP-Hem model with required input data [*Shatalov et al*., 2003].

3.5. Input information

The MSCE-POP-Hem model input information includes emission data, meteorological and geophysical information, and physical-chemical properties of POPs. MSCE-POP-Hem and MSCE-HM-Hem models use the same meteorological data, land cover information (Annex C), and data on OH radical content in the atmosphere (Section 2.5. “Chemical reactants data”). In addition to them MSCE-POP-Hem model requires also data on leaf area index, organic carbon content in soil, data on specific aerosol surface in air and data on sea currents.

Emissions of selected POPs

The preparation of emission data for modelling is made on the basis of official data submitted to the UN ECE Secretariat by countries and available expert estimates of POP emissions. The official data on POP emissions (PAHs, PCDD/Fs, PCBs, HCB and γ-HCH) for the period from 1990 to 2001 (at least for one year) were submitted by 32 Parties to the Convention. Data on other pollutants (Aldrin, Chlordane, Chlordecone, Dieldrin, Endrin, Heptachlor, Hexabromobiphenyl, Mirex, Toxaphene, DDT, PCP and SCCP) were submitted by 16 countries. It is worth to note that in recent years, the number of countries submitting data on POP emissions and their spatial distribution over the EMEP domain increased. For countries for which official emission data were not available, expert estimates are used.

Emission data for polycyclic aromatic hydrocarbons were compiled with the usage of officially submitted data and available expert estimates of [*Pacyna et al*., 1999; *Tsibulsky et al*., 2001; *Berdowski et al.,* 1997; *Baart et al.*, 1995]. In the model computations seasonal variations of PAH emissions are considered in accordance with [*Baart et al*., 1995].

Data on polychlorinated dibenzo-p-dioxins and dibenzofurans (PCDD/Fs) emissions of European countries were prepared using official emissions and expert estimates of PCDD/F total emissions and their spatial distribution of [*Pacyna et al*., 1999]. For model calculations splitting of the overall toxicity of PCDD/F mixture between different congeners was performed and spatial distributions of emissions for each congener were prepared on the basis of the data from [*Pacyna et al.,* 1999].

Emissions of polychlorinated biphenyls (PCBs) for European region are based on global emission inventory of 22 PCB congeners for the period 1930-2000 [*Breivik et al*., 2002]. These data were redistributed into MSCE-POP-Hem model grid using the information on population density.

Information on HCB and γ-HCH emissions of European countries was compiled on the basis available official information and expert estimates of [*Pacyna et al*., 1999]. Seasonal variations of γ-HCH emissions due to its application for agricultural purposes in spring and early summer are taken into account in modelling.

Detailed description of emission data used for modelling can be found in MSC-E/CCC technical reports 7/2002 and 4/2003 [*Shatalov et al.*, 2002; *Shatalov et al.*, 2003].

Physical-chemical properties of selected POPs and substance-specific parameters

Basic differences in the long-range transport of POPs mainly result from peculiarities of their physical-chemical properties and degradation rates in the main environmental media. The key characteristics required for POP modelling are the following:

- subcooled liquid vapour pressure (p^0_L);
- air-water Henry's law constant (K_H);
- washout ratio for the particulate (W_p) and gaseous phase (W_g);
- degradation rate constants for different environmental compartments;
- coefficients of partitioning between different media (octanol-water partition coefficient (K_{OW}), octanol-air partition coefficient (K_{OA}), organic carbon-water partition coefficient (K_{OC}));
- data on the distribution of low volatile POPs with particle sizes in the atmosphere;
- and molecular diffusion coefficients (D_A, D_W , m^2/s).

These physical-chemical properties were prepared for the evaluation of environmental pollution with MSCE-POP-Hem model for selected POPs, namely, PAHs (B[a]P, B[b]F, B[k]F and I_P), PCDD/Fs (17 congeners), PCBs (5 congeners), γ-HCH and HCB. The mentioned above characteristics used for modelling of considered POPs are presented below in Annex C. For some of these POPs temperature dependencies of subcooled liquid-vapour pressure, Henry's law constant, octanol-air partition coefficient and degradation rate constants are also given.

The selection of parameters was carried out on the basis of literature data on POP physical-chemical properties and measurement data. Many studies report data on experimentally determined or theoretically derived physical-chemical properties of individual POPs. At that base values of some physical-chemical properties and/or coefficients of temperature dependencies vary substantially. The scattering of the values reported can to some extent characterize the uncertainty of particular parameter.

Geophysical data

Leaf Area Index (LAI) data set is used for the description of POP gaseous exchange between the atmosphere and vegetation. The Leaf Area Index for a given grid cell implies the ratio between the area of leaves in this cell to its total area (m^2/m^2). The geographically resolved leaf area index data with monthly resolution was adopted from CD-ROM of NASA Goddard Space Flight Center [*Sellers et al*., 1994, 1995] and converted to MSCE-POP-Hem model grid. Consistency of these data in relation to the land cover information was investigated by correlation analysis.

Data on sea currents were obtained from ocean general circulation model (OGCM) [*Resnyansky and Zelenko*, 1991; 1992; 1999]. These data describe three-dimensional structure of velocity fields in the oceanic depth and the surface mixed layer depths within the EMEP grid. The velocity fields and the upper mixed layer thickness are defined for every two days with linear interpolation of values obtained within this period of time. Description of this information can be found in MSC-E Technical Note 5/2000 [*Strukov et al.*, 2000].

REFERENCES

Aas W. and Breivik K. [2004] Heavy Metals and POPs measurements, 2002. EMEP/CCC Report 7/2004. Norwegian Institute for Air Research, Kjeller, Norway.

Acker K., Moller D., Wieprecht W., Kalass D., Auel R. [1998] Investigations of ground-based clouds at the Mt. Brocken. Fresenius. Anal. Chem., vol. 361, pp.59-64.

Anderson P.N. and R.A. Hites [1996] OH Radical Reactions: The Major Removal Pathway for Polychlorinated Biphenyls from the Atmosphere, Environ. Sci. Technol., vol. 30, No. 5, pp. 1756 – 1763.

Andersson M., Wängberg I., Gårdfeldt K., Munthe J. [2004] Investigation of the Henry's low coefficient for elemental mercury. Proceedings of the 7th Conference "Mercury as a global pollutant". RMZ – Materials and Geoenvironment, Ljubljana, June 2004.

Andrinache C. [2003] Estimated variability of below-cloud aerosol removal by rainfall for observed aerosol size distributions. Atmos. Chem. Phys., vol. 3, pp.131-143.

Andrinache C. [2004] Estimates of sulfate aerosol wet scavenging coefficient for locations in the Eastern United States. Atmos. Environ., vol. 38, pp.795-804.

Ariya P.A., Khalizov A., Gidas A. [2002] Reactions of gaseous mercury with atomic and molecular halogens: kinetics, product studies, and atmospheric implications. J. Phys. Chem., vol. 106, pp.7310-7320.

Asman W.A.H. [1995] Parameterization of below-cloud scavenging of highly soluble gases under convective conditions. Atmos. Environ., vol. 29, pp.1359-1368.

Atmosphere Handbook [1991]. L., Hydrometeoizdat, p.179 (in Russian).

Baart A., J.Berdowski, J. van Jaarsveld and K.Wulffraat [1995] Calculation of atmospheric deposition of contaminants on the North Sea. TNO-MEP-R 95/138, Delft, The Netherlands.

Banic C. M., Schroeder W. H., and Steffen A. [1999] Vertical distribution of total gaseous mercury in Canada. Book of abstracts, 5th International Conference on Mercury as a Global Pollutant, 23-28 May 1999, Rio de Janeiro.

Barries L.A. [1985] Scavenging ratios, wet deposition, and in-cloud oxidation: an application to the oxides of sulphur and nitrogen. J. Geophys. Res., vol. 90(D3), pp.5789-5799.

Berdowski J.J.M., Baas J., Bloos J.P.J., Visschedijk A.J.H., Zandveld P.Y.J. [1997] The European Emission Inventory of Heavy Metals and Persistent Organic Pollutants for 1990. TNO Institute of Environmental Sciences, Energy Research and Process Innovation, UBA-FB report 104 02 672/03, Apeldoorn, 239 p.

Berg T. and A.-G.Hjellbrekke [1998] Heavy metals and POPs within the ECE region. Supplementary data for 1989-1996. Kjeller, Norwegian Institute for Air Research (NILU EMEP/CCC-Report 7/98).

Berg T., A.-G. Hjellbrekke and J.E. Skjelmoen [1996]: Heavy metals and POPs within the ECE region. EMEP/CCC-Report 8/96. Norwegian Institute for Air Research.

Berg T., A.-G. Hjellbrekke and Larsen R. [2001] Heavy metals and POPs within the EMEP region 1999. EMEP/CCC – Report 9/2001.

Berg T., A.-G. Hjellbrekke and N. Ritter [1997] Heavy metals and POPs within the ECE region. Additional data. EMEP/CCC-Report 9/97, ref. O-95038, August.

Berg T., A.-G. Hjellbrekke and R. Larsen [2002] Heavy metals and POPs within the EMEP region 2000., EMEP/CCC-Report 9/2002.

Berg T., A.-G.Hjellbrekke and R.Larson [2000] Heavy metals and POPs within the ECE region 1998. Kjeller, Norwegian Institute for Air Research (NILU EMEP/ÑÑÑ-Report 2/2000).

Berg T., Sekkester S., Steines E., Valdal A., Wibetoe G. [2001] Arctic springtime depletion of mercury as observed in the European Arctic. Book of Abstracts, 6th International Conference on Mercury as a Global Pollutant, 15-19 October 2001, Minamata, Japan.

Beyer A and M.Matthies [2001] Criteria for Atmospheric Long-range Transport Potential and Persistence of Pesticides and Industrial Chemicals. Umweltforschungsplan des Bundesministerium fur Umwelt, Naturschutz und Reaktorsicherheit. Stoffbewertung, Gentechnik, Forderkennzeichen (UFOPLAN) 299 65 402.

Beyer A. and M. Matthies [2002] Criteria for Atmospheric long-range Transport Potential and Persistence of Pesticides and Industrial Chemicals, Umweltbundesamt.- Berlin: Erich Schmidt, Berichte/Umweltbundesamt, No. 7, p. 244.

Bott A. [1989a] A positive definite advection scheme obtained by nonlinear renormalization of the advective fluxes. Mon. Wea. Rev., vol.117, pp.1006-1015.

Bott A. [1989b] Reply to comment on "A positive definite advection scheme obtained by nonlinear renormalization of the advective fluxes." Mon. Wea. Rev., vol. 117, pp.2633-2636.

Brandt J., Christensen J.H., Frohn L.M. [2002] Modelling transport and deposition of caesium and iodine from the Chernobyl accident using the DREAM model. Atmos. Chem. Phys., vol. 2, vol.397-417.

Breivik K., A.Sweetman, J.M.Pacyna and K. Jones [2002] Towards a global historical emission inventory for selected PCB congeners – a mass balance approach. 2. Emissions. The Science of the Total Environment, vol. 290, pp. 199-224.

Brosset C., Lord E. [1991] Mercury in precipitation and ambient air – a new scenario. WASP, vol. 56, pp.493-506.

Brubaker W.W. and R.A. Hites [1997] Polychlorinated dibenzo-p-dioxins and dibenzofurans: gas-phase hydroxyl radical reactions and related atmospheric removal. Environ. Sci. Technol., vol.31, No. 6, pp.1805-1810.

Brubaker W.W. and R.A. Hites [1998] OH reaction kinetics of gase-phase α - and γ - Hexachlorocyclohexane and hexachlorobenzene, Environ. Sci. Technol., vol. 32, No. 6, pp. 766-769.

Bruce P.B., C. Hunke, C.M. Bitz, B. Lipscomb and V. Schramm [2001] DRAFT description of the CCSM2 Sea Ice Model: CSIM4, (http://www.ccsm.ucar.edu/models/ice-csim4).

Bulgakov A., D.Ioannisian, B.Moisseev, A.Zelenko, Yu.Resnyansky and L.Erdman [1998] Review of physical – chemical properties of polychlorinated dibenzo-p-dioxins (PCDDs) and dibenzofurans (PCDFs) in respect to their long-range transport in the atmosphere // Long-range transport of selected POPs. Part II. Physical-chemical properties of dioxins and furans and factors influencing the transport and accumulation of Persistent Organic Pollutants. EMEP/MSC-E Report 2/98, Part II.

Chin M. et al. [1996] A global three-dimensional model of tropospheric sulfate, J. Geophys. Res. v.101, pp.18667-18690.

Chu W. and K.-H.Chan [2000] The prediction of partitioning coefficients for chemicals causing environmental concern, The Science of the Total Environment, vol. 248, pp. 1-10.

Dabdub D., Seinfeld J. H. [1994] Numerical advective schemes used in air quality models – sequential and parallel implementation. Atmos. Environ., vol. 28, pp.3369-3385.

Dunnivant F.M., A.W.Elzerman, P.C.Jurs and M.N.Hasan [1992] Quantitative Structure-Property Relationships for Aqueous Solubilities and Henry s Law Constants of Polychlorinated Biphenyls, Environ. Sci. Technol., vol. 23, No. 10, pp. 1250 – 1253.

Duyzer J. H. and R.F. van Oss [1997] Determination of deposition parameters of a number of persistent organic pollutants by laboratory experiments. TNO-Report TNO-MEP-R97/150.

Easter R. C. [1993] Two modified versions of Bott's positive-definite numerical advection scheme. Mon. Wea. Rev., vol.121, pp.297-304.

Ebinghaus R., Kock H. H., Temme C., Einax J. W., Löwe A. G., Richter A., Birrows J. P., Schroeder W. H. [2002] Antarctic Springtime Depletion of Atmospheric Mercury. Environ. Sci. Technol., vol. 36, pp.1238-1244.

Ebinghaus R., Tripathi R. M., Walischlager D., and Lindberg S. E. [1999] Natural and anthropogenic mercury sources and their impact on the air-surface exchange of mercury on regional and global scales. In: Ebinghaus R., Turner R. R., Lacerda de L. D., Vasiliev O., and Salomons W. (Eds.) Mercury contaminated sites. Springer, Berlin, pp.3-50.

Eisenreich S.J., B.B.Looney and J.D.Thornton [1981] Airborne organic contaminants in the Great Lakes ecosystem. Environ. Sci. Technol., vol. 15, pp. 30-38.

Erisman J.W., van Pul A., Wyers P. [1994] Parameterization of surface resistance for the quantification of atmospheric deposition of acidifying pollutants and ozone. Atmos. Environ., vol. 28, pp.2595-2607.

Falconer R.L. and T.F. Bidleman [1994] Vapor pressures and predicted particle/gas distributions of polychlorinated biphenyl congeners as functions of temperature and ortho-chlorine substitution. Atmos. Environ., vol.28, pp.547-554

Fitzgerald J.W. [1975] Approximation formulas for the equilibrium size of an aerosol particle as a function of its dry size and composition and the ambient relative humidity. J. Appl. Meteorol., vol.14, No.6, pp.1044-1049.

Fitzgerald W.F., Mason R.P., Vandal G.M. [1991] Atmospheric cycling and air-water exchange of mercury over mid-continental lacustrine regions. WASP, vol. 56, pp.745-767.

Franz T.P. and S.J. Eisenreich [1998] Snow scavenging of polychlorinated biphenyls and polycyclic aromatic hydrocarbones in Minnesota. Environ. Sci Technol., vol.32, pp.1771-1778.

Frolov A., A.Vaznik, E.Astahova, J.Alferov, D.Kiktev, I.Rosinkina and K.Rubinstein [1997a] A System of diagnosis of lower atmosphere for monitoring transboundary pollutant transport. Meteorology and Hydrology, No 4, pp.5-15.

Frolov A., A.Vaznik, E.Astahova, J.Alferov, D.Kiktev, I.Rosinkina and K.Rubinstein [1997b] A System of diagnosis of lower atmosphere for monitoring transboundary pollutant transport. The main algorithms. Meteorology and Hydrology, No 5, pp.5-13.

Frolov A., A.Vaznik, E.Astahova, J.Alferov, D.Kiktev, I.Rosinkina and K.Rubinstein [1997c] A System of diagnosis of lower atmosphere for monitoring transboundary pollutant transport: Precipitation and clouds. Meteorology and Hydrology, No.6, pp.5-15.

Frolov A., K.Rubinstein, I.Rosinkina, A.Vajnik, D.Kiktev, E.Astachova and J.Alferov [1994] A System of diagnosis of lower atmosphere for of transboundary air pollutant transport. EMEP/MSC-E and RHMC report 1/94.

Galarneau E., C.V.Audette, A.Bandemehr, I.Basu, T.F.Bidleman, K.A.Brice, D.A.Burniston, C.H.Chan, F.Froude, R.A.Hites, M.L.Hulting, M.Neilson, D.Orr, M.F.Simcik, W.M.J.Strachan and R.M.Hoff [2000] Atmospheric Deposition of Toxic Substances to the Great Lakes: IADN Results to 1996. Environment Canada and the United States Environmental Protection Agency.

Gårdfeldt K., Sommar J., Strömberg D., Feng X. [2001] Oxidation of atomic mercury by hydroxyl radicals and photoinduced decomposition of methylmercury in the aqueous phase. Atmos. Environ., vol.35, pp.3039-3047.

Garrat J.R. [1999] The atmospheric boundary layer. Cambridge University Press. 316 p.

Giorgi F. [1986] A particle dry deposition parameterization scheme for use in tracer transport models. J. Geophys. Res., vol. 91, pp.9794-9806.

Govers H.A.J. and H.B.Krop [1998] Partition constants of chlorinated dibenzofurans and dibenzo-p-dioxins.

Chemosphere, vol.37, No.9-12, pp.2139-2152.

Guo, Y.-R., and S. Chen [1994] Terrain and land use for the fifth-generation Penn State/NCAR mesoscale modelling system (MM5): Program TERRAIN. NCAR Tech. Note, NCAR/TN-397+IA, 119 pp. [Available from the National Center for Atmospheric Research, P. O. Box 3000, Boulder, CO 80307.]

Hall B. [1995] The gas phase oxidation of mercury by ozone. WASP, vol. 80, pp.301-315.

Harner T. and D.Mackay [1995] Measurement of octanol-air partition coefficients for chlorobenzenes, PCB, and DDT, Environ. Sci. Technol., vol. 29, No.6, pp. 1599 - 1606.

Harner T. and T.F. Bidleman [1996] Measurements of octanol-air partition coefficients for polychlorinated biphenyls. Chem. Eng. Data, vol.41, pp.895-899.

Harner T., H.Kylin, T.F.Bidleman, and M.J.Strachan [1999] Removal of a- and g-hexachlorocyclohexane and enantiomers of a-hexachlorocyclohexane in the Eastern Arctic Ocean. Environ. Sci. Technol., vol.33, pp. 1157-1164.

Harrad S.J and D.J.T.Smith [1997] Evaluation of a terrestrial food chain model for estimating foodstuff concentrations of PCDD/Fs, Chemosphere, vol. 34, No.8, pp.1723-1737.

Hawker D.W. and D.W.Connell [1988] Octanol-water partition coefficients of polychlorinated biphenyl congeners. Environ. Sci. Technol., vol.22, pp.382-387.

Hoff R.M., W.M.J.Strachan, C.W.Sweet, C.H.Chan, M.Shackleton, T.F.Bidleman, K.A.Brice, D.A.Butniston, S.Cussion, D.F.Gatz, K.Harlin and W.H. Schroeder [1996] Atmospheric deposition of toxic chemicals to the Great Lakes: a review of data through 1994. Atmos. Environ., vol. 30, No.20, pp. 3505-3527.

Jacobs C.M.J. and W.A.J. van Pul [1996] Long-range atmospheric transport of persistent organic pollutants. 1: Description of surface - Atmosphere exchange modules and implementation in EUROS. National Institute of Public Health and the Environment, Bilthoven, The Netherlands. Report No. 722401013.

Jacobson M. Z. [1999] Fundamentals of atmospheric modeling. Cambridge University Press. 656 p.

Junge C.E. [1977] Basic considerations about trace constituent in the atmosphere is related to the fate of global pollutant. In: Fate of pollutants in the air and water environment. Part I, I.H. Suffet (ed.) (Advanced in Environ. Sci. Technol., vol.8, Wiley-Interscience, New York.

Karikhoff S. W. [1981] Semiempirical estimation of sorbtion of hydrophobic pollutants on natural sediments and soil, Chemosphere, vol.10, pp.833-846.

Kasper A., Puxbaum H., Brantner B., Paleczek S. [1998] Scavenging efficiency of lead and sulfate in supercooled clouds at Sonnblick, 3106 m a.s.l., Austria. Atmos. Environ., vol.23, pp.3967-3974.

Keene W.C., M. Aslam, K. Khalil, D.J. Erickson, III , A. McCulloch, T.E. Graedel, J.M. Lobert, M.L. Aucott, S.L. Gong, D.B. Harper, G. Kleiman, P. Midgley, R.M. Moore, C. Seuzaret, W.T. Sturges, C.M. Benkovitz, V. Koropalov, L.A. Barrie, and Y.F. Li [1999] Composite global emissions of reactive chlorine from anthropogenic and natural sources: Reactive Chlorine Emissions Inventory. J. Geophys. Res., v.104(D7), pp.8429-8440.

Koester C.J. and R.A. Hites [1992] Wet and dry deposition of chlorinated dioxins and furans. Environ. Sci. Technol., vol.26, 1375-1382.

Kucklick J.R., D.A.Hinckley and T.F.Bidleman [1991] Determination of Henry's law constants for hexachlorocyclohexanes in distilled water and artificial seawater as a function of temperature. Marine chemistry, vol.34, pp.197-209.

Lamborg C. H., Fitzgerald W. F., O'Donnell J., Torgersen T. [2002] A non-steady-state compartmental model of global-scale mercury biogeochemistry with interhemispheric atmospheric gradients. Geochimica et Cosmochimica Acta, vol. 66, No.7, pp.1105-1118.

Lamborg C. H., Fitzgerald W. F., Vandal G. M., Rolfhus K. R. [1995] Atmospheric mercury in northern Wisconsin: sources and species. WASP, vol. 80, pp.189-198.

Ligocki M.P., C.Leuenberger and J.F.Pankow [1985] Trace organic compounds in rain - III. Particle scavenging of neutral organic compounds, Atmos. Environ., vol. 19, pp. 1619-1626.

Lin C.-J., Pehkonen S. O. [1999] The chemistry of atmospheric mercury: a review. Atmos. Environ., vol.33, pp.2067-2079.

Lindberg S. E., Brooks S., Lin C.-J., Scott K. J., Landis M. S., Stevens R. R., Goodsite M., Richter A. [2002] Dynamic oxidation of gaseous mercury in the Arctic troposphere at polar sunrise. Environ. Sci. Technol., vol.36, pp.1245-1256.

Lindfors V., S.M.Joffre and J.Damski [1991] Determination of the wet and dry deposition of sulphur and nitrogen compounds over the Baltic Sea using actual meteorological data. Finnish Meteorological Institute Contributions No.4, Helsinki.

Lu J. Y., Schroeder W. H., Barrie L. A., Steffen A., Welch H. E., Martin K., Lockhart W. L., Hunt R. V., Boila G., Richter A. [2001] Magnification of atmospheric mercury deposition to polar regions in springtime: the link to tropospheric ozone depletion chemistry. Geophys. Res. Letters., vol. 28, No.17, pp.3219-3222.

Lurie Yu. Yu. [1971] Handbook for Analytical Chemistry. Khimiya, Moscow, 454 p.

Ma J., S.Daggupaty, T.Harner and Y. Li [2003] Impacts of Lindane Usage in the Canadian Prairies on the Great Lakes Ecosystem. 1. Coupled Atmospheric Transport Model and Modeled Concentrations in Air and Soil. Environ. Sci. Technol., vol.37, pp.3774-3781.

Mackay D., W.Y.Shiu and K.C.Ma [1992a] Illustrated Handbook of Physical-Chemical properties and environmental fate for organic chemicals, vol.1: Monoaromatic Hydrocarbons, Chlorobenzenes, and PCBs'. Lewis Publishers, INC.

Mackay D., W.Y.Shiu and K.C.Ma [1992b] Illustrated Handbook of Physical-Chemical properties and environmental fate for organic chemicals, vol.2: Polynuclear aromatic hydrocarbons, Polychlorinated Dioxins, and Dibenzofurans'. Lewis Publishers, INC.

Mackay D., W.Y.Shiu and K.C.Ma [1997] Illustrated Handbook of Physical-Chemical properties and environmental Fate of Organic Chemicals, vol. V, Pesticide Chemicals, pp. 431-434, 599 – 571.

Mantseva E., A.Malanichev and N.Vulykh [2002] Polyaromatic hydrocarbons in the environment. MSC-E Technical Note 9/2002.

Marchuk G. I. [1975] Methods of numerical mathematics. Springer-Verlag, New York. 316 p.

Mclachlan M. and M.Horstmann [1998] Forests as filters of airborne organic pollutants: a model. Environ. Sci. Technol., vol.32, pp.413-420.

McLachlan M., J. Czub and F. Wania [2002] The Influence of Vertical Sorbed Phase Transport on the Fate of Organic Chemicals in Surface Soils. Environ. Sci. Technol. vol. 36, pp.4860-4867.

McRae G. J., Goodin W. R., Seifeld J. H. [1982] Numerical solution of the atmospheric diffusion equation for chemically reacting flows. J. Comp. Phys., vol. 45, pp.1-42.

Meneses M., M.Schuhmacher and J.L.Domingo [2002] A desing of two simple models to predict PCDD/F concentrations in vegetation and soils. Chemosphere, vol. 46, pp. 1393 – 1402.

Meylan W.M. and P.H. Howard [1993] Chemosphere, vol.26: pp.2293-99.

Milford J. B., Davidson C. I. [1985] The size of particulate trace elements in the atmosphere – a review. JAPCA, vol.35, No.12, pp.1249-1260.

Munthe J. [1992] The aqueous oxidation of elemental mercury by ozone. Atmos. Environ. vol.26A, pp.1461-1468.

Ngabe B., T.F.Bidleman and R.L.Falconer [1993] Base Hydrolysis of α - and γ - Hexachlorocyclohaxane, Environ. Sci. Technol., vol. 27, No. 9, pp. 1930-1933.

Odman M. T. and Russell A. G. [2000] Mass conservative coupling of non-hydrostatic meteorological models with air quality models. In: Gryning S.-E. and Batchvarova E. (Eds.) Air pollution modelling and its application XIII. Kluwer Academic/Plenum Publishers, New York, 651-660.

Okita T., Hara H and Fukuzaki N. [1996] Measurements of atmospheric SO2 and SO4 , and determination of the wet scavenging of sulfate aerosol for the winter monsoon season over the sea of Japan. Atmos. Environ. , vol.30, pp.3733-3739.

Paasivirta J., S. Sinkkonen, P.Mikelson, T.Rantio and F. Wania [1999] Estimation of vapor pressures, solubilities and Henry s law constants of selected persistent organic pollutants as functions of temperature, Chemosphere, vol. 39, No. 5, pp. 811-832.

Pacyna J.M. et al. [1999] Final report for Project POPCYCLING-Baltic. EU DGXII, Environment and Climate Program ENV4-CT96-0214. Available on CD-rom including technical report, the emission and environmental databases as well as the POPCYCLING-Baltic model. NILU, P.O. Box 100, N-2027 Kjeller, Norway

Pacyna, J. M., Pacyna, E. G., Steenhuisen, F., Wilson, S. [2003] Mapping 1995 global anthropogenic emissions of mercury. Atmos. Environ., vol. 37, Supplement No. 1, pp.109-117.

Pal B., Ariya P. [2004] Atmospheric transformation of elemental mercury upon hydroxyl radicals under near tropospheric conditions. Proceedings of the 7th Conference "Mercury as a global pollutant". RMZ – Materials and Geoenvironment. Ljubljana, June 2004.

Pankow J.F. [1987] Review and comparative analysis of the theories on partitioning between the gas and aerosol particulate phases in the atmosphere. Atmos. Environ., vol.21, pp.2275-2283.

Pekar M. [1996] Regional models LPMOD and ASIMD. Algorithms, parametrization and results of application to Pb and Cd in Europe scale for 1990. EMEP/MSC-E Technical Report 9/96, Meteorological Synthesizing Centre – East, Moscow, Russia.

Pekar M., N. Pavlova, A. Gusev, V. Shatalov, N. Vulikh, D. Ioannisian, S. Dutchak, T. Berg and A.-G. Hjellbrekke [1999] Long-Range transport of selected persistent organic pollutants. EMEP Report 4/99.

Penner J.E., Atherton C.S., Dignon J., Ghan S.J., Walton J.J. and Hameed S. [1991] Tropospheric nitrogen: A three-dimensional study of sources, distributions, and deposition. J. Geophys. Res., vol.96(D1), pp.959-990.

Peters K., Eiden R. [1992] Modelling the dry deposition velocity of aerosol particles to a spruce forest. Atmos. Environ., vol. 26, pp.2555-2564.

Petersen G., Iverfeldt A. and Munthe J. [1995] Atmospheric mercury species over central and northern Europe. Model calculations and comparison with observations from the nordic air and precipitation network for 1987 and 1988. Atmos. Environ., vol.29, pp.47-67.

Petersen G., Munthe J., Pleijel K., Bloxam R. and A.V.Kumar [1998] A comprehensive Eulerian modeling framework for airborne mercury species: Development and testing of the tropospheric chemistry module (TCM). Atmos. Environ., vol. 32, No.5, pp.829-843.

Pleijel K., and Munte J. [1995] Modeling the atmospheric mercury cycle - chemistry in fog droplets. Atmos. Environ., vol. 29, pp.1441-1457.

Poster D.L. and J.E.Baker [1996] Influence of submicron particles on hydrophobic organic contaminants in precipitation.1. Consentrations and distributions of polycyclic aromatic hydrocarbons and polychlorinated biphenyls in rainwater. Environ. Sci. Technol., vol. 30, No.1, pp. 341-348.

Pryor S.C., Barthelmie R.J., Geernaert L.L.S., Ellermann T., Perry K.D. [1999] Speciated particle dry deposition to the

sea surface: results from ASEPS '97. Atmos. Environ., vol. 33, pp.2045-2058.

Ragland K.W., Wilkening K.E. [1983] Intermediate-range grid model for atmospheric sulfur dioxide and sulfate concentrations and depositions. Atmos. Environ., vol. 17, pp.935-947.

Resnyansky Yu.D. and A.A. Zelenko [1999] Effects of synoptic variations of atmospheric impacts in the model of ocean general circulation: direct and indirect manifectation. Meteorology and Hydrology, No.9, pp.66-71, (in Russian).

Resnyansky Yu.D. and A.A.Zelenko [1991] Parametrization of the upper mixed layer in an ocean general circulation model. - Izvestiya of the USSR Academy of Sciences. Atmosphere and Ocean Physics, vol.27, No 10, pp.1080-1088.

Resnyansky Yu.D. and A.A.Zelenko [1992] Numerical realization of the ocean general circulation with parametrization of the upper mixed layer. Proceedings of the USSR Hydrometcentre, vol.323, pp.3-31.

Ruelle P. and U.W. Kesselring [1997] Aqueous solubility prediction of environmentally important chemicals from the mobile order thermodinamics. Chemosphere, vol. 34, No. 2, pp. 275-298.

Ruijgrok W. H.Tieben and P.Eisinga [1997] The dry deposition of particles to a forest canopy: a comparison of model and experimental results. Atmospheric Environment, vol.31, pp. 399-415.

Ryaboshapko A., Ilyin I., Bullock R., Ebinghaus R., Lohman K., Munthe J., Petersen G., Segneur C., Wangberg I. [2001] Intercomparison study of numerical models for long-range atmospheric transport of mercury. Stage I: Comparison of chemical modules for mercury transformations in a cloud/fog environment. EMEP/MSC-E Technical report 2/2001, Meteorological Synthesizing Centre – East, Moscow, Russia.

Rubinstein K. and D.Kiktev [1998] Comparison System of the Atmospheric Lower-Layer Diagnostic System(SDA) for Pollution Transfer Modeling of MSC - East(Moscow) and MSC - West(Oslo). Proceeding of International Conference of Air Pollution Modeling and Simulation. Paris, 26-29 October 1998.

Rubinstein K., Frolov A., Vaznik A., Astachova E., Rosinkina I., Kiktev D. and J.Alferov [1997] Diagnostic System of Atmosphere Lower-Layer for Pollution Transfer Modelling. Revista. International de Contaminational. Ambienal, v.13, No.1, pp.23-34.

Sander R. [1997] Henry's law constants available on the Web. EUROTRAC Newsletter, vol. 18, pp.24-25 (www.mpch-mainz.mpg.de/~sander/res/henry).

Schroeder W. H. and Munthe J. [1998] Atmospheric mercury - an overview. Atmos. Environ., vol.32, pp.809-822.

Schroeder W., Anlauf K., Barrie L. A., Lu J., Steffen A., Schneeberger D., Berg T. [1998] Arctic springtime depletion of mercury. Nature, vol.394, pp.331-332.

Schwarzenbach R.P., P.M.Gschwend and D.M.Imboden [1993] Environmental organic chemistry. John Wiley&Sons Inc., New York.

Scott B. C. [1982] Theoretical estimates of the scavenging coefficient for soluble aerosol particles as a function of precipitation type, rate and attitude. Atmos. Environ., vol. 16, p.1753-1762.

Sehmel G. A. [1980] Particle and gas dry deposition: a review. Atmos. Environ. vol.14, pp. 983-1011.

Seigneur C., Karamchandani P., Lohman K., Vijayaraghavan K., and Shia R.-L. [2001] Multiscale modeling of the atmospheric fate and transport of mercury. J. Geophys. Res., vol.106(D21), pp.27795-27809.

Seigneur C., Wrobel J. and Constantinou E. [1994] A chemical kinetic mechanism for atmospheric inorganic mercury. Environ. Sci. and Technol, vol.28, No.9, pp.1589-1597.

Seinfeld J.H., Pandis S.N. [1997] Atmospheric chemistry and physics: From air pollution to climate change, John Wiley, New York.

Sellers P.J., S.O. Los, C.J. Tucker, C.O. Justice, D.A. Dazlich, G.J. Collatz and D.A. Randall [1994] A global 1 by 1 degree NDVI data set for climate studies. Part 2: The generation of global fields of terrestrial biophysical parameters from the NDVI. International Journal of Remote Sensing, vol.15, No.17, pp.3519-3545.

Sellers P.J., S.O. Los, C.J. Tucker, C.O. Justice, D.A. Dazlich, G.J. Collatz and D.A. Randall [1995]. A revised land surface parameterization (SiB2) for atmospheric GCMs. Part 2: The generation of global fields of terrestrial biophysical parameters from satellite data. Submitted to Journal of Climate.

Sergeev Yu.N. (ed), A.A.Kolodochka, Hk.D.Krummel, V.P.Kulesh and O.P.Savchuk [1979] Modelling of substance transport and transformation processes in the sea; Modelling of substance transport and transformation processes in the sea. L., published by Leningrad State University, p. 291.

Shatalov V., A.Malanichev and N.Vulykh [2002] Assessment of POP transport and accumulation in the environment. MSC-E Technical Report 7/2002.

Shatalov V., A.Malanitchev, T.Berg and R.Larsen [2000] Investigation and assessment of POP transboundary transport and accumulation in different media, EMEP Report 4/2000, Part 1,2.

Shatalov V., M.Fedyunin, E.Mantseva, B.Strukov, N.Vulykh [2003] Persistent organic pollutants in the environment. MSC-E/Technical Report 4/2003.

Sijm D.T.H.M., H.Wever, P.J. de Vries and A.Opperhuizen [1989] Octan-1-ol/ water partition coefficients of polychlorinated dibenzo-p-dioxins and dibenzofurans: experimental values determined with a stirring method, Chemosphere, vol.19, No.1-6, pp.263-266.

Simpson D., Fagerli H., Jonson J.E., Tsyro S., Wind P., Tuovinen J-P. [2003] Transboundary acidification, eutrophication and ground level ozone in Europe. Part I: Unified EMEP Model Description. EMEP Report 1/2003, Meteorological Synthesizing Centre – West, Oslo, Norway.

Sinkkonen S. and J.Paasivirta [2000] Degradation half-life times of PCDDs, PCDFs and PCBs for environmental fate modelling. Chemosphere, vol.40, pp.943-949.

Slinn S. A., Slinn W.G.N. [1980] Predictions for particle deposition on natural waters. Atmos. Environ., vol.14, pp.1013-1016.

Slinn W.G.N. [1982] Predictions for particle deposition to vegetative canopies. Atmos. Environ., vol.16, pp.1785-1794.

Sommar J., Gårdfeldt K., Feng X., Lindquist O. [1999] Rate coefficients for gas-phase oxidation of elemental mercury by bromine and hydrocyl radicals. In: Mercury as a Global Pollutant. 5th International Conference, May 23-28, 1999, Rio de Janeiro, Brazil. Book of abstracts, p. 87.

Sommar J., Gårdfeldt K., Strömberg D., Feng X. [2001] A kinetic study of the gas-phase reaction between the hydroxyl radical and atomic mercury. Atmos. Environ. vol.35, pp.3049-3054.

Spivakovsky C.M., J.A.Logan, S.A.Montzka, Y.J.Balkanski, M.Foreman-Fowler, D.B.A.Jones, L.W.Horowitz, A.C.Fusco, C.A.M.Brenninkmeijer, M.J.Prather, S.C.Wofsy, M.B.McElroy [2000] Three-dimensional climatological distribution of tropospheric OH: Update and evaluation, J. Geophys. Res. vol.105, pp. 8931-8980.

SRC Chemfate [2001] Chemfate Search Result (SRC CSR) (http://www.syrres.com/) found via the database ChemIDplus [2001]: http://chem.sis.nlm.nih.gov/chemidplus.

SRC PhysProp Database (SRC PPD) [2001] found via the database ChemIDplus [2001]: http://chem.sis.nlm.nih.gov/chemidplus.

Strukov B., Yu. Resnyansky, A.Zelenko, A.Gusev and V.Shatalov [2000] Modelling long-range transport and deposition of POPs in the European region with emphasis to sea currents. EMEP/MSC-E Report 5/2000.

Sweetman A.J. and K.C.Jones [2000] Declining PCB concentrations in the U.K. atmosphere: evidence and possible causes. Environmental Science and Technology, vol.34, No. 5, pp.863-869.

ten Hulscher Th.E.M., L.E. van der Velde and W.A. Bruggeman [1992] Temperature Dependence of Henry's Law Constants for Selected Chlorobenzenes, Polychlorinated Biphenyls and Polycyclic Aromatic Hydrocarbons. Environ. Toxicol. Chem., vol.11, pp.1595-1603.

Thomas G., A.J.Sweetman, W.A.Ockenden, D.Mackay and K.C.Jones [1998] Environ. Science and Technology, vol.32, pp.936-942.

Tokos J. J. S., Hall B., Calhoun J. A., and Prestbo E. M. [1998] Homogeneous gas-phase reaction of Hg0 with H2O2, O3, CH3I, and (CH3)2S: implications for atmospheric Hg cycling. Atmos. Environ., vol.32, pp.823-827.

Travnikov O. [2001] Hemispheric Model of Airborne Pollutant Transport. EMEP/MSC-E Technical note 8/2001, Meteorological Synthesizing Centre - East, Moscow, Russia.

Travnikov O., Ryaboshapko A. [2002]. Modelling of mercury hemispheric transport and depositions. EMEP/MSC-E Technical Report 6/2002, Meteorological Synthesizing Centre - East, Moscow, Russia.

Tsibulsky V., V.Sokolovsky, S.Dutchak and V. Shatalov [2001] MSC-E contribution to the HM and POP emission inventories. Technical Note 7/2001. June 2001.

Tsyro S. and L.Erdman [2000] Parametrization of aerosol deposition processes in EMEP MSC-E and MSC-W transport models. EMEP/MSC-W Technical Note.

US EPA [1997] Mercury Study Report to Congress. Vol. III, Fate and Transport of Mercury in the Environment. US-EPA-452/R-97003.

Vassilyeva G. and V. Shatalov [2002] Behaviour of persistent organic pollutants in soil. MSC-E Technical Note 1/2002.

Walton J.J., MacCracken M.C. and Ghan S.J. [1988] A global-scale Lagrangian trace species model of transport, transformation, and removal processes. J. Geophys. Res., vol. 93(D7), pp.8339-8354.

Wang Y. J. et al. [1998] Global simulation of tropospheric O3-NOx-hydrocarbon chemistry 2: Model evaluation and global ozone budget. J. Geophys. Res. vol.103, pp. 10727-10755.

Wania F. [1997] Modelling Sea-Air Exchange of Persistent Organic Pollutants: Focus on Temperature and Other Seasonal Parameters. In: Sea-Air Exchange: Processes and Modelling. Ed. by J.M.Pacyna, D.Broman and E.Lipiatou 1998, pp.161-190.

Wania F. and J.-E. Haugen [1999] Long term measurements of wet deposition and precipitation scavenging of hexachlorocyclohexanes in Southern Norway, Environmental Pollution, vol.105, pp. 381-386.

Wesely M.L. and Hicks B.B. [2000] A review of the current status of knowledge on dry deposition. Atmos. Environ. vol.34, pp.2261-2282.

Wesely M.L., Cook D.R., Hart R.L. [1985] Measurements and parameterization of particulate sulfur dry deposition over grass. J. Geophys. Res., vol.90(D1), pp.2131-2143.

Williams R.M. [1982] A model for the dry deposition of particles to natural water surfaces. Atmos. Environ., vol. 16, pp.1933-1938.

Wu J. [1979] Oceanic whitecaps and sea state. J. Phys. Oceanogr., vol. 9, pp.1064-1068.

Yanenko N. N. [1971] The method of fractional steps. The solution of problems of mathematical physics in several variables. Springer-Verlag, New York. 160 p.

Zhang L., Gong S., Padro J., Barrie L. [2001] A size-segregated particle dry deposition scheme for an atmospheric aerosol module. Atmos. Environ., vol. 35, pp.549-560.

Annex A

CALCULATION OF THE VERTICAL VELOCITY

A possible approach to adjust the input meteorological fields to the model discritization is derivation of vertical wind velocity $\dot{\sigma}$ from the continuity equation for air at each time step [*Odman and Russel*, 2000]. For the exact mass conservation it is important to apply the same numerical scheme used for description of species advection to solution of the continuity equation. The solution is performed in two steps:

Step 1. Solution of the horizontal constituent of the air continuity equation for p^* using Bott advection scheme:

$$\frac{\partial p^*}{\partial t} = -m^2 \nabla_H \cdot \left(p^* \frac{\mathrm{V}_H}{m} \right) \tag{A.1}$$

For the initial condition the surface pressure at the beginning of the time step $(p^*)_t$ is used. As a result a tree-dimensional distribution of the intermediate pressure $(p^*)_{t+\Delta t/2} = f(x,y,\sigma)$ is obtained.

Step 2. Solution of the vertical constituent of the air continuity equation for the vertical velocity $\dot{\sigma}$:

$$\frac{\partial p^*}{\partial t} = -\frac{\partial}{\partial \sigma}\left(p^* \dot{\sigma}\right) \tag{A.2}$$

The intermediate pressure $(p^*)_{t+\Delta t/2}$ from the Step 1 is used as the initial condition; and the surface pressure at the end of the time step $(p^*)_{t+\Delta t} = f(x,y)$ interpolated from the input data is considered as a final condition. Keeping notations from [*Bott*, 1989a] the surface pressure at the end of the time step can be express as follows for each layer k of the model domain

$$\left(p^*\right)_{t+\Delta t} = \left(p_k^*\right)_{t+\Delta t/2} - I_k^{up} - I_k^{down} + \frac{\Delta\sigma_{k-1}}{\Delta\sigma_k} I_{k-1}^{up} + \frac{\Delta\sigma_{k+1}}{\Delta\sigma_k} I_{k+1}^{down}, \qquad k = 1, K_{max}, \tag{A.3}$$

where the integrals of mass coming up and down through the upper and lower borders of the gridcell, respectively, are given by :

$$I_k^{up} = \int_{-1/2}^{-1/2+\alpha_k^{up}} p^*(\xi)\,d\xi, \qquad I_k^{down} = \int_{1/2-\alpha_k^{down}}^{1/2} p^*(\xi)\,d\xi, \tag{A.4}$$

pressure distribution in a gridcell is approximated by the 2nd order polynomial:

$$p^*(\xi) = \sum_{n=0}^{2} a_{k,n}\xi^n, \qquad \xi = \frac{\sigma - \sigma_k}{\Delta\sigma_k} \tag{A.5}$$

and the local Courant numbers are calculated as follows:

$$\alpha_k^{up} = \frac{\left|\dot{\sigma}_k^{up}\right|\Delta t}{\Delta\sigma_k}, \qquad \alpha_k^{down} = \frac{\left|\dot{\sigma}_k^{down}\right|\Delta t}{\Delta\sigma_k} \tag{A.6}$$

The integrals of mass coming through the gridcell borders are derived from Eq. (A.3):

$$\begin{cases} I_k^{up} = \left(p_k^*\right)_{t+\Delta t/2} - \left(p^*\right)_{t+\Delta t} - I_k^{down} + \dfrac{\Delta\sigma_{k-1}}{\Delta\sigma_k} I_{k-1}^{up}, & I_k^{up} > 0 \\ I_{k+1}^{down} = \dfrac{\Delta\sigma_k}{\Delta\sigma_{k+1}} \left(\left(p^*\right)_{t+\Delta t} - \left(p_k^*\right)_{t+\Delta t/2} + I_k^{down} - \dfrac{\Delta\sigma_{k-1}}{\Delta\sigma_k} I_{k-1}^{up} \right), & I_k^{up} \le 0 \end{cases}, \qquad k = 1, K_{max}. \tag{A.7}$$

The calculation is started from the lowest layer where the mass flux through the ground surface is absent: $I_0^{up} = 0$ and $I_1^{down} = 0$. Substituting the polynomial approximation (A.5) to the Eqs. (A.4) and equating the obtained expressions to the values of the mass integrals calculated in Eq. (A.7) one can derive linear algebraic equations for the local Courant numbers α_k^{up} or α_k^{down} at borders of each gridcell (k = 1, K_{max}):

$$\sum_{n=0}^{2} \frac{a_{k,n}}{(n+1)2^{n+1}} (-1)^n \left[1 - \left(1 - 2\alpha_k^{up}\right)^{n+1} \right] = I_k^{up} \tag{B.8}$$

$$\sum_{n=0}^{2} \frac{a_{k+1,n}}{(n+1)2^{n+1}} \left[1 - \left(1 - 2\alpha_{k+1}^{down}\right)^{n+1} \right] = I_{k+1}^{down} \tag{B.9}$$

Only one of Eqs. (A.8) and (A.9) is taken for each gridcell border. For example, for the upper border of gridcell k Eq. (A.8) is chosen if $I_k^{up} > 0$ and Eq. (A.9) in the opposite case. The Eqs. (A.8) or (A.9) are solved for α_k^{up} or α_k^{down}, respectively, using the Newton's method. Vertical velocities are derived from the appropriate Courant numbers using expressions (A.6).

Annex B

PHYSICAL CHEMICAL PROPERTIES OF SELECTED POPs AND SUBSTANCE-SPECIFIC PARAMETERS

The values of physical-chemical properties, substance-specific parameters and degradation rates of POPs in the main environmental media (atmosphere, soil, seawater and vegetation) are presented below in Tables B.1-B.11.

B.1. Subcooled liquid-vapour pressure

The value of subcooled liquid-vapour pressure (p_{OL}, Pa) is used in the modelling of the process of POP partitioning between its particulate and gaseous phase in the atmosphere in accordance with the Junge-Pankow adsorption model [*Junge*, 1977; *Pankow*, 1987]. Thus, the value of p_{OL} determining the particle-bound fraction of a pollutant in air strongly influences such subsequent important processes as dry and wet deposition and degradation in air.

The value of subcooled liquid-vapour pressure (p_{OL}, Pa) depends on the air temperature and is included in the model in the following form:

$$p_{OL} = p_{OL}^0 \exp\left[-a_P\left(\frac{1}{T}-\frac{1}{T_0}\right)\right], \quad \text{(B.1)}$$

where T is the ambient temperature, K;
T_0 is the reference temperature, K;
p_{OL}^0 is the value of p_{OL} at the reference temperature T_0;
a_P is the coefficient of the vapour pressure temperature dependence, K.

Coefficients of p_{OL} temperature dependence and base values given at the temperature 283.15 K (T_0) for the selected POPs are presented in Table B.1. The way in which these coefficients of the temperature dependence were obtained or recalculated from original data presented in the literature used is specified in the field "Comments".

The temperature dependence of p_{OL} essentially affects the long-range transport of a pollutant. It increases with increasing temperature for all considered compounds. POPs with the lowest values of vapour pressure the same as PAHs, heavier congeners of PCDD/Fs and PCBs exist in the atmosphere preferably sorbed on atmospheric aerosol particles thereby increasing the probability of their subsequent deposition and washout with precipitation.

Table B.1. *Coefficients of p_{OL} temperature dependence used in model parameterization*

Compound		Values			Comments	Reference
		p^0_{OL}, Pa	a_P, K	T_0, K		
PAHs	B[a]P	$9.34 \cdot 10^{-7}$	11488	283.15	Coefficients of the exponential equation are recalculated from the standard form of temperature dependence: $\log p_{OL}$ (Pa) = $-A/T(K) + B$ with the help of the following formulas: $a_p = \ln(10) \cdot A$, $p^0_{OL} = 10^{(-A/To + B)}$ where for: B[a]P A = 4989, B = 11.59; B[b]F A = 4578, B = 9.48; B[k]F A = 4427, B = 9.48; I_P A = 4839, B = 9.6.	*Hinckley et al*., 1990
	B[b]F	$2.05 \cdot 10^{-7}$	10541	283.15		*Paasivirta et al*., 1999
	B[k]F	$7.00 \cdot 10^{-7}$	10194	283.15		
	I_P	$3.24 \cdot 10^{-8}$	11142	283.15		
PCDDs	2,3,7,8-TCDD	$8.11 \cdot 10^{-5}$	10113	283.15	Coefficients of the exponential equation are recalculated from the standard form of temperature dependence: $\log p_{OL}$ (Pa) = $-A/T(K) + B$ with the help of the following formulas: $a_p = \ln(10) \cdot A$, $p^0_{OL} = 10^{(-A/To + B)}$ where for: 2,3,7,8-TCDD A = 4392, B = 11.42 1,2,3,7,8-PeCDD A = 4778, B = 11.90 1,2,3,4,7,8–HxCDD A = 4840, B = 11.75 1,2,3,6,7,8-HxCDD A = 4803, B = 11.41 1,2,3,7,8,9-HxCDD A = 4957, B = 12.01 1,2,3,4,6,7,8-HpCDD A = 5017, B = 11.91 OCDD A = 4676, B = 11.20	*Bulgakov and Ioannisian*, 1998
	1,2,3,7,8-PeCDD	$1.06 \cdot 10^{-5}$	11002	283.15		
	1,2,3,4,7,8–HxCDD	$4.54 \cdot 10^{-6}$	11145	283.15		
	1,2,3,6,7,8-HxCDD	$2.8 \cdot 10^{-6}$	11059	283.15		
	1,2,3,7,8,9-HxCDD	$3.19 \cdot 10^{-6}$	11414	283.15		
	1,2,3,4,6,7,8-HpCDD	$1.55 \cdot 10^{-6}$	11552	283.15		
	OCDD	$4.85 \cdot 10^{-6}$	10767	283.15		
PCDFs	2,3,7,8-TCDF	$1.31 \cdot 10^{-4}$	10002	283.15	Coefficients of the exponential equation are recalculated from the standard form of temperature dependence: $\log p_{OL}$ (Pa) = $-A/T(K) + B$ with the help of the following formulas: $a_p = \ln(10) \cdot A$, $p^0_{ol} = 10^{(-A/To + B)}$ where for: 2,3,7,8-TCDF A = 4344, B = 11.46 1,2,3,7,8-PeCDF A = 4504, B = 11.54 2,3,4,7,8–PeCDF A = 4607, B = 11.70 1,2,3,4,7,8–HxCDF A = 4655, B = 11.54 1,2,3,6,7,8-HxCDF A = 4645, B = 11.49 1,2,3,7,8,9-HxCDF A = 4643, B = 11.51 2,3,4,6,7,8-HxCDF A = 4629, B = 11.49 1,2,3,4,6,7,8-HpCDF A = 4735, B = 11.49 1,2,3,4,7,8,9-HpCDF A = 4777, B = 11.43 OCDF A = 4805, B = 11.24	*Bulgakov and Ioannisian*, 1998
	2,3,4,7,8–PeCDF	$2.69 \cdot 10^{-5}$	10608	283.15		
	1,2,3,4,7,8–HxCDF	$1.26 \cdot 10^{-5}$	10719	283.15		
	1,2,3,6,7,8-HxCDF	$1.22 \cdot 10^{-5}$	10696	283.15		
	1,2,3,7,8,9-HxCDF	$1.30 \cdot 10^{-5}$	10691	283.15		
	2,3,4,6,7,8-HxCDF	$1.39 \cdot 10^{-5}$	10659	283.15		
	1,2,3,4,6,7,8-HpCDF	$5.85 \cdot 10^{-6}$	10903	283.15		
	1,2,3,4,7,8,9-HpCDF	$3.62 \cdot 10^{-6}$	10999	283.15		
	OCDF	$1.86 \cdot 10^{-6}$	11064	283.15		
PCBs	PCB-28	$6.43 \cdot 10^{-3}$	9383	283.15	Coefficients of the exponential equation are recalculated from the standard form of temperature dependence: $\log p_{OL}$ (Pa) = $-A/T(K) + B$ with the help of the following formulas: $a_p = \ln(10) \cdot A$, $p^0_{OL} = 10^{(-A/To + B)}$ where for: PCB-28 A = 4075, B = 12.20 PCB-105 A = 4758, B = 12.9 PCB-118 A = 4664, B = 12.72 PCB-153 A = 4775, B = 12.85 PCB-180 A = 5042, B = 13.03	*Falconer and Bidleman,* 1994
	PCB-105	$1.25 \cdot 10^{-4}$	10956	283.15		
	PCB-118	$1.77 \cdot 10^{-4}$	10739	283.15		
	PCB-153	$9.69 \cdot 10^{-5}$	10995	283.15		
	PCB-180	$1.67 \cdot 10^{-5}$	11610	283.15		
γ-HCH		$1.424 \cdot 10^{-2}$	8474	283.15	Coefficients of the exponential equation are recalculated from the standard form of temperature dependence: $\log p_{OL}$ (Pa) = $- 3680/T(K) + 11.15$ with the help of the following formulas: $a_p = \ln(10) \cdot 3680$, $p^0_{OL} = 10^{(-3680/To + 11.15)}$	*Hinckley et al*., 1990
HCB		$2.88 \cdot 10^{-2}$	8248	283.15	Coefficients of the exponential equation are recalculated from the standard form of temperature dependence: $\log p_{OL}$ (Pa) = $-3582/T(K) + 11.11$ with the help of the following formulas: $a_p = \ln(10) \cdot 3582$, $p^0_{OL} = 10^{(-3582/To + 11.11)}$	*Hinckley et al*., 1990

B.2. Henry's law constant and air/water partition coefficient

The value of the air-water Henry's law constant or the air/water partition coefficient are used in the description of the gaseous exchange process between the atmosphere and soil, between the atmosphere and seawater, as well as of wet deposition of the POP gaseous phase. Relation between the air-water Henry's law constant, (K_H, Pa·m^3/mol) and the air/water partition coefficient (K_{aw}, dimensionless) is as follows:

$$K_{aw} = K'_H = \frac{K_H}{RT}, \tag{B.2}$$

where T - temperature, K;
R = 8.314 J/(mol·K) - universal gas constant.

The temperature dependence of Henry's law constant in the dimensionless form (K'_H) used in the model parameterization is expressed by the following equation:

$$K'_H = \frac{K_{H0}}{RT} \exp\left[-a_H \left(\frac{1}{T} - \frac{1}{T_0} \right) \right], \tag{B.3}$$

where T is the ambient air temperature, K;
T_0 is the reference temperature;
R is the universal gas constant, J/(mol·K),
a_H is the coefficient of Henry's law constant temperature dependence, K;
K_{H0} is the value of Henry's law constant at reference temperature, Pa·m^3/mol.

Coefficients of the temperature dependence of the Henry's law constant for the selected POPs are presented in Table B.2. The way in which these coefficients of the temperature dependence were obtained or recalculated from original data presented in the literature used is specified in the field "Comments".

Table B.2. *Coefficients of temperature dependence of Henry`s law constant used in model parameterization*

Compound		Values			Comments	Reference
		K_{H0}, Pa·m^3/mol	a_H, K	T_0, K		
PAHs	B[a]P	$5.44 \cdot 10^{-2}$	7866	283.15	Coefficients of the exponential equation are recalculated from the standard form of temperature dependence: log K_H (Pa·m^3/mol) = -A/T(K) + B with the help of the following formulas: a_H = ln(10) · A, $K_{H0} = 10^{(-A/To + B)}$ where for: B[a]P A = 3416, B = 10.8; B[b]F A = 3416, B = 10.4; B[k]F A = 3416, B = 10.7; I_P A = 3416, B = 10.0	*Ten Hulscher et al.,* 1992 cited by *Galarneau et al*., 2000
	B[b]F	$2.166 \cdot 10^{-2}$	7866	283.15		
	B[k]F	$4.322 \cdot 10^{-2}$	7866	283.15		
	I_P	$8.684 \cdot 10^{-3}$	7866	283.15		
PCDDs	2,3,7,8-TCDD	0.333	10104	283.15	Coefficients of the exponential equation are recalculated from the standard form of temperature dependence: log K_H (Pa·m^3/mol) = -A/T(K) + B with the help of the following formulas: a_H = ln(10) · A, $K_{H0} = 10^{(-A/To + B)}$ where for: 2,3,7,8-TCDD A = 4388, B = 15.02; 1,2,3,7,8-PeCDD A = 4522, B = 15.32; 1,2,3,4,7,8–HxCDD A = 4978, B = 16.08; 1,2,3,6,7,8-HxCDD A = 4936, B = 15.92; 1,2,3,7,8,9-HxCDD A = 5090, B = 16.60; 1,2,3,4,6,7,8-HpCDD A = 5621, B = 17.95; OCDD A = 4004, B = 13.27	*Bulgakov and Ioannisian*, 1998
	1,2,3,7,8-PeCDD	0.224	10412	283.15		
	1,2,3,4,7,8–HxCDD	$3.16 \cdot 10^{-2}$	11462	283.15		
	1,2,3,6,7,8-HxCDD	$3.07 \cdot 10^{-2}$	11366	283.15		
	1,2,3,7,8,9-HxCDD	$4.2 \cdot 10^{-2}$	11720	283.15		
	1,2,3,4,6,7,8-HpCDD	$1.25 \cdot 10^{-2}$	12943	283.15		
	OCDD	0.135	9219.6	283.15		

Table B.2. *(continued)*

PCDFs	2,3,7,8-TCDF	0.274	8998.5	283.15	Coefficients of the exponential equation are recalculated from the standard form of temperature dependence: $\log K_H$ (Pa·m^3/mol) = $-A/T(K) + B$ with the help of the following formulas: $a_H = \ln(10) \cdot A$, $K_{H0} = 10^{(-A/To + B)}$ where for: 2,3,7,8-TCDF A = 3908, B = 13.24 1,2,3,7,8-PeCDF A = 4392, B = 14.11 2,3,4,7,8–PeCDF A = 4468, B = 14.69 1,2,3,4,7,8–HxCDF A = 4832, B = 16.35 1,2,3,6,7,8-HxCDF A = 4816, B = 15.91 1,2,3,7,8,9-HxCDF A = 4816, B = 16.00 2,3,4,6,7,8-HxCDF A = 4801, B = 15.93 1,2,3,4,6,7,8-HpCDF A = 5211, B = 16.42 1,2,3,4,7,8,9-HpCDF A = 5241, B = 16.62 OCDF A = 4537, B = 14.59	
	1,2,3,7,8-PeCDF	$3.97 \cdot 10^{-2}$	10113	283.15		
	2,3,4,7,8–PeCDF	$8.14 \cdot 10^{-2}$	10288	283.15		
	1,2,3,4,7,8–HxCDF	0.193	11126	283.15		
	1,2,3,6,7,8-HxCDF	$7.97 \cdot 10^{-2}$	11089	283.15		
	1,2,3,7,8,9-HxCDF	$9.80 \cdot 10^{-2}$	11089	283.15		
	2,3,4,6,7,8-HxCDF	$9.43 \cdot 10^{-2}$	11055	283.15		
	1,2,3,4,6,7,8-HpCDF	$1.04 \cdot 10^{-2}$	11999	283.15		
	1,2,3,4,7,8,9-HpCDF	$1.29 \cdot 10^{-2}$	12068	283.15		
	OCDF	$3.69 \cdot 10^{-2}$	10447	283.15		
PCBs	PCB-28	7.642	7430	283.15	Coefficients of the exponential equation are recalculated from the standard form of temperature dependence: $\log K_H$ (Pa·m^3/mol)= $-A/T$(K) + B with the help of the following formulas: $a_H = \ln(10) \cdot A$, $K_{H0} = 10^{(-A/To + B)}$; where $A = \Delta H_W / 2.303R$; $B = \log H_{298} + \Delta H_W / 2.303R(298)$. H_{298} is Henry's law constant (Pa·m^3/mol) at 25^{0}C taken from [*Dunnivant et al.*, 1992]: PCB-28: 28.58 PCB-105: 10.03 PCB-118: 12.69 PCB-153: 16.48 PCB-180: 10.74 ΔH_W is the enthalpy of volatilization from water, kJ/mol taken from [*Burkhard et al*., 1985 cited in *Wania*, 1997]: PCB-28: 61.8 PCB-105: 67.2 PCB-118: 67.2 PCB-153: 69.4 PCB-180: 71.3	estimated
	PCB-105	2.365	8082	283.15		
	PCB-118	3.046	8082	283.15		
	PCB-153	3.781	8347	283.15		
	PCB-180	2.388	8575	283.15		
γ-HCH		0.1341	5485	283.15	Coefficients of the exponential equation are recalculated from the standard form of temperature dependence: $\log K_H$ (Pa·m^3/mol) = $-A/T(K) + B$ with the help of the following formulas: $a_H = \ln(10) \cdot A$, $K_{H0} = 10^{(-A/To + B)}$ where for: distilled water A = 2382, B = 7.54 sea water A = 2703, B = 8.68.	distilled water: *Kucklick et al.,* 1991
		0.1361	6224	283.15		sea water*:* *Kucklick et al*., 1991
HCB		26.4	6190	283.15	Coefficients of the exponential equation are recalculated from the standard form of temperature dependence: $\log K_H$ (Pa·m^3/mol) = $-A/T(K) + B$ with the help of the following formulas: $a_H = \ln(10) \cdot A$, $K_{H0} = 10^{(-A/To + B)}$ where for HCB: A = 2715 , B = 11.009 A and B were estimated with the use of temperature dependencies of p_{OL} and S_{WL} given in [*Beyer and Matthies*, 2001] $\log K_H = \log p_{OL} - \log S_{WL}$	estimated

B.3. Dry deposition velocities over land, sea, and forest

Velocities of dry deposition over land, sea, and forest are used for modelling of PAHs, PCDD/Fs, and PCBs which exist in the atmosphere mainly particle bounded. For γ-HCH and HCB, these parameters are not required because these pollutants are assumed to occur in the atmosphere only in the gas-phase.

Based on the measurement data on the distribution of low volatile POPs with particle sizes in the atmosphere, the velocity of dry deposition to different underlying surfaces for PAHs and PCDD/Fs is calculated for particles-carriers with effective aerodynamic diameter 0.84 μm and for PCBs – for particles with effective diameter 0.55 μm [*Tsyro and Erdman*, 2000; *Pekar et al.,* 1999*; Shatalov et al*., 2000; *Mantseva et al.,* 2002].

Dry deposition velocities over sea from 10 m height and over land (except forests) from 1 m height are determined using Eq. 3.5 and 3.6 in Section "Dry deposition of the particulate phase" with the use of constants presented in Table B.3. The table also provides the constants defining velocities of dry deposition to a forest, which are calculated by Eq. 3.7 and 3.8 in Section "Dry deposition of the particulate phase".

Table B.3. *Constants for the calculation of dry deposition velocities over land, sea, and forest used in the model parameterization*

Compound		Aerodynamic diameter of particle-carriers, μm	Values							
			Dry deposition velocity over land			Dry deposition velocity over sea		Dry deposition velocity over forest		
			A_{soil}	B_{soil}	C_{soil}	A_{sea}	B_{sea}	α	β	γ
PAHs	B[a]P	0.84	0.04	0.02	0.3	0.15	0.023	0.06	0.3	0.25
	B[b]F		0.04	0.02	0.3	0.15	0.023	0.06	0.3	0.25
	B[k]F		0.04	0.02	0.3	0.15	0.023	0.06	0.3	0.25
	I_P		0.04	0.02	0.3	0.15	0.023	0.06	0.3	0.25
PCDDs	2,3,7,8-TCDD	0.84	0.04	0.02	0.3	0.15	0.023	0.06	0.3	0.25
	1,2,3,7,8-PeCDD		0.04	0.02	0.3	0.15	0.023	0.06	0.3	0.25
	1,2,3,4,7,8–HxCDD		0.04	0.02	0.3	0.15	0.023	0.06	0.3	0.25
	1,2,3,6,7,8-HxCDD		0.04	0.02	0.3	0.15	0.023	0.06	0.3	0.25
	1,2,3,7,8,9-HxCDD		0.04	0.02	0.3	0.15	0.023	0.06	0.3	0.25
	1,2,3,4,6,7,8-HpCDD		0.04	0.02	0.3	0.15	0.023	0.06	0.3	0.25
	OCDD		0.04	0.02	0.3	0.15	0.023	0.06	0.3	0.25
PCDFs	2,3,7,8-TCDF		0.04	0.02	0.3	0.15	0.023	0.06	0.3	0.25
	1,2,3,7,8-PeCDF		0.04	0.02	0.3	0.15	0.023	0.06	0.3	0.25
	2,3,4,7,8-PeCDF		0.04	0.02	0.3	0.15	0.023	0.06	0.3	0.25
	1,2,3,4,7,8-HxCDF		0.04	0.02	0.3	0.15	0.023	0.06	0.3	0.25
	1,2,3,6,7,8-HxCDF		0.04	0.02	0.3	0.15	0.023	0.06	0.3	0.25
	1,2,3,7,8,9-HxCDF		0.04	0.02	0.3	0.15	0.023	0.06	0.3	0.25
	2,3,4,6,7,8-HxCDF		0.04	0.02	0.3	0.15	0.023	0.06	0.3	0.25
	1,2,3,4,6,7,8-HpCDF		0.04	0.02	0.3	0.15	0.023	0.06	0.3	0.25
	1,2,3,4,7,8,9-HpCDF		0.04	0.02	0.3	0.15	0.023	0.06	0.3	0.25
	OCDF		0.04	0.02	0.3	0.15	0.023	0.06	0.3	0.25
PCBs	PCB-28	0.55	0.02	0.01	0.33	0.15	0.013	0.048	0.3	0.25
	PCB-105		0.02	0.01	0.33	0.15	0.013	0.048	0.3	0.25
	PCB-118		0.02	0.01	0.33	0.15	0.013	0.048	0.3	0.25
	PCB-153		0.02	0.01	0.33	0.15	0.013	0.048	0.3	0.25
	PCB-180		0.02	0.01	0.33	0.15	0.013	0.048	0.3	0.25

B.4. Washout ratio

In the model parameterization for HCB total washout ratio determined on the basis of measurement data (W_T, dimensionless) is used. For other considered POPs, wet depositions of the gaseous and particulate phases are considered separately in the model (See Eqs. (3.11) and (3.13) in Section "Wet deposition"). In the model description of gaseous phase scavenging with precipitation it is assumed that equilibrium between the vapour phase and the dissolved phase in a raindrop is attained rapidly and washout ratios for the gaseous phase (W_g, dimensionless) of PAHs, PCDD/Fs and PCBs is determined as inverse values to dimensionless Henry's law constant:

$$W_g = 1/K'_H \qquad \text{(B.5)}$$

where K'_H is the dimensionless Henry's law constant.

W_g may be also defined experimentally by the relationship of a substance concentration in the dissolved phase in wet depositions and in the gaseous phase in air. In particular, γ-HCH washout ratio for the gaseous phase is empirically obtained on the basis of simultaneous measurements in air and precipitation [*Wania et al.*, 1999].

For the description of particle bound phase scavenging of PAHs, PCDD/Fs, and PCBs with precipitation (W_p, dimensionless), values of the washout ratio determined experimentally or derived theoretically are used. Wet deposition of POP particle bound phase is the dominant removal mechanism by precipitation for pollutants, which are present in the atmosphere in the most part associated with particles.

Table B.4 gives washout ratio values of the considered pollutants used in the model parameterization. The way in which these values were selected is specified in the field "Comments".

Table B.4. *Washout ratio, (dimensionless) used in the model parameterization*

Compound		Values rain	Comments	Reference
PAHs	B[a]P B[b]F B[k]F I_P	$5.0 \cdot 10^4$	W_p selected on the basis of geometric mean values of 4 indicator PAHs estimated from measurement data: B[a]P $7.37 \cdot 10^4$ B[k]F $5.90 \cdot 10^4$ B[b]F $2.62 \cdot 10^4$ I_P $9.03 \cdot 10^4$	*Ligocki et al*., 1985, *Poster and Baker*, 1996, *Hoff et al.,* 1996, *Franz and Eisenreich,* 1998
PCDDs	2,3,7,8-TCDD	$5.50 \cdot 10^4$	Values of W_p (homologue-specific) determined experimentally were selected in [*Harrad and Smith*, 1997; *Meneses et al*., 2002] for modelling; For 2,3,7,8-TCDD the value is assumed to equal that of TCDFs.	*Koester and Hites,* 1992*; Standley and Hites,* 1991 *cited by Harrad and Smith*, 1997; *Meneses et al*., 2002
	1,2,3,7,8-PeCDD	$1.80 \cdot 10^4$		
	1,2,3,4,7,8–HxCDD	$1.20 \cdot 10^4$		
	1,2,3,6,7,8-HxCDD	$1.20 \cdot 10^4$		
	1,2,3,7,8,9-HxCDD	$1.20 \cdot 10^4$		
	1,2,3,4,6,7,8-HpCDD	$5.90 \cdot 10^4$		
	OCDD	$7.20 \cdot 10^4$		
PCDFs	2,3,7,8-TCDF	$5.50 \cdot 10^4$	Values of W_p (homologue-specific) determined experimentally were selected in [*Harrad and Smith*, 1997; *Meneses et al*., 2002] for modelling	*Koester and Hites,* 1992*; Standley and Hites,* 1991 *cited by Harrad and Smith*, 1997; *Meneses et al*., 2002
	1,2,3,7,8-PeCDF	$1.80 \cdot 10^4$		
	2,3,4,7,8–PeCDF	$1.80 \cdot 10^4$		
	1,2,3,4,7,8–HxCDF	$1.0 \cdot 10^4$		
	1,2,3,6,7,8-HxCDF	$1.0 \cdot 10^4$		
	1,2,3,7,8,9-HxCDF	$1.0 \cdot 10^4$		
	2,3,4,6,7,8-HxCDF	$1.0 \cdot 10^4$		
	1,2,3,4,6,7,8-HpCDF	$3.0 \cdot 10^4$		
	1,2,3,4,7,8,9-HpCDF	$3.0 \cdot 10^4$		
	OCDF	$1.2 \cdot 10^4$		
PCBs	PCB-28	$1.5 \cdot 10^5$	W_p for PCB-28, PCB-105, PCB-118, PCB-180 is assumed to be equal W_p of PCB-153, which experimentally determined value is selected in [*Sweetman and Jones* 2000] for modelling	*Swackhamer, et al.,* 1988 cited by *Sweetman and Jones*, 2000
	PCB-105			
	PCB-118			
	PCB-153			
	PCB-180			
γ-HCH		$3.7 \cdot 10^4$	Experimentally determined value of W_g [*Ma et al.,* 2003]	*Atlas and Giam,* 1988 *cited by Ma et al.,* 2003
HCB		$1.0 \cdot 10^4$	W_t selected on the basis of measurement data	*Berg and Hjellbrekke,* 1998, 1999*; Berg et al.,* 1996, 1997, 2000, 2001, 2002; *Hoff et al.,* 1996*; Eisenreich et al.,* 1981

B.5. Degradation rate constants in environmental media

Degradation process of POPs in the atmosphere is considered as the gas-phase reaction of pollutants with hydroxyl radicals and all other reactions are neglected. In MSCE-POP model, the degradation process in the atmosphere is expressed by the equation of the second order (see Eq. (3.14) in Section “Degradation in air”). Temperature dependence of degradation rate constant of the gas-phase reaction with OH-radical is taken in the form of Arrenius equation:

$$k_{air} = A \cdot \exp(-E_a / RT), \qquad \text{(B.6)}$$

where A is the pre-exponential multiplier; $cm^3/(molec \cdot s)$;

E_a is the activation energy of interaction with OH-radical in air, J/mol;

R is the universal gas constant, J/(mol · K);

T is the ambient temperature, K.

This equation is applied for the gaseous phase of a pollutant only. Values of the pre-exponential multiplier and the activation energy for the temperature dependence of degradation rate constant in the atmosphere for the considered pollutants are displayed in Table B.5. Temperature dependent degradation rate constant are implied for PCBs, γ-HCH and HCB. Of note that for PAHs and PCDD/Fs no such temperature dependence exists in the literature and the values of second order rate constant for the gas-phase reaction with OH-radical at 25°C are used in the calculations.

Table B.5. *Coefficients of temperature dependence of degradation rate constants in air k_{air}, used in model parameterization*

Compound		Values		Reference
		A, $cm^3/(molec \cdot s)$	E_A, J/mol	
PAHs	B[a]P	$5 \cdot 10^{-11}$	-	*Meylan and Howard,* 1993 cited in *SRC PhysProp Database*
	B[b]F	$1.86 \cdot 10^{-11}$	-	
	B[k]F	$5.36 \cdot 10^{-11}$	-	
	I_P	$6.447 \cdot 10^{-11}$	-	
PCDDs	2,3,7,8-TCDD	$1.05 \cdot 10^{-12}$	-	*Brubaker and Hites*, 1997
	1,2,3,7,8-PeCDD	$5.6 \cdot 10^{-13}$	-	
	1,2,3,4,7,8–HxCDD	$2.7 \cdot 10^{-13}$	-	
	1,2,3,6,7,8-HxCDD	$2.7 \cdot 10^{-13}$	-	
	1,2,3,7,8,9-HxCDD	$2.7 \cdot 10^{-13}$	-	
	1,2,3,4,6,7,8-HpCDD	$1.3 \cdot 10^{-13}$	-	
	OCDD	$5.0 \cdot 10^{-14}$	-	
PCDFs	2,3,7,8-TCDF	$6.1 \cdot 10^{-13}$	-	*Brubaker and Hites*, 1997
	1,2,3,7,8-PeCDF	$3.0 \cdot 10^{-13}$	-	
	2,3,4,7,8–PeCDF	$3.0 \cdot 10^{-13}$	-	
	1,2,3,4,7,8–HxCDF	$1.4 \cdot 10^{-13}$	-	
	1,2,3,6,7,8-HxCDF	$1.4 \cdot 10^{-13}$	-	
	1,2,3,7,8,9-HxCDF	$1.4 \cdot 10^{-13}$	-	
	2,3,4,6,7,8-HxCDF	$1.4 \cdot 10^{-13}$	-	
	1,2,3,4,6,7,8-HpCDF	$6.0 \cdot 10^{-14}$	-	
	1,2,3,4,7,8,9-HpCDF	$6.0 \cdot 10^{-14}$	-	
	OCDF	$3.0 \cdot 10^{-14}$	-	
PCBs	PCB-28	$2.7 \cdot 10^{-10}$	13720	*Anderson and Hites*, 1996; *Beyer and Matthies,* 2001
	PCB-105	$6.15 \cdot 10^{-11}$	12920	
	PCB-118	$6.15 \cdot 10^{-11}$	12920	
	PCB-153	$8.12 \cdot 10^{-11}$	15380	
	PCB-180	$1.4 \cdot 10^{-10}$	17840	
γ-HCH		$6 \cdot 10^{-11}$	14200	*Brubaker and Hites*, 1998
HCB		$4.9 \cdot 10^{-10}$	24300	*Brubaker and Hites,* 1998

In the MSCE-POP model the degradation process of POPs in soil and seawater is described as a first-order process by Eq. (3.28) (Section “Degradation in soil”) and Eq. (3.36) (Section “Degradation in seawater”). The degradation rate constants in these media for the considered POPs are presented in Table B.6. Of note that degradation rate constant for γ-HCH hydrolysis in seawater at pH = 8 used in model parameterization is taken to be temperature dependent.

Table B.6. *Degradation rate constants in environmental media k_{soil} and k_{sea} used in model parameterization*

Compound		Values		Comments	Reference
PAHs	B[a]P	k_{soil}, s^{-1}	$1.13 \cdot 10^{-8}$	Temperature independent; recalculated from recommended half-lives	*Mackay et al*., 1992b
		k_{sea}, s^{-1}	$1.13 \cdot 10^{-7}$		
	B[b]F	k_{soil}, s^{-1}	$1.13 \cdot 10^{-8}$		
		k_{sea}, s^{-1}	$1.13 \cdot 10^{-7}$		
	B[k]F	k_{soil}, s^{-1}	$1.13 \cdot 10^{-8}$		
		k_{sea}, s^{-1}	$1.13 \cdot 10^{-7}$		
	I_P	k_{soil}, s^{-1}	$1.13 \cdot 10^{-8}$		
		k_{sea}, s^{-1}	$1.13 \cdot 10^{-7}$		
PCDDs	2,3,7,8-TCDD	k_{soil}, s^{-1}	$2.14 \cdot 10^{-10}$	Temperature independent; recalculated from recommended half-lives	*Sinkkonen and Paasivirta,* 2000
		k_{sea}, s^{-1}	$4.81 \cdot 10^{-8}$		
	1,2,3,7,8-PeCDD	k_{soil}, s^{-1}	$1.93 \cdot 10^{-10}$		
		k_{sea}, s^{-1}	$2.67 \cdot 10^{-8}$		
	1,2,3,4,7,8–HxCDD	k_{soil}, s^{-1}	$8.02 \cdot 10^{-11}$		
		k_{sea}, s^{-1}	$1.30 \cdot 10^{-8}$		
	1,2,3,6,7,8-HxCDD	k_{soil}, s^{-1}	$3.50 \cdot 10^{-10}$		
		k_{sea}, s^{-1}	$1.30 \cdot 10^{-8}$		
	1,2,3,7,8,9-HxCDD	k_{soil}, s^{-1}	$2.75 \cdot 10^{-10}$		
		k_{sea}, s^{-1}	$1.30 \cdot 10^{-8}$		
	1,2,3,4,6,7,8-HpCDD	k_{soil}, s^{-1}	$2.14 \cdot 10^{-9}$		
		k_{sea}, s^{-1}	$6.42 \cdot 10^{-9}$		
	OCDD	k_{soil}, s^{-1}	$1.48 \cdot 10^{-10}$		
		k_{sea}, s^{-1}	$2.44 \cdot 10^{-9}$		
PCDFs	2,3,7,8-TCDF	k_{soil}, s^{-1}	$3.50 \cdot 10^{-10}$	Temperature independent; recalculated from recommended half-lives	*Sinkkonen and Paasivirta,* 2000
		k_{sea}, s^{-1}	$3.01 \cdot 10^{-8}$		
	1,2,3,7,8-PeCDF	k_{soil}, s^{-1}	$4.28 \cdot 10^{-10}$		
		k_{sea}, s^{-1}	$1.46 \cdot 10^{-8}$		
	2,3,4,7,8–PeCDF	k_{soil}, s^{-1}	$3.50 \cdot 10^{-10}$		
		k_{sea}, s^{-1}	$1.46 \cdot 10^{-8}$		
	1,2,3,4,7,8–HxCDF	k_{soil}, s^{-1}	$3.21 \cdot 10^{-10}$		
		k_{sea}, s^{-1}	$6.88 \cdot 10^{-9}$		
	1,2,3,6,7,8-HxCDF	k_{soil}, s^{-1}	$2.75 \cdot 10^{-10}$		
		k_{sea}, s^{-1}	$6.88 \cdot 10^{-9}$		
	1,2,3,7,8,9-HxCDF	k_{soil}, s^{-1}	$3.85 \cdot 10^{-10}$		
		k_{sea}, s^{-1}	$6.88 \cdot 10^{-9}$		
	2,3,4,6,7,8-HxCDF	k_{soil}, s^{-1}	$4.28 \cdot 10^{-10}$		
		k_{sea}, s^{-1}	$6.88 \cdot 10^{-9}$		
	1,2,3,4,6,7,8-HpCDF	k_{soil}, s^{-1}	$5.50 \cdot 10^{-10}$		
		k_{sea}, s^{-1}	$3.01 \cdot 10^{-9}$		
	1,2,3,4,7,8,9-HpCDF	k_{soil}, s^{-1}	$6.42 \cdot 10^{-10}$		
		k_{sea}, s^{-1}	$3.01 \cdot 10^{-9}$		
	OCDF	k_{soil}, s^{-1}	$7.70 \cdot 10^{-10}$		
		k_{sea}, s^{-1}	$1.00 \cdot 10^{-9}$		
PCBs	PCB-28	k_{soil}, s^{-1}	$7.4 \cdot 10^{-9}$	Temperature independent (on the average for +7 ºC); recalculated from recommended half-lives	*Sinkkonen and Paasivirta,* 2000
		k_{sea}, s^{-1}	$1.33 \cdot 10^{-7}$		
	PCB-105	k_{soil}, s^{-1}	$2.20 \cdot 10^{-9}$		
		k_{sea}, s^{-1}	$3.21 \cdot 10^{-9}$		
	PCB-118	k_{soil}, s^{-1}	$3.21 \cdot 10^{-9}$		
		k_{sea}, s^{-1}	$3.21 \cdot 10^{-9}$		
	PCB-153	k_{soil}, s^{-1}	$1.17 \cdot 10^{-9}$		
		k_{sea}, s^{-1}	$1.6 \cdot 10^{-9}$		
	PCB-180	k_{soil}, s^{-1}	$5.83 \cdot 10^{-10}$		
		k_{sea}, s^{-1}	$8.02 \cdot 10^{-10}$		
γ-HCH		k_{soil}, s^{-1} for soil depth <5cm	$5.73 \cdot 10^{-7}$	Temperature independent; recalculated from half-lives	*Dowd et al.,* 1993 *cited by Mackay et al.,* 1997
		k_{soil}, s^{-1} for soil depth 5-20cm	$8.91 \cdot 10^{-8}$		
		k_{soil}, s^{-1} Bio-degradation	$4.46 \cdot 10^{-8}$		*Rao and Davidson* 1980 *cited by Mackay et al.,* 1997
		k_{sea}^{0}, s^{-1}	$1.905 \cdot 10^{-9}$	The following temperature dependence is used: $k_{sea}=k_{sea}^{0} \cdot \exp(-B(1/T-1/T_0) - C\cdot(T-T_0))$ where T_0 = 283.15 $B = Ea/R + 4471 \cdot \ln(10)$; C = 0.03928 Ea = 84.6 kJ/mol; R = 8.314 J/(mol·K)	*Ngabe et al.,* 1993; *Harner et al.,* 1999
HCB		k_{soil}, s^{-1}	$5.24 \cdot 10^{-9}$	Temperature independent; recalculated from half-lives	*Sheringer,* 1997
		k_{sea}, s^{-1}	$5.24 \cdot 10^{-9}$		

B.6. Octanol-water partition coefficient

The octanol-water partition coefficient ($K_{OW,}$ dimensionless) is a measure of substance hydrophoby and characterizes its partitioning between water and lipid media substituted for octanol. K_{OW} is used for the estimation of the partition coefficient in the organic carbon-water system (K_{OC}), the partition coefficient in the octanol-air system (K_{OA}), and the bioconcentration factor (BCF). For the considered POPs partition coefficients in the "octanol-water" system selected for modelling are given in Table B.7.

Table B.7. *Octanol-water partition coefficient (K_{OW}), dimensionless used in the model parameterization*

Compound		Value K_{OW}	Comments	References
PAHs	B[a]P	$1.1 \cdot 10^6$	Temperature independent B[a]P log K_{OW} = 6.04 B[b]F log K_{OW} = 5.80 B[k]F log K_{OW} = 6.00 I_P log K_{OW} = 6.584	*Mackay et al.,* 1992b
	B[b]F	$6.31 \cdot 10^5$		
	B[k]F	$1.00 \cdot 10^6$		
	I_P	$3.84 \cdot 10^6$		*SRC Calculated Values,* 1988 cited in database *SRC Chemfate,* 2001
PCDDs	2,3,7,8-TCDD	$9.12 \cdot 10^6$	Temperature independent; 2,3,7,8-TCDD log K_{OW} = 6.96 1,2,3,7,8-PeCDD log K_{OW} = 7.27 1,2,3,4,7,8–HxCDD log K_{OW} = 7.80 1,2,3,6,7,8-HxCDD log K_{OW} = 7.96 1,2,3,7,8,9-HxCDD log K_{OW} = 7.76 1,2,3,4,6,7,8-HpCDD log K_{OW} = 8.0 OCDD log K_{OW} = 8.20	*Govers and Krop,* 1998
	1,2,3,7,8-PeCDD	$1.86 \cdot 10^7$		*Paasivirta et al.,* 1999
	1,2,3,4,7,8–HxCDD	$6.31 \cdot 10^7$		*Beyer and Matthies,* 2002
	1,2,3,6,7,8-HxCDD	$9.12 \cdot 10^7$		*Paasivirta et al.,* 1999
	1,2,3,7,8,9-HxCDD	$5.75 \cdot 10^7$		
	1,2,3,4,6,7,8-HpCDD	$1.00 \cdot 10^8$		*Beyer and Matthies,* 2002
	OCDD	$1.58 \cdot 10^8$		
PCDFs	2,3,7,8-TCDF	$3.80 \cdot 10^6$	Temperature independent; 2,3,7,8-TCDF log K_{OW} = 6.58 1,2,3,7,8-PeCDF log K_{OW} = 6.79 2,3,4,7,8–PeCDF log K_{OW} = 6.90 1,2,3,4,7,8–HxCDF log K_{OW} = 7.54 1,2,3,6,7,8-HxCDF log K_{OW} = 7.57 1,2,3,7,8,9-HxCDF log K_{OW} = 7.76 2,3,4,6,7,8-HxCDF log K_{OW} = 7.62 1,2,3,4,6,7,8-HpCDF log K_{OW} = 7.92 1,2,3,4,7,8,9-HpCDF log K_{OW} = 7.99 OCDF log K_{OW} = 8.0	*Paasivirta et al*., 1999
	1,2,3,7,8-PeCDF	$6.17 \cdot 10^6$		*Sijm et al.,* 1989
	2,3,4,7,8–PeCDF	$7.94 \cdot 10^6$		*Paasivirta et al*., 1999
	1,2,3,4,7,8–HxCDF	$3.47 \cdot 10^7$		
	1,2,3,6,7,8-HxCDF	$3.72 \cdot 10^7$		*Govers and Krop*, 1998
	1,2,3,7,8,9-HxCDF	$5.75 \cdot 10^7$		
	2,3,4,6,7,8-HxCDF	$4.17 \cdot 10^7$		*Paasivirta et al*., 1999
	1,2,3,4,6,7,8-HpCDF	$8.32 \cdot 10^7$		*Sijm et al*., 1989
	1,2,3,4,7,8,9-HpCDF	$9.77 \cdot 10^7$		*Paasivirta et al*., 1999
	OCDF	$1.00 \cdot 10^8$		*Beyer and Matthies*, 2002
PCBs	PCB-28	$6.31 \cdot 10^5$	Temperature independent; PCB-28 log K_{OW} = 5.8 PCB-105 log K_{OW} = 6.65 PCB 118 log K_{OW} = 6.74 PCB-153 log K_{OW} = 6.9 PCB-180 log K_{OW} = 7.36	*Mackay et al.,* 1992a
	PCB-105	$4.47 \cdot 10^6$		*Hawker and Connell,* 1988
	PCB-118	$5.5 \cdot 10^6$		
	PCB-153	$7.94 \cdot 10^6$		*Mackay et al.,* 1992a
	PCB-180	$2.29 \cdot 10^7$		*Hawker and Connell,* 1988
γ-HCH		$7.943 \cdot 10^3$	Temperature independent log K_{OW} = 3.9	*Chu and Chan,* 2000
HCB		$2.426 \cdot 10^5$	Temperature independent; estimated with the use of K_{OA} from [*Harner and Mackay*, 1995] and used value of K_H obtained on the basis of data from [*Beyer and Matthies*, 2001]	estimated

B.7. Organic carbon-water partition coefficient

The organic carbon-water partition coefficient (K_{OC}, m^3/kg) is used for the description of POP sorption by soil and bottom sediments. K_{OC} values used in the model parameterization for the most part of the considered POPs were obtained from K_{OW} values using the following relation:

$$K_{OC} = 0.41 K_{OW} \text{ [Karikhoff, 1981]} \quad \text{(B.7)}$$

Partition coefficients in the "organic carbon-water" system selected for modelling are presented in Table B.8.

***Table B.8**. Organic carbon-water partition coefficient (K_{OC}), m^3/kg used in the model parameterization*

Compound		Values K_{oc}, m^3/kg	Comments	Reference
PAHs	B[a]P	$4.496 \cdot 10^2$	calculated from K_{OW} by Eq. (B.7) from *Karikhoff,* 1981	estimated
	B[b]F	$2.59 \cdot 10^2$		
	B[k]F	$4.10 \cdot 10^2$		
	I_P	$1.57 \cdot 10^3$		
PCDDs	2,3,7,8-TCDD	$3.74 \cdot 10^3$	calculated from K_{OW} by Eq. (B.7) from *Karikhoff,* 1981	
	1,2,3,7,8-PeCDD	$7.63 \cdot 10^3$		
	1,2,3,4,7,8–HxCDD	$2.59 \cdot 10^4$		
	1,2,3,6,7,8-HxCDD	$3.74 \cdot 10^4$		
	1,2,3,7,8,9-HxCDD	$2.36 \cdot 10^4$		
	1,2,3,4,6,7,8-HpCDD	$4.10 \cdot 10^4$		
	OCDD	$6.50 \cdot 10^4$		
PCDFs	2,3,7,8-TCDF	$1.56 \cdot 10^3$		
	1,2,3,7,8-PeCDF	$2.53 \cdot 10^3$		
	2,3,4,7,8–PeCDF	$3.26 \cdot 10^3$		
	1,2,3,4,7,8–HxCDF	$1.42 \cdot 10^4$		
	1,2,3,6,7,8-HxCDF	$1.52 \cdot 10^4$		
	1,2,3,7,8,9-HxCDF	$2.36 \cdot 10^4$		
	2,3,4,6,7,8-HxCDF	$1.71 \cdot 10^4$		
	1,2,3,4,6,7,8-HpCDF	$3.41 \cdot 10^4$		
	1,2,3,4,7,8,9-HpCDF	$4.01 \cdot 10^4$		
	OCDF	$4.10 \cdot 10^4$		
PCBs	PCB-28	$2.59 \cdot 10^2$	calculated from K_{OW} by Eq. (B.7) from *Karikhoff,* 1981	
	PCB-105	$1.83 \cdot 10^3$		
	PCB-118	$2.255 \cdot 10^3$		
	PCB-153	$3.26 \cdot 10^3$		
	PCB-180	$9.39 \cdot 10^3$		
γ-HCH		1.08	predicted	*Chu and Chan,* 2000
HCB		$9.946 \cdot 10^1$	calculated from K_{OW} by Eq. (B.7) from *Karikhoff,* 1981	estimated

B.8. Octanol-air partition coefficient

The octanol-air partition coefficient ($K_{OA,}$ dimensionless) is used for the description of a substance partitioning between air and the cuticle of plants, between the gaseous phase and the organic film of atmospheric aerosol particles, etc. In experiments this coefficient is determined by the ratio of equilibrium concentrations of a substance in octanol and air. Additionally, this coefficient can be defined with the use of coefficients “octanol-water” and “air-water”.

$$K_{OA} = C_O / C_A = K_{OW} / K_{AW} = K_{OW} \cdot RT / K_H, \quad \text{(B.8)}$$

where C_O is the equilibrium concentration of a substance in octanol;

C_A is the equilibrium concentration of a substance in air;

K_{OW} is octanol-water partition coefficient;

R is universal gas constant equal to 8.314 J/(mol·K);

T is temperature, K;

K_H is Henry’s law constant, $Pa \cdot m^3/mol$.

Parameter K_{OA} of the considered POPs depends on temperature. The temperature dependence of partition coefficient in the “octanol-air” system is expressed in the following form:

$$K_{OA} = K_{OA}^0 \exp\left[a_K\left(\frac{1}{T} - \frac{1}{T_0}\right)\right], \quad \text{(B.9)}$$

where T_0 = 283.15 K is the reference temperature;

K^0_{OA} is the K_{OA} value at the reference temperature;

a_K is the coefficient of K_{OA} temperature dependence, K.

Coefficients for K_{OA} temperature dependence of the considered POPs used for modelling are presented in Table B.9. The way in which these coefficients of the temperature dependence were obtained or recalculated from original data presented in the literature used is specified in the field "Comments".

Table B.9. *Octanol-air partition coefficient (K_{OA}), dimensionless used in the model parameterization*

Compound		Values			Comments	Reference
		K^0_{OA} dimensionless	a_K K	T_0 K		
PAHs	B[a]P	$4.99 \cdot 10^{10}$	7866	283.15	Coefficients of the exponential equation are recalculated from the standard form of temperature dependence: log K_{OA} = $A/T(K)$ - B with the help of the following formulas: a_k = ln(10)· A, $K^0_{OA} = 10^{(A/To - B)}$ where for: B[a]P A = 3416, B = 1.37; B[b]F A = 3416, B = 1.21; B[k]F A = 3416, B = 1.31 estimated with the use of basic value of K_{OA} at 25^{0}C calculated by equation: $K_{OA} = K_{OW} \cdot R \cdot T/K_H$ (K_{OW} from *Mackay et al.,* 1992b*;* K_H from *Ten Hulscher et al.,* 1992*)* together with temperature dependence coefficient for Henry's law constant	estimated
	B[b]F	$7.16 \cdot 10^{10}$	7866	283.15		
	B[k]F	$5.69 \cdot 10^{10}$	7866	283.15		
	I_P	$1.11 \cdot 10^{12}$	7866	283.15	Coefficients of the exponential equation are recalculated from the standard form of temperature dependence: log K_{OA} = $A/T(K) - B$ with the help of the following formulas: a_k = ln(10)· A, $K^0_{OA} = 10^{(A/To - B)}$ where for: I_P A = 3416, B = 0.02. estimated with the use of basic value of K_{OA} at 25^{0}C calculated by equation: $K_{OA} = K_{OW} \cdot R \cdot T/K_H$ (K_{OW} from *Database SRC Chemfate* 2001*;* K_H from *Ten Hulscher et al.,* 1992*)* together with temperature dependence coefficient for Henry's law constant	
PCDDs	2,3,7,8-TCDD	$6.44 \cdot 10^{10}$	10104	283.15	Coefficients of the exponential equation are estimated with the use of basic value of K_{OA} at 10^{0}C calculated by equation: $K_{OA} = K_{OW} \cdot R \cdot T/K_H$ (K_{OW} from *Govers and Krop*,1998; K_H from *Bulgakov and Ioannisian,* 1998) together with temperature dependence coefficient for Henry's law constant	estimated
	1,2,3,7,8-PeCDD	$1.96 \cdot 10^{11}$	10412	283.15	Coefficients of the exponential equation are estimated with the use of basic value of K_{OA} at 10^{0}C calculated by equation: $K_{OA} = K_{OW} \cdot R \cdot T/K_H$ (K_{OW} from *Paasivirta et al.,* 1999*;* K_H from *Bulgakov and Ioannisian*, 1998*)* together with temperature dependence coefficient for Henry's law constant	estimated
	1,2,3,4,7,8-HxCDD	$4.71 \cdot 10^{12}$	11462	283.15	Coefficients of the exponential equation are estimated with the use of basic value of K_{OA} at 10^{0}C calculated by equation $K_{OA} = K_{OW} \cdot R \cdot T/K_H$ (K_{OW} from *Beyer and Matthies,* 2002*;* K_H from *Bulgakov and Ioannisian*, 1998*)* together with temperature dependence coefficient for Henry's law constant	estimated
	1,2,3,6,7,8-HxCDD	$6.99 \cdot 10^{12}$	11366	283.15	Coefficients of the exponential equation are estimated with the use of basic value of K_{OA} at 10^{0}C calculated by equation: $K_{OA} = K_{OW} \cdot R \cdot T/K_H$ (K_{OW} from *Paasivirta et al.,* 1999*;* K_H from *Bulgakov and Ioannisian*, 1998*)* together with temperature dependence coefficient for Henry's law constant	estimated
	1,2,3,7,8,9-HxCDD	$3.22 \cdot 10^{12}$	11720	283.15		estimated
	1,2,3,4,6,7,8-HpCDD	$1.88 \cdot 10^{13}$	12943	283.15	Coefficients of the exponential equation are estimated with the use of basic value of K_{OA} at 10^{0}C calculated by equation: $K_{OA} = K_{OW} \cdot R \cdot T/K_H$ (K_{OW} from *Beyer and Matthies,* 2002*;* K_H from *Bulgakov and Ioannisian*, 1998*)* together with temperature dependence coefficient for Henry's law constant	estimated
	OCDD	$2.77 \cdot 10^{12}$	9219.6	283.15		estimated

Table B.9. *(continued)*

Compound		Values			Comments	Reference
		$K°_{OA}$ dimensionless	a_K K	T_0 K		
PCDFs	2,3,7,8-TCDF	$3.26 \cdot 10^{10}$	8998.5	283.15	Coefficients of the exponential equation are estimated with the use of basic value of K_{OA} at 10^0C calculated by equation: $K_{OA} = K_{OW} \cdot R \cdot T/K_H$ (K_{OW} from *Paasivirta et al*., 1999*; K_H* from *Bulgakov and Ioannisian*, 1998*)* together with temperature dependence coefficient for Henry's law constant	estimated
	1,2,3,7,8-PeCDF	$3.66 \cdot 10^{11}$	10113	283.15	Coefficients of the exponential equation are estimated with the use of basic value of K_{OA} at 10^0C calculated by equation: $K_{OA} = K_{OW} \cdot R \cdot T/K_H$ (K_{OW} from *Sijm et al.,* 1989*; K_H* from *Bulgakov and Ioannisian*, 1998*)* together with temperature dependence coefficient for Henry's law constant	estimated
	2,3,4,7,8–PeCDF	$2.30 \cdot 10^{11}$	10288	283.15	Coefficients of the exponential equation are estimated with the use of basic value of K_{OA} at 10^0C calculated by equation: $K_{OA} = K_{OW} \cdot R \cdot T/K_H$ (K_{OW} from *Paasivirta et al*., 1999*; K_H* from *Bulgakov and Ioannisian*, 1998*)* together with temperature dependence coefficient for Henry's law constant	estimated
	1,2,3,4,7,8–HxCDF	$4.24 \cdot 10^{11}$	11126	283.15		estimated
PCDFs	1,2,3,6,7,8-HxCDF	$1.10 \cdot 10^{12}$	11089	283.15	Coefficients of the exponential equation are estimated with the use of basic value of K_{OA} at 10^0C calculated by equation: $K_{OA} = K_{OW} \cdot R \cdot T/K_H$ (K_{OW} from *Govers and Krop*, 1998*; K_H* from *Bulgakov and Ioannisian*, 1998*)* together with temperature dependence coefficient for Henry's law constant	estimated
	1,2,3,7,8,9-HxCDF	$1.38 \cdot 10^{12}$	11089	283.15		estimated
	2,3,4,6,7,8-HxCDF	$1.04 \cdot 10^{12}$	11055	283.15	Coefficients of the exponential equation are estimated with the use of basic value of K_{OA} at 10^0C calculated by equation: $K_{OA} = K_{OW} \cdot R \cdot T/K_H$ (K_{OW} from *Paasivirta et al*., 1999*; K_H* from *Bulgakov and Ioannisian*, 1998*)* together with temperature dependence coefficient for Henry's law constant	estimated
	1,2,3,4,6,7,8-HpCDF	$1.89 \cdot 10^{13}$	11999	283.15	Coefficients of the exponential equation are estimated with the use of basic value of K_{OA} at 10^0C calculated by equation: $K_{OA} = K_{OW} \cdot R \cdot T/K_H$ (K_{OW} from *Sijm et al*., 1989*; K_H* from *Bulgakov and Ioannisian*, 1998*)* together with temperature dependence coefficient for Henry's law constant	estimated
	1,2,3,4,7,8,9-HpCDF	$1.78 \cdot 10^{13}$	12068	283.15	Coefficients of the exponential equation are estimated with the use of basic value of K_{OA} at 10^0C calculated by equation: $K_{OA} = K_{OW} \cdot R \cdot T/K_H$ (K_{OW} from *Paasivirta et al*., 1999*; K_H* from *Bulgakov and Ioannisian*, 1998*)* together with temperature dependence coefficient for Henry's law constant	estimated
	OCDF	$6.38 \cdot 10^{12}$	10447	283.15	Coefficients of the exponential equation are estimated with the use of basic value of K_{OA} at 10^0C calculated by equation: $K_{OA} = K_{OW} \cdot R \cdot T/K_H$ (K_{OW} from *Beyer and Matthies*, 2002*; K_H* from *Bulgakov and Ioannisian*, 1998*)* together with temperature dependence coefficient for Henry's law constant	estimated
PCBs	PCB-28	$5.78 \cdot 10^8$	8731	283.15	Coefficients of the exponential equation are recalculated from the standard form of temperature dependence: $\log K_{OA} = A/T(K) - B$ with the help of the following formulas: $a_k = \ln(10) \cdot A$, $K^0_{OA} = 10^{(A/To - B)}$ where for: PCB-28 $A = 3792$, $B = 4.63$ A was taken to be equal to the corresponding coefficient for PCB-29 taken from [*Harner and Bidleman,* 1996], B was estimated from the formula $B = A/293 - \log K_{OA}^{293}$; where $\log K_{OA}^{293} = (-1.268) \log p^0_L + 6.135$ [*Harner and Bidleman,* 1996]	estimated
	PCB-105	$6.94 \cdot 10^{10}$	10772	283.15	Coefficients of the exponential equation are recalculated from the standard form of temperature dependence: $\log K_{OA} = A/T(K) - B$ with the help of the following formulas: $a_k = \ln(10) \cdot A$, $K^0_{OA} = 10^{(A/To - B)}$ where for: PCB-105 A = 4678, B = 5.68; PCB-118 A = 4693, B = 5.92; PCB-153 A = 4695, B = 6.02; PCB-180 A = 4535, B = 4.70	*Harner and Bidleman,* 1996
	PCB-118	$4.51 \cdot 10^{10}$	10806	283.15		
	PCB-153	$3.64 \cdot 10^{10}$	10811	283.15		
	PCB-180	$2.07 \cdot 10^{11}$	10442	283.15		
γ-HCH		$1.45 \cdot 10^8$	5485	283.15	Coefficients of the exponential equation are recalculated from the standard form of temperature dependence: $\log K_{OA} = 2382/T(K) - 0.25$ estimated with the use of basic value of K_{OA} at 25^0C calculated by equation: $\log K_{OA} = \log K_{OW} - \log K_H/RT$ (K_{OW} from *Chu and Chan,* 2000*; K_H* from *Kucklick et al.,* 1991*)* together with temperature dependence coefficient for Henry's law constant for fresh water	estimated
HCB		$3.74 \cdot 10^7$	9045	283.15	Coefficients of the exponential equation are recalculated from the standard form of temperature dependence: $\log K_{OA} = 3928/T(K) - 6.3$ with the help of the following formulas: $a_k = \ln(10) \cdot 3928$, $K^0_{OA} = 10^{(3928To - 6.3)}$	*Harner and Mackay*, 1995

B.9. Molecular diffusion coefficients in air and water

Molecular diffusion coefficients (D_A, D_W, cm^2/s) are used in the description of the POP air-soil exchange process. The molecular diffusion coefficient of an organic compound in air (D_A, cm^2/s) can be estimated by the formula [*Schwarzenbach et al.,* 1993]:

$$D_A = 10^{-3} \cdot \frac{T^{1.75}\left[(1/M_{air}) + (1/M)\right]^{1/2}}{p\left[\overline{V}_{air}^{1/3} + \overline{V}_m^{1/3}\right]^2} \qquad \text{(B.10)}$$

where T is the absolute temperature, 298 K;
M_{air} is the mean molecular air weight, ~29 g/mol;
M is the molecular weight of an organic substance, g/mol;
p is the pressure, 1 atm;
$\overline{V}_{air}$ is the mean molar gas volume in the air, ~20.1 cm^3/mol;
$\overline{V}_m$ is the molar volume of an organic substance, cm^3/mol.

For the determination of molecular diffusion coefficients for organic substances in water (D_W, cm^2/s), the following ratio [*Schwarzenbach et al.,* 1993] can be used:

$$D_W = \frac{13.26 \times 10^{-5}}{\mu^{1.14} \cdot (\overline{V}_m)^{0.589}} \qquad \text{(B.11)}$$

where μ is the solution viscosity in centipoise at a certain temperature, taken to be equal to water viscosity, 0.894 cps at 298K;
$\overline{V}_m$ is the mean molar volume of a substance, cm^3/mol.

In order to calculate molecular diffusion coefficients for the selected POPs, molecular weights (M) and molar volumes (V_m) of these compounds found in the literature (Table B.10) were used.

Table B.11 demonstrates values of molecular diffusion coefficients for air and water calculated with the use of data from Table B.10.

Table B.11. *Molecular diffusion coefficients in air and water, m^2/s used in the model parameterization*

Compound		Values		Comments	Reference
		D_A	D_W		
PAHs	B[a]P	$5.44 \cdot 10^{-6}$	$6.24 \cdot 10^{-10}$	calculated by Eqs. (B.10) and (B.11) taken from [*Schwarzenbach et al.,* 1993]	estimated
	B[b]F	$5.44 \cdot 10^{-6}$	$6.24 \cdot 10^{-10}$		
	B[k]F	$5.44 \cdot 10^{-6}$	$6.24 \cdot 10^{-10}$		
	I_P	$5.3 \cdot 10^{-6}$	$6.06 \cdot 10^{-10}$		
PCDDs	2,3,7,8-TCDD	$5.575 \cdot 10^{-6}$	$6.534 \cdot 10^{-10}$		
	1,2,3,7,8-PeCDD	$5.40 \cdot 10^{-6}$	$6.30 \cdot 10^{-10}$		
	1,2,3,4,7,8–HxCDD	$5.24 \cdot 10^{-6}$	$6.09 \cdot 10^{-10}$		
	1,2,3,6,7,8-HxCDD	$5.24 \cdot 10^{-6}$	$6.09 \cdot 10^{-10}$		
	1,2,3,7,8,9-HxCDD	$5.24 \cdot 10^{-6}$	$6.09 \cdot 10^{-10}$		
	1,2,3,4,6,7,8-HpCDD	$5.10 \cdot 10^{-6}$	$5.90 \cdot 10^{-10}$		
	OCDD	$4.97 \cdot 10^{-6}$	$5.73 \cdot 10^{-10}$		
PCDFs	2,3,7,8-TCDF	$5.67 \cdot 10^{-6}$	$6.66 \cdot 10^{-10}$		
	1,2,3,7,8-PeCDF	$5.49 \cdot 10^{-6}$	$6.42 \cdot 10^{-10}$		
	2,3,4,7,8–PeCDF	$5.49 \cdot 10^{-6}$	$6.42 \cdot 10^{-10}$		
	1,2,3,4,7,8–HxCDF	$5.32 \cdot 10^{-6}$	$6.20 \cdot 10^{-10}$		
	1,2,3,6,7,8-HxCDF	$5.32 \cdot 10^{-6}$	$6.20 \cdot 10^{-10}$		
	1,2,3,7,8,9-HxCDF	$5.32 \cdot 10^{-6}$	$6.20 \cdot 10^{-10}$		
	2,3,4,6,7,8-HxCDF	$5.32 \cdot 10^{-6}$	$6.20 \cdot 10^{-10}$		
	1,2,3,4,6,7,8-HpCDF	$5.17 \cdot 10^{-6}$	$6.00 \cdot 10^{-10}$		
	1,2,3,4,7,8,9-HpCDF	$5.17 \cdot 10^{-6}$	$6.00 \cdot 10^{-10}$		
	OCDF	$5.03 \cdot 10^{-6}$	$5.82 \cdot 10^{-10}$		
PCBs	PCB-28	$5.43 \cdot 10^{-6}$	$6.08 \cdot 10^{-10}$	recalculated from molecular diffusion coefficients in air and water for PCB-153	estimated
	PCB-105	$4.82 \cdot 10^{-6}$	$5.40 \cdot 10^{-10}$		
	PCB-118	$4.82 \cdot 10^{-6}$	$5.40 \cdot 10^{-10}$		
	PCB-153	$4.59 \cdot 10^{-6}$	$5.14 \cdot 10^{-10}$	calculated by Eqs. (B.10) and (B.11) taken from [*Schwarzenbach et al.,* 1993]	
	PCB-180	$4.38 \cdot 10^{-6}$	$4.91 \cdot 10^{-10}$	recalculated from molecular diffusion coefficients in air and water for PCB-153	
γ-HCH		$6 \cdot 10^{-6}$	$7 \cdot 10^{-10}$	calculated by Eqs. (B.10) and (B.11) taken from [*Schwarzenbach et al.,* 1993]	estimated
HCB		$6.166 \cdot 10^{-6}$	$7.399 \cdot 10^{-10}$		

Table B.10. *Molar volume and molar masses*

Compound		Values		Reference
		M, g/mol	V_m, cm^3/mol	
PAHs	B[a]P	252.29	222.8	*Paasivirta et al.,* 1999*;* *Ruelle and Kesselring*, 1997
	B[b]F	252.29	222.8	
	B[k]F	252.29	222.8	
	I_P	276.31	233.8	
PCDDs	2,3,7,8-TCDD	321.98	206	*Mackay et al.,* 1992b; *Ruelle and Kesselring*, 1997
	1,2,3,7,8-PeCDD	356.40	218.9*	
	1,2,3,4,7,8–HxCDD	390.87	231.8	
	1,2,3,6,7,8-HxCDD	390.87	231.8	
	1,2,3,7,8,9-HxCDD	390.87	231.8	
	1,2,3,4,6,7,8-HpCDD	425.2	244.7	
	OCDD	460.0	257.6	
PCDFs	2,3,7,8-TCDF	306.00	199.4	
	1,2,3,7,8-PeCDF	340.42	212.3	
	2,3,4,7,8-PeCDF	340.42	212.3	
	1,2,3,4,7,8-HxCDF	374.87	225.2	
	1,2,3,6,7,8-HxCDF	374.87	225.2	
	1,2,3,7,8,9-HxCDF	374.87	225.2	
	2,3,4,6,7,8-HxCDF	374.87	225.2	
	1,2,3,4,6,7,8-HpCDF	409.31	238.1	
	1,2,3,4,7,8,9-HpCDF	409.31	238.1	
	OCDF	443.8	251	
PCBs	PCB-28	257.5	247.3	*Mackay et al.,* 1992a
	PCB-105	326.4**	289.1**	
	PCB-118	326.4	289.1	
	PCB-153	360.9	310	
	PCB-180	395.3	330.9	
γ-HCH		290.85	179.5	*Mackay et al.,* 1997; *Ruelle and Kesselring*, 1997
HCB		284.8	166.8	*Mackay et al.,* 1992a; *Ruelle and Kesselring*,1997

* molar volume is given for congener – 1,2,3,4,7- PeCDD

** - this congener description is not presented in detail in [*Mackay et al.,* 1992a]. However, parameter values are taken to be equal to these values of other pentachlorobiphenyls given in [*Mackay et al.,* 1992a].

Annex C

INPUT DATA

C.1. Meteorological data

The System of Diagnosis of the Lower Atmosphere (SDA) developed by Hydrometeorological Centre of Russia [*Frolov et al.*, 1994; *Rubinstein et al.*, 1997,1998; *Frolov et al.*, 1997 a,b,c] provides a set of meteorological data for the hemispheric multi-compartment models. The list of these parameters is presented in Table C.2. The horizontal resolution of information produced by SDA system is 2.5ºx2.5º. Along the vertical σ-coordinates are used with 9 layers up to the level of 0.26 hPa.

The SDA system consists of the following main units:

- unit of initial data including the control and correction of errors,
- unit of boundary conditions,
- hydrodynamic prognostic model,
- post-processing unit.

Table C.1. *Meteorological parameters supplied by the SDA system for the Northern Hemisphere with resolution of 2.5ºx2.5º*

Parameter	Notation	Type
Wind velocity	V_Λ, V_Φ	bulk
Air temperature	T_a	bulk
Surface pressure	p_s	surface
Precipitation rate	I_p	bulk
Water vapour mixing ratio	q_w	bulk
Large-scale cloudiness	C_L	bulk
Convective cloudiness	C_C	bulk
Surface temperature	T_s	surface
Vertical eddy diffusion coefficient	K_z	bulk
Roughness of the underlying surface	z_0	surface
Friction velocity	u_*	surface
Monin-Obukhov length	L_{MO}	surface
Soil humidity	M_s	surface
Snow cover height	h_s	surface

C.2. Land cover data

Land cover information is used for correct description of deposition and exchange processes between atmosphere and different types of underlying surface. For this purpose we use 24-category USGS Land Use/Land Cover dataset obtained from NCAR Mesoscale Modeling System (MM5) [*Guo and Chen*, 1994]. This selection is conditioned by the availability of more detailed information on underlying surface types with high spatial resolution (10'x10'). Each grid cell is characterized by several types of surface proportional their area. Table C.2 contains the description of USGS Land Use/Land Cover System Legend.

Table C.2. *USGS Land Use/Land Cover System Legend*

No	Description
1	Urban and Built-Up Land
2	Dryland Cropland and Pasture
3	Irrigated Cropland and Pasture
4	Mixed Dryland/Irrigated Cropland and Pasture
5	Cropland/Grassland Mosaic
6	Cropland/Woodland Mosaic
7	Grassland
8	Shrubland
9	Mixed Shrubland/Grassland
10	Savanna
11	Deciduous Broadleaf Forest
12	Deciduous Needleleaf Forest
13	Evergreen Broadleaf Forest
14	Evergreen Needleleaf Forest
15	Mixed Forest
16	Water Bodies
17	Herbaceous Wetland
18	Wooded Wetland
19	Barren or Sparsely Vegetated
20	Herbaceous Tundra
21	Wooded Tundra
22	Mixed Tundra
23	Bare Ground Tundra
24	Snow or Ice

Since the formulation of the models described in this report does not require detailed specification of data on the underlying surface, the original 24-categories of land cover were reduced to six general categories (deciduous forests, coniferous forests, grassland, urban and built-up land, bare land and glaciers, water bodies) and redistributed over the model grid.